44th International Physics Olympiad
IPhO 2013

Final Report

IPhO
44th
Copenhagen Denmark 7-15 July 2013

www.ipho2013.dk

Contents

IPhO 2013 links

Main IPhO 2013 website: http://www.ipho2013.dk

Presentations of problems: http://www.ipho2013.dk/ipho2013-presentations.htm
The problems: http://www.ipho2013.dk/ipho2013-problems.htm
The solutions: http://www.ipho2013.dk/ipho2013-solutions.htm
Results: http://www.ipho2013.dk/ipho2013-results.htm

Videos: http://www.ipho2013.dk
Photo gallery: http://www.ipho2013.dk/ipho2013-photos.htm
Daily newsletter: http://www.ipho2013.dk/ipho2013-newsletter.htm
Press clippings: http://www.ipho2013.dk/ipho2013-press-clips.htm

Organizing committee: http://www.ipho2013.dk/ipho2013-committee.htm
Sponsors: http://www.ipho2013.dk/ipho2013-sponsors.htm

Main IPhO website: http://ipho.phy.ntnu.edu.tw/

Preface

In 1999, the Minister of Education accepted on behalf of Denmark the honorable task of hosting the 44th International Physics Olympiad, IPhO 2013, one of the most prestigious scientific competitions for pre-university students. The particular year 2013 and the host city Copenhagen were chosen to celebrate the centennial anniversary of Niels Bohr's groundbreaking 1913-papers on the quantum model of the hydrogen atom. The Bohr model led to the foundation of modern quantum physics and is naturally reflected in the IPhO 2013 logo.

The preparations for IPhO 2013 began in earnest five years ago by the formation of a steering committee. As the great event drew closer, more and more people from the two host universities, University of Copenhagen (KU) and Technical University of Denmark (DTU), became involved in the preparations. In particular, students and faculty from the Niels Bohr Institute (KU), DTU Physics, DTU Nanotech, DTU Photonics, and DTU Admission Course as well as administrative staff from KU and DTU participated enthusiastically on all levels in creating the big event. A great and sincere thank goes to all these people, without whom IPhO 2013 would not have been possible to run.

However, a great staff does not do it alone. Substantial funding is also required to host an IPhO with more than 80 participating countries sending delegations totaling more than 700 people. Fortunately, the Ministry of Education, the two host universities, and eight private foundations provided the necessary financial means and facilities. We gratefully acknowledge this generous support, which showed the wide-spread understanding in Denmark for the importance of the International Physics Olympiad.

The core of an IPhO is the scientific competition, and more than 20 people from KU and DTU worked on formulating the theoretical and experimental exams. The aim was to provide problems involving actual phenomena in nature and technology, thus showing the relevance of physics in everyday life. Another aim was to ensure that all the problems had a reasonable entrance level, allowing most students to get a good start, followed by increasingly difficult questions to challenge even the most talented students. We hope that the students, the leaders and the 85 markers assisting in correcting the exams, felt that these aims were indeed fulfilled.

A secondary goal in the planning of IPhO 2013 was to present Denmark, Copenhagen and the two host universities in such a way that all participants, students, leaders, observers and visitors, would like to return here for scientific, educational, and/or touristic reasons in the future. To this end, more than 120 student guides volunteered to help making our guests have a great time in Denmark.

Finally, on behalf of the organizers, we would like not only to thank the students who participated in the competition and demonstrated high skills, but also all the leaders, observers and visitors for their participation in IPhO-2013. They all contributed to the success of the event.

Copenhagen, fall 2013

Senior Lecturer Niels Hartling
President of IPhO 2013

Professor Henrik Bruus
Vice President of IPhO 2013

Welcome note from His Royal Highness Crown Prince Frederik

As patron of the 44th International Physics Olympiad in Denmark, it is a great pleasure for me to bid each of you from all over the world a cordial welcome to this inspiring event. At the opening ceremony of IPhO 2013, physicists from more than 80 countries are present; physicists on all levels including professors, researchers, teachers from high schools and universities, and, not least, about 400 young and very talented students. A special welcome to you.

In the coming days you are going to engage each other in an academically demanding, but friendly competition involving a series of challenging physics problems. I wish you the best of luck in your endeavors. Regardless of your achievements in the competition, remember that you have already, through your qualification to your national team, shown an outstanding talent for physics.

In addition to the competition itself, you will enjoy several days here in Denmark as visitors, and hopefully you will carry home dear memories that will one day make you wish to return. Most importantly, during the coming week you will have a unique opportunity to create an international network and to initiate lasting friendships with other people sharing your passion for physics.

Physics is a unique subject that is above political, cultural, and societal differences between people. Physics provides an exceptional insight into nature and its inner workings, and physics is a crucial prerequisite for technology, which is a pivotal part of modern societies. Your talent can be of great personal joy for you in your future life, and it will most likely be of benefit for those countries that you represent here today.

I hope you will enjoy your stay in Denmark and represent your country well at the 44th International Physics Olympiad.

Public sponsors and hosts

Ministry of Education

UNDERVISNINGS MINISTERIET

University of Copenhagen

Niels Bohr Institutet

Technical University of Denmark

DTU

List of private sponsors in alphabetical order

A.P. Møller og Hustru Chastine Mc-Kinney Møllers Fond til Almene Formaal

A.P. MØLLER FONDEN

Augustinus Fonden

CHR AUGUSTINUS FABRIKKERS FOND

AUGUSTINUS FONDEN

STIFTET 25. MARTS 1942

Carlsbergs Mindelegat

CARLSBERGS MINDELEGAT

Jorcks Fond

KONSUL GEORGE JORCK OG HUSTRU EMMA JORCK'S FOND

Knud Højgaards Fond

Knud Højgaards Fond

Lundbeckfonden

THE LUNDBECK FOUNDATION

Otto Mønsteds Fond

Otto Mønsted

- FREMMER DANSK HANDEL OG INDUSTRI

Villum Fonden

VILLUM FONDEN

The opening ceremony of the 44th International Physics Olympiad
DTU, Monday 8 July 2013 (see the video at www.ipho2013.dk)

1. Pre-show at 09:00: The Tivoli Guard and still photos from Denmark
2. Opening at 09:30 by the New Bigband led by Andreas Vetö
and show hosts Flemming Enevold and Sofie Lassen-Kahlke
3. Speech. Martin Schmidt, National Advisor of Physcis, Ministry of Education




4. Show. Violinist Monika Malmquist plays *Tango Jalusie* by Jacob Gade
5. Show. Professor Emeritus Mogens Andresen demonstrates the ancient Danish instrument the lure
6. Speech. Professor Anders O. Bjarklev, President of Technical University of Denmark
7. Speech. Professor Robert K. Feidenhans'l, Director of Niels Bohr Institute



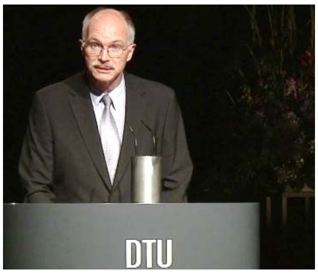

8. Show. Jazz and rock artist Cæcilie Norbye
9. Show. Flemming Enevold and Monika Malmquist, *Der stode tre skjalke*, (traditional song)
10. Speech. Mayor Søren P. Rasmussen, Lyngby-Taarbæk Municipality
11. Speech. President of the Danish IPhO Committee, Senior Lecturer Niels Hartling




12. Speech. President of IPhO, Dr. Hans Jordens, Official opening of IPhO 2013
13. Presentation of the participating countries
14. Show. Vocalist, instrumentalist, and songwriter Eivør Pálsdóttir



15. Closing at 11:30 followed by lunch buffet

DTU, Dyrehaven, Niels Bohr Institute, Tivoli on 8, 9, and 10 July

(see more at http://www.ipho2013.dk/ipho2013-photos.htm)

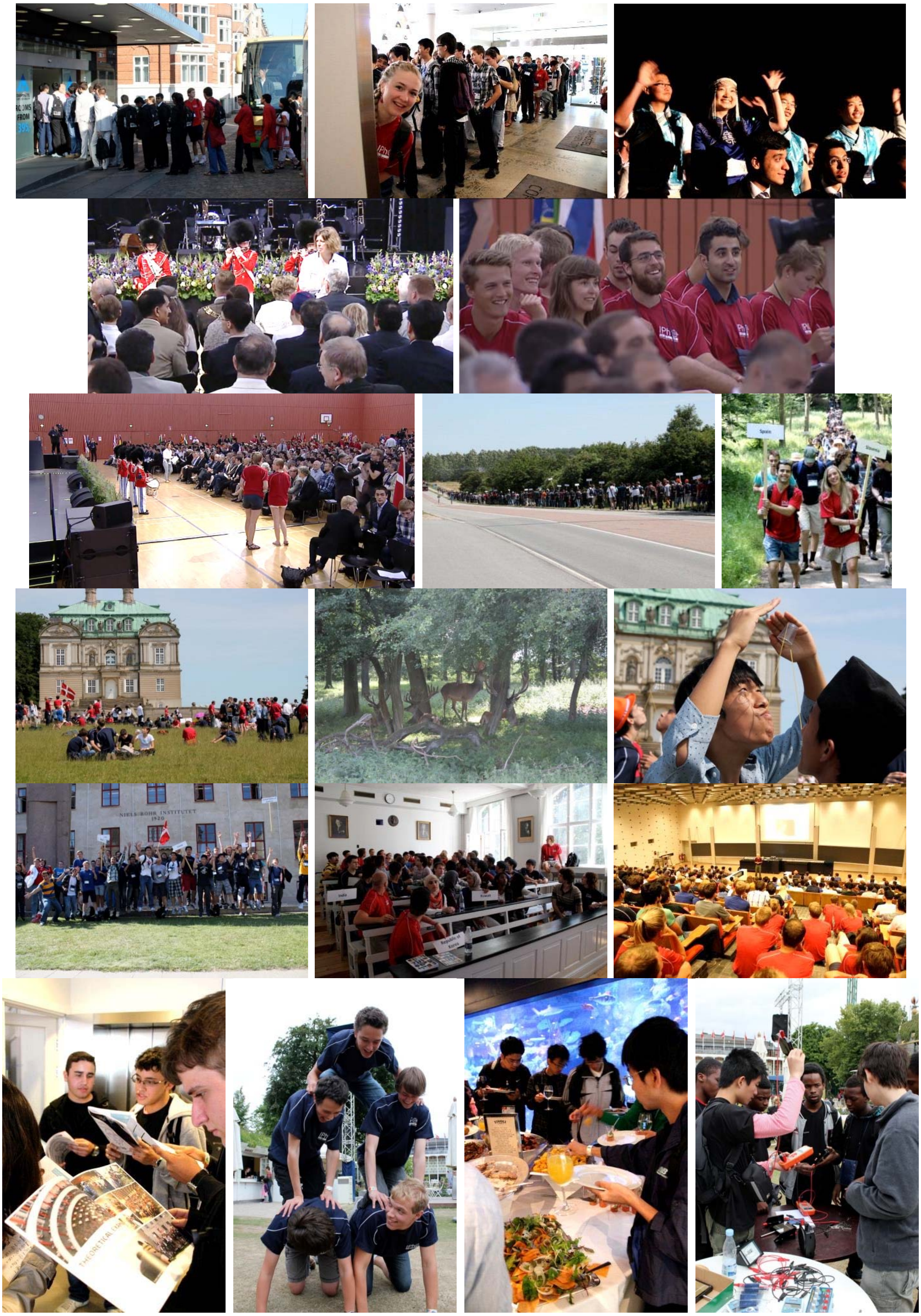

Participants

Armenia (AM)

Leaders: Gagik Grigoryan, Bilor Kurghinyan
Students: Razmik Hovhannisyan, Aleksandr Petrosyan, Arsen Vasilyan Gevorg Martirosyan, Vardges Mambreyan

Australia (AU)

Leaders: Matthew Verdon, Alix Verdon
Students: Dmitry Brizhinev, Liam Hayes, Eric Huang, Jack Spilecki, Simon Swan

Austria (AT)

Leaders: Helmuth Otto Mayr, Engelbert Stütz
Students: Oliver Edtmair, Christian Schuster, Florian Kanitschar, Moritz Theissing, Florian Riedl

Azerbaijan (AZ)

Leaders: Mirzali Murguzov, Rana Mammadova
Students: Nurlan Avazli, Rafail Gadirov, Rauf Mahmudzade, Tural Aliyev, Abdullah Bazarov
Observer: Rashadat Gadmaliyev. **Visitor:** Shahin Murguzov

Bangladesh (BD)

Leaders: M. Arshad Momen, Fayez Ahmed Jahangir Masud
Students: Shinjini Saha, Shovon Biswas, Kinjol Barua, Saquib Musavi Hassan, Mohammed Abid Abrar

Belarus (BY)

Leaders: Anatoli Slabadzianiuk , Anton Mishchuk
Students: Akvukh Jeims Aye, Aliaksandr Hancharuk , Aliaksei Duduk , Maksim Litskevich , Ivan Mitskovets

Belgium (BE)

Leaders: Philippe Leonard, Bernadette Hendrickx
Students: Nick Van Den Broeck, Marcel M Goeminne Nelis, Engelen Wouter, Deprez Xavier, Gaëtan Cassiers
Observer: Sophie Houard

Bolivia (BO)

Leader: Marko Jorge Andrade Uzieda
Students: Adriana Nayra Alvarez Pari, Francisco Antonio Camacho Mendieta

Bosnia And Herzegovina (BA)

Leaders: Rajfa Musemic, Sinisha Ignjatovich
Students: Benjamin Cerimagic, Nudzeim Selimovic, Suad Krilasevic, Enes Krijestorac, Slavko Ivanovic

Brazil (BR)

Leaders: Euclydes Marega Junior, Fernando Wellysson De Alencar Sobreira
Students: Jose Luciano De Morais Neto, Guilherme Renato Martis Unzer, Fernando Frota Junior, Matheus Carius Castro, Fabio Kenji Arai
Observers: Joselaine Aparecida Martinez Migliato Marega, Francisco Odivaldo Teixeira Junior, Leonardo Bruno Pedroza Pontes De Lima, Fred Uesono Basso

Bulgaria (BG)
Leaders: Viktor Genchev Ivanov, Miroslav Vergilov Abrashev
Students: Katerina Marinova Naydenova, Ivan Krasimirov Poryazov, Kaloyan Ognyanov Darmonev, Yordan Stefanov Yordanov, Kaloyan Georgiev Metodiev

Canada (CA)
Leaders: Andrzej Kotlicki, Mohammadreza Mohammadi
Students: Henry Wu, Bailey Gu, Hao Zhe Sheng, Jiaxi (Jannis) Mei, Shun Da Suo
Visitor: Chantal Luise Haussmann

China (CN)
Leaders: Song Feng, Zhang Chunling
Students: Jiang Jiaqi, Wang Sizhen, Yu Yue, Zhang Chengkai, Zhang Zhengxing
Observers: Lu Wenqiang, Liu Yubin

Colombia (CO)
Leaders: Fernando Vega Salamanca, Eduardo Zalamea Godoy
Students: Jorge Alberto Garcia Perez, Daniel Eduardo Fajardo Fajardo, Oscar O. Ojito Navarro
Observer: Elena Patricia Losada Falk

Croatia (HR)
Leaders: Kreso Zadro, Mario Basletic
Students: Antonio Bjelcic, Samuel Bosch, Tvrtko Doresic, Ivan Porin Tolic, Matej Vilic

Cuba (CU)
Leader: Alberto Mawad Santos
Student: Leonardo Martín De La Nuez

Cyprus (CY)
Leaders: Andreas Panagi, Demetrios Philippou
Students: Andreas Stavrou, Angelos Ermogenous, Rafail Panagi, Rafail Dimitriou, Andreas Kiourlappos

Czech Republic (CZ)
Leaders: Jan Kříž, Filip Studnička
Students: Lubomír Grund, Jiří Guth, Jakub Vančura, Jakub Rösler, Miroslav Hanzelka

Denmark (DK)
Leaders: Niels Christian Jensen, Kirstine Berg-Sørensen
Students: Sebastian Tim Holdum, Frederik Ravn Klausen, Michael Blom Hermansen, Tai Mathias Skadegaard Thorsen, Markus Emil Jacobsen

Ecuador (EC)
Leaders: None (assistance from the Spanish leaders)
Students: Gustavo Antonio Costa Kozhaya, Martin Trapero Laos, Luis Gilberto Escobar Nunez, Andony Landivar Macias

El Salvador (SV)
Leaders: Carlos Armando Alberti Arroyo, Raúl Alfonso Alvarenga Gómez
Students: Alejandra María Fuentes Núñez, Mario Fernando Alvarado Lazo

Estonia (EE)
Leaders: Jaan Kalda, Mihkel Kree, Stanislav Zavjalov
Students: Kaur Aare Saar, Andres Põldaru, Joonas Kalda, Kristo Ment, Kristjan Kongas

Finland (FI)
Leaders: Heikki Jalo Jalmari Mäntysaari, Lasse Aatos Franti
Students: Timo Takala, Heikki Oskari Timonen, Einari Junter, Tomi Mäkinen, Joonas Latukka

France (FR)
Leaders: Nicolas Billy, Christian Brunel
Students: Sébastien Chevaleyre, Matthieu De Rochemonteix, Anatole Gosset, Jean Doucot, Cédric Viry
Observers: Solène Thery, Dominique Obert

Georgia (GE)
Leaders: Tsimakuridze, Paverman
Students: Chalauri, Maludze, Sokhashvili, Tskhadadze, Gobejishvili
Observer: Dalakishvili

Germany (DE)
Leaders: Stefan Petersen, Axel Boeltzig
Students: Lars Dehlwes, Sascha Lill, Lucas Rettenmeier, David Schmidt, Michael Sonner
Observer: Jochen Kröger

Greece (GR)
Leaders: Georgios Kalkanis , Panagiotis Tsakonas
Students: Stavros Eythymiou , Grigorios Sergentanis , Filippos Kyriakidis , Krinio Marouda, Evangelos-Damianos Lazaris

Hong Kong (HK)
Leaders: Du Shengwang, Yung Lit Hung
Students: Lum Kai Chun, Man Siu Hang, Shing Ming Tong, Tam Pok Man, Wong Yiu Man
Observers: Lam Wang Yuen, Szeto Chung Wang Godwin, Zhang Shanchao

Hungary (HU)
Leaders: Tasnádi Tamás Péter, Vigh Máté
Students: Jenei Márk, Juhász Péter, Kovács Áron Dániel, Papp Roland, Szabó Attila
Observer: Simon Péter

Iceland (IS)
Leaders: Ingibjörg Haraldsdóttir, Viðar Ágústsson
Students: Snorri Tómasson, Tryggvi Kalman Jónsson, Pétur Rafn Bryde, Jón Sölvi Snorrason, Davíð Ólafsson
Visitor: Helga Hilmarsdóttir

India (IN)
Leaders: Mukund Laxman Ogalapurkar, Praveen Pathak
Students: Abhijit Lavania, Abhishek Anand, Prafulla Susil Dhariwal, Shouvanik Chakrabarti, Yash Gupta
Observer: Vijay Awadesh Singh

Indonesia (ID)
Leaders: Kamsul Abraha, Mohammad Syamsu Rosid
Students: Paulus Anthony Halim, Mikael Harseno Subianto, Joshua Christian Nathanael, I Made Gita Narendra Kumara, Andres Bethavan Situmorang
Observers: Bobby Eka Gunara, Budhy Kurniawan. **Visitor:** Hari Sugiharto

Iran (IR)
Leaders: Hossein Mirzaei, Mehdi Saadat
Students: Amir Zareh, Nader Mostaan, Aminparsa Zivari, Mohamadreza Lotfinamin, Koosha Rezaiezadeh
Observer: Seyyed Nader Rasuli. **Visitor:** Hassan Saeidehghan

Israel (IL)
Leaders: Eli Raz Somech, Igor Lisenker
Students: Ofer Moshe Kopelevitch, Gil Ad Kishony, Guy Segall, Dan Karliner, Jacoby Shoham Joshoa
Observer: Michael Averbukh

Italy (IT)
Leaders: Dennis Luigi Censi, Francesco Minosso
Students: Roberto Albesiano, Federico Belliardo, Michele Fava, Leonardo Fiore, Luigi Pagano
Observer: Alberto Meroni

Japan (JP)
Leaders: Tsutomu Nakayashiki , Kazuo Kitahara
Students: Kenji Ueda , Yuichi Enoki, Hidenobu Ema, Tasuku Omori, Hiromitsu Sawaoka
Observers: Yuto Ashida, Tadao Sugiyama, Yuya Tanizaki, Mitsuoka Kaoru

Kazakhstan (KZ)
Leaders: Askar Davletov, Yernur Rysmagambetov
Students: Amir Bralin , Mussa Rajamov, Aidar Zhetessov, Nurislam Tursynbek, Dinmukhammed Nurbek
Observers: Guliya Nurbakova , Pavel Levchenko, Sholpan Kirabayeva, Murat Abenov

Korea (KR)
Leaders: Dong Ryul Jeon, Moolee Lee
Students: Donghoi Kim, Jaewon Kim, Jaeha Lee, Changhyon Lee, Sangsu Jeong
Observers: Gunsang Jeon, Jaewan Kim, Jaehyuk Huh, Jongtak Park, Sungkook Kim

Kuwait (KW)
Leaders: Tareq A M Abdullah, Eman A Hamad
Students: Abrar Kh A M A Almutairi, Laila S M N H Bu Abbas, Annah H S T E Busalehah, Sarah S F J J Alotaibi, Lojain A H M J
Observers: Nozhah A A Almatrodo, Anoud M Y H A Alkandari

Kyrgyzstan (KG)
Leaders: Raia Sultanalieva, Seitbek Djanbaev
Students: Andrei Gagin, Arapbai Musaev, Atay Dobrynin, Salizhan Kylychbekov, Zakirbek Mamatair Uulu
Observer: Ainur Konushbaeva

Latvia (LV)
Leaders: Vjačeslavs Kaščejevs, Paulis Paulins
Students: Luka Ivanovskis, Māris Seržāns, Sergejs Blakunovs, Rūdolfs Treilis, Armands Garančs

Liechtenstein (LI)
Leaders: Fritz Epple, Daniel Oehry
Students: Lukas Lang , David Hälg

Lithuania (LT)
Leaders: Pavelas Bogdanovicius, Andrius Stikonas
Students: Vilius Cepaitis, Gintautas Kamuntavicius, Daumantas Kavolis
Vilda Kornelija Markeviciute, Justinas Rumbutis

Macao (MO)
Leaders: Iat Neng Chan, Chon Fai Kam
Students: Chon Man Sou, Chon Lok Lei, Pui Un Tang, Ka Kit Kong, Chi Chong Lam

Macedonia (MK)
Leaders: Stanisha Veljkovikj
Students: Biljana Mitreska, Filip Simeski

Malaysia (MY)
Leaders: Wee Choi Chiang, Wan Mohd Aimran Bin Wan Mohd Kamil
Students: Poh Wai Chang, Yeoh Chin Vern, Man Chee Seng, Koong Zhe Xian,
Muhammad Asyraf Hafizuddin Bin Azahar

Mexico (MX)
Leaders: Raul Arturo Espejel Morales, Victor Manuel Romero Rochin
Students: Jose Alberto De La Paz Espinosa, Jorge Torres Ramos, Leonel Medina Varela,
Eduardo Israel Acosta Reynoso, Siddhartha Emmanuel Morales Guzman
Observer: Eleazar Neri Medina

Moldova (MD)
Leaders: Victor Paginu, Igor Evtodiev
Students: Cristian Zanoci, Nicoleta Colibaba, Ilie Popanu, Dinu Purice, Cristian Telescu

Mongolia (MN)
Leaders: Bat-Ochir Bat-Otgon, Munkhuu Ganbat
Students: Bat-Erdene Bat-Amgalan, Duinkharjav Budmonde, Ulziisaikhan Khishigdelger,
Manlaibaatar Tugsbayasgalan, Zorigoo Garid
Observer: Duger Ulam-Orgikh

Montenegro (ME)
Leaders: Sanja Damjanovic, Tatijana Carapic
Students: Petar Tadic, Miodrag Joksimovic

Netherlands (NL)
Leaders: Arie Mooldijk, Jan Enno Van Der Laan
Students: Tim Baanen, Arthur Christianen, Freddie Hendriks, Jozef Barnabas Houben,
Matthijs Niels Albert Vernooij

Nepal (NP)
Leaders: Deependra Parajuli, Ram Babu Ray
Students: Niranjan Bhujel, Bindesh Tripathi, Pradeep Niroula, Sulav Lal Shrestha, Gaurav Gyawali

Nigeria (NG)
Leaders: Lewis Obagboye, Yaman Ayhan
Students: John Nwankwo Chijioke, Ayomide Andrae Bamidele, Musa Muhammad Damina, Joseph Rotdirnen Chikak, Ikechukwu Anthony Okonkwo
Visitors: Okike Okorie, Mohammed Jazuli Musa, Aisha Mohammed Jazuli

Norway (NO)
Leaders: Torbjørn Mehl, Øyvind Tordar Guldahl
Students: Gjert Magne Knutsen, Carl Andreas Julsvoll, Arnoldas Seputis, Tobias Valentin Rye Torben, Åsmund Hausken Sande

Pakistan (PK)
Leaders: Muhammad Aftab Rafiq, Shahid Qamar
Students: Uzair Akbar, Muhammad Umair Qazi, Muhammad Irfan Kaleem, Muhammad Saad Qureshi, Zulfiqar Haider Zaidi

Peru (PE)
Leader: Hugo Luyo Sánchez

Poland (PL)
Leaders: Jan Mostowski, Jacek Jasiak
Students: Jakub Supel, Kacper Oreszczuk, Adam Krasuski, Jakub Mrożek, Kamil Kaczmarek

Portugal (PT)
Leaders: Fernando Manuel Da Silva Nogueira, Rui Davide Martins Travasso
Students: Rita Barrocas Dias Teixeira Da Costa, Tomás M- De Oliveira De Albuquerque Reis, Carlos M. Cardoso Garrido, Filipe M.A. De Matos, Carlos Diogo Monteiro Fernandes
Observer: Maria Teresa De Matos Paiva

Puerto Rico (PR)
Leader: Hector Jesus Jimenez
Students: Logan Brendan Abel

Romania (RO)
Leaders: Delia Constanta Davidescu, Adrian Dafinei
Students: Dan-Cristian Andronic, Tudor Ciobanu, Denis Turcu, Cristian-Alexandru Frunza, Sebastian Florin Dumitru

Russian Federation (RU)
Leaders: Stanislav Kozel, Valery Slobodyanin
Students: Mikhail Kurenkov, Ilya Fradkin, Ivan Maslov, Daniil Kalinov, Maksim Velikanov
Observers: Mikhail Osin, Maksim Karmanov, Vitaly Shevchenko

Saudi Arabia (SA)
Leaders: Najm Misfer Alhosiny, Jaan Kalda
Students: Mohammad Alhejji, Ibrahim Alnami, Ali Alhulaymi, Abdulmohsen Alowayed, Fysal Alkhayyal
Observers: Abdulaziz Salem Alharthi, Talal Alrashidi

Serbia (RS)
Leaders: Aleksandar Krmpot, Nenad Vukmirović
Students: Milan Krstajić, Ilija Burić, Luka Bojović, Uroš Ristivojević, Ivan Tanasijević

Singapore (SG)
Leaders: Rawat Rajdeep Singh, Lim Kim Yong
Students: Sean S. X. En, Lim Jeck, Tan W.L. Byorn, Daniel M. K. Kay, Ashwin Venkidachalam
Observers: Kwek Wei Hong, Tao Ye, Bobba V. Rao Chowdari, Feng Yuan Ping, Lim Yeow Heng
Visitors: Bobba Rajyalashmi, Huang Zhilan, Xu Shuyan

Slovakia (SK)
Leaders: Ivo Čáp, Ľubomír Mucha
Students: Patrik Turzak, Ján Ondráš, Tomáš Gonda, Jakub Kvorka, Ladislav Ürge
Observer: Ľubomír Konrád. **Visitor:** Klára Čápová

Slovenia (SI)
Leaders: Jurij Bajc, Barbara Rovšek
Students: Michel Adamič, Bine Brank, Žan Kokalj, Žiga Krajnik, Žiga Nosan

South Africa (ZA)
Leaders: Mervlyn Moodley, Jagathesan Govender
Students: Shailin Govender, Lloyd Mahadeo, Carrie-Anne Rubidge, Shihal Munesher Sapry, Ehsaan Rajak

Spain (ES)
Leaders: Juan Jose Leon Garcia, Jose Francisco Romero Garcia
Students: Marc Santigosa I Pinilla, Angel Jesus Murcia Gil, Pablo Gomez Perez, Raul Gonzalez Molina, Francisco Javier Gonzalez Rodriguez
Observer: Maria Matilde Ariza Montes

Sri Lanka (LK)
Leaders: Sellappulige Rexy Denzil Rosa, Geetha Rathnamalee Rosa
Students: Jayan Chathuranga Vidanapathirana, Thelasingha H.M.N. Chandrajith Thelasingha, Herath Mudiyanselage K. Sananthana Herath, Ranasinghe M.N.I. Herath Ranasinghe, Edirisooriya Arachchi A.N. Eranga Edirisooriya

Suriname (SR)
Leader: Tjien Bing Tan
Students: Santosh B. Gangaram-Panday, Raynesh A.V. Kanhai

Sweden (SE)
Leaders: Bo Söderberg, Max Kesselberg
Students: Emil Ejbyfeldt, Mattias Ekre, Henrik Gingsjö, Andréas Sundström
Observer: Christian Karlsson

Switzerland (CH)
Leaders: Lionel Philippoz, Markus Meier
Students: William Borgeaud, Sven Pfeiffer, Alain Rossier, Quentin Wenger, Rafael Winkler
Observer: Richard Heimgartner. **Visitor:** Ingeborg Meier-Kälin

Syrian Arab Republic (SY)
Leaders: Emad Alazeb, Akil Salloum
Students: Osama Yaghi, Ghadeer Shaaban, Hasan Khalil, Anas Hlal, Mohamed Alrazzouk
Observer: Farkad Alramadani. **Visitors:** Reem Kouaider, Yara Alazab, Mouafak Alazab

Taiwan (TW)
Leaders: Chih-Ta Chia, Shang-Fang Tsai
Students: Yu-Kai Lo, Zong-You Luo, Ching-Chung Hsueh, Chuan-I Yen, Wen-Yu Chang
Observer: Hao-Chi Wang, Jiun-Huei Wu, Chia-Hung Chang, Chung-Yu Mou, Chon Saar Chu

Tajikistan (TJ)
Leaders: Ilkhom Khotami, Zokir Abdurakhmanov
Students: Adhamzhon Shukurov, Safarkhon Sayhomid, Shakhzodi Rustamdzhon, Isfandiyor Safarov, Ismoil Odinaev
Observer: Ilkhom Khotamov

Thailand (TH)
Leaders: Sujint Wangsuya, Ratchapak Chitaree
Students: Kann Ruaytae, Kittipatr Poopong, Peerasak Sae-Ung, Phurint Siripanthong, Sorawitch Wathanapenpaiboon
Observers: Sutthida Boontawee, Suwan Kusamran

Turkey (TR)
Leaders: Ibrahim Gunal, Inanc Kanik
Students: Atinc Cagan Sengul, Ekin Akyurek, Huseyin Anil Gunduz, Bilal Cark, Fatih S. Saglam
Observer: Melih Gunes

Turkmenistan (TM)
Leaders: Halit Coşkun, Gylychmammet Orazov
Students: Dovran Amanov, Dovrangeldi Jumageldiyev, Nazar Ilamanov, Omargeldi Atanov, Dayanch Yazberdiyev

Ukraine (UA)
Leaders: Borys Kreminskyi, Igor Anisimov
Students: Oleksii Lubynets, Igor Sholom, Volodymyr Biloshytskyi, Artem Oliinyk, Taras Antoshchuk
Observer: Olga Robak

United Kingdom (GB)
Leaders: Robin William Minto Hughes, Adam John Patchett
Students: Daniel Y. Hu, George T. Fortune, Elango Madhivanan, Yuting Li, Matei F. Mandache
Observer: Anson Chee Hann Cheung

United States of America (US)
Leaders: Paul Elliott Stanley, Marianna Yuling Mao
Students: Jeffrey Cai, Calvin Lin Huang, Jeffrey Yan, Samuel Zbarsky, Kevin Zhou

Vietnam (VN)
Leaders: Nguyen The Khoi, Luc Huy Hoang
Students: Bui Quang Tu, Ngo Phi Long, Le Duy Anh, My Duy Hoang Long, Tran Thi Thu Huong
Observers: Bui Thu Ha, Tran La Giang, Kim Ngoc Chinh, Nguyen Cong Toan, Pham Van Dai
Visitors: Trinh Tho Truong, Nguyen Van Huyen, Cam Thinh

IPhO 2013 organizers

Steering committee

Niels Hartling   Henrik Bruus   Christian Thune Jacobsen   Jens Paaske

Organizing committee

Niels Hartling	Dorte Glass	Marianne Hartling
Henrik Bruus	Niels Østergård	Lisbeth Kronborg Jensen
Christian Thune Jacobsen	Michael Clasen Jacobsen	Freja Elbro
Jens Paaske	Michael Brix Pedersen	

Academic committee, theory

Henrik Bruus	Andrei Lavrinenko	Henning Haack
Niels Hartling	Andrei Andryieuski	Irvin Silberling Svensson
Jens Paaske	Erik Both	Christine Schøtt Hvidberg
Michael Brix Pedersen	Michael Hallundbæk	

Academic committee, experiment

Christian Thune Jacobsen	Christian Petresch	Malte Olsen
Ole Trinhammer	Niels Erik Wegge	Mogens Stibius Jensen
Jens Ulrik Lefmann	Jakob Gade Kofoed	Miroslava Smrcinova
Niels Christian Jensen	Nicholas Gauguin	Erik Hansen

IT committee

Niels Østergård   Michael Clasen Jacobsen   Joakim C. Allerup

PR committee

Turi Schäffer   Miriam Ortwed   Ellen Valentin Christensen

Support and assistants

Torben Christoffersen	Gitte Andresen	Marianne Tranberg Pii
Louise Kjær	Oliver Balco	Mette Agertoft
Hanne Busk	Rene Hansen	Bruno Padborg
Andreas Kallesøe	Hans Peter Ærstrøm	Jesper Toft Rasmussen
Christian Emil Bech	Irene Kongstad	Kirsten Bruus
Jens Paulsen	Mads Wegelby Birkvig	Asmus Blædel Jørgensen
Michael Kjeldsen	Franz Heinemeier	Fabian Thune Jacobsen
Gertie Skaarup	Astrid Degerbøl	

Markers

Adam Mielke
Alexander Bruun Christiansen
Alexander Simon Christensen
Alisa Javadi
Anders Thyssen
Anders Nysteen
Anders Dahl Henriksen
Anders Øhrberg Schreiber
Andrei Andryieuski
Andrei Laurynenka
Cecilie Drost Aakjær
Chengjun Jin
Christian Berrig
Christian Laut Ebbesen
Christoffer Østfeldt
Christoffer Peder Nielsen
Erik J. Both
Erikas Gaidamauskas
Filip Anselm Rasmussen
Finn Berg Rasmussen
Frank Borum
Frederik Sønderby Nathan
Gediminas Kirsanskas
Hairun Guo
Haiyan Ma
Hajrah Tabassam
Helle Greisen
Henrik Bohr
Hjalte Axel Frellesvig
Hualong Bao
Ivan-Lazar Bundalo
Jacob Gade Koefoed
Jakob Nordheim Riedel
Jakob Rosenkrantz de Lasson
Jens Paaske
Jens-Søren Kjær Andersen
Jeppe Clausen
Jeppe Trøst Nielsen
Jette Oddershede
Jonas Tobias Karlsen
Jørn Dines Hansen
Kasper Astrup Eriksen
Kasper Bayer Frøhling
Kasper Meldgaard Røge
Kim Bertelsen
Louise Dyregaard Nielsen
Mads Søgaard
Maksim Zalkovskij
Malte Olsen
Marta Majkut
Michael Brix Pedersen
Mikkel Settnes
Mikkel W. H. Ley
Mohnish Pandey
Morten Niklas Gjerding
Nicholas G. Houghton-Larsen
Niels Erik Wegge
Niels Theis Bendtsen
Niels-Kristian Kjøller
Nikolaj Kofoed Mandsberg
Nis Korsgaard Andersen
Oleg Lysenko
Paul Jespersgaard
Pengfei Tian
Per Simmendefeldt Schmidt
Peter Barkholt Muller
Peter Friis Østergaard
Petru Tighineanu
Pétur Gordon Hermannsson
Qiao Gu
Rasmus Dybbro Engelsholm
Rasmus Schmidt Davidsen
Rijun Huang
Sakse Dalum
Sergei Zhukovsky
Supannee Learkthanakhachon
Søren Raza
Søren Vang Fischer
Thomas Christensen
Tianwu Wang
Tobias Sommer Thune
Ulrik Grønbjerg Vej-Hansen
Vladimir Posvyanskiy
Xiaolong Zhu
Xing Liu
Zohreh Lali Dastjerdi

Behind the scenes

Guides

Coordinators: Lisbeth Kronborg Jensen, Freja Elbro
Assistant coordinators: Anna Olesen, Kristina Rose, Mikkel Bjørn, Kim Ettrup
Guides for the leaders: Alexander Krabbe, Anders Hedegaard Jensen, Anders Schlaikjer, Andreas Kristoffersen, Asbjørn Arvad Jørgensen, Asger Fuhr Høyer, Ditte Marie R. Jensen, Emil Tosti, Lars Lynne Hansen, Mille Lærke Nielsen, Nanna Overby, Nanna Sander, Olfert Holte, Sara Tviis Hansen, Steffen Kjær,
Hostel guides: Anna Frandsen, Jeppe B. Schou Jensen, Nina-Marie Dovmark, Rikke Lilo Thiesson

4-country coordinators

Andreas M. Christiansen (TW, ID, JP, VN)
Bolette B. Jensen (MN, HK, MO, CN)
Cecilie Rasch (FI, EE, LT, LV)
Christoffer Ceutz (KG, TM, UZ, TA)
Daniel Nielsen (SY, SA, PK, IR)
Gertrud Dam-Dalgeir (FR, RO, MD, BE)
Kristine C.-Rotne (BR, CO, SV, PE)
Line Steiness D. Jensen (LI, AT, DE, NL)
Line Worm Christiansen (PL, HU, CZ, SK)
Lisbeth Malinowski (GE, UA, BY, RU)
Mathias Bruhn (EC, BO, SR, PR)
Mikkel Kolding (BG, SI, CH)
Molte Emil Strange Andersen (BA, HR, ME, RS)
Natasha Cosgrave (KW, LK, IN, KR)
Nikolaj Thams (AU, SG, ZA, NG)
Patrik Reppien (MK, ES, PT, IT)
Pernille K. H. Szöcs (KZ, AM, TR, AZ)
Rasmus Emig (IL, GB, CY, GR)
Simone Wehnert (IS, NO, DK, SE)
Stine Elnegaard (BD, CU, TH, MY)
Susanne Riis (CA, US, MX, NP)

Single-country guides

Alexander Sandahl (TM)
Ali Mohebbi (IR)
Anders B. Marstrand (SE)
Anders Aamand (CN)
Andreas Junker-Holst (RO)
Anette Ester Andersen (KW)
Ann Sophie Høg (BE)
Anna Leth-Espensen (NP)
Anne Sofie Munk (US)
Asger Sørensen (SY)
Aya Hjortshøj Lindgren (ME)
Birthe Wohlenberg (HR)
Bo S. Schmidt (DE)
Camilla Marie Jensen (NL)
Camilla Nygaard (MK)
Carita H.-Knudsen (IS)
Charlotte H. Frausing (PT)
Christian Brams (GB)
Christian W. Nygaard (AT)
Christina Hansen (NG)
Christine Johnsen (CA)
Daniel Juhász Vigild (HU)
Dennis Hansen (MO)
Emilia Wodzka (RU)
Emilie Knudsen Brun (PE)
Filip Dahl Olsen (CU)
Frederik Ceutz (BD)
Gro Dyrting (NO)
Guillermo S. Briega (IT)
Henriette Aa. Petersen (FI)
Henrik Teglborg (KR)
Isabel J. A. Becker (SR)
Jakob Thorsbro (BY)
Joakim Schack (CY)
Johan Byrgesen (DK)
Jorge Peiro (ES)
Karen Marie Arentoft (KZ)
Kasper Tolborg (AZ)
Katja Fliedner Gantriis (TW)
Katrine S.Haaning (LI)
Katrine Tolvang (KG)
Kirsten B. Kjærgård (AM)
Kristian L. Jensen (SA)
Kristina Linde (BA)
Lars Lindberg (MD)
Line Gammelby Jensen (MN)
Line Ledsgaard Jensen (LT)
Line Pedersen (GR)
Linea Sofie Skov (ID)
Louise Green Pedersen (CH)
Lærke Philipsen (PR)
Majbrit Lyngsøe (LV)
Manuel de N. Peifedo (BR)
Marina Ejlertsen (TH)
Martin Thygesen (EE)
Mathias R. Jensen (CO)
Mathis Isaksen (SG)
Mette Falkesgaard (SK)
Mette L.V. Lauridsen (FR)
Mickey Nielsen (LK)
Mika Lanzky (UZ)
Mikkel M.Madsen (MX)
Nadine B. Sørenen (SI)
Nicolai Frost-Jensen (IN)
Niklas Hjuler (PK)
Niklas Mørch Secher (BG)
Nikolaj Knøsgaard (UA)
Philip Rasmussen (PL)
Randi Juel Olsen (BO)
Raul Zarecki (RS)
Richard Vinding Krus (GE)
Rikke Dag Randløv (TJ)
Rikke Langhede (HK)
Sebastian Reinert (SV)
Servet Coskun (TR)
Sidsel Sørensen (AU)
Signe S.Jakobsen (MY)
Solvej Knudsen (JP)
Stefan M. Rathmann (ZA)
Stine Louise Antons (CZ)
Thomas Lunde Hygum (VN)
Thomas R. L. Nielsen (EC)
Tommas Munkholm (IL)

Program
(http://www.ipho2013.dk/ipho2013-program.htm)

Date	Leaders and Observers	Students
Sunday 7 July	Arrival and registration	Arrival and registration
Monday 8 July	Official opening ceremony, discussion and translation of theoretical problems	Official opening ceremony, Excursion to Dyrehaven [fun and games], Dinner at the amusement park Bakken.
Tuesday 9 July	Tour at Niels Bohr Institute (NBI), walk in Copenhagen, Canal Tour, and visit at Carlsberg	Theoretical examination. Tour at Niels Bohr Institute (NBI) and H.C. Ørsted Institute (including entertainment lectures)
Wednesday 10 July	Discussion and translation of experimental problems	Free time in Copenhagen, Excursion to Tivoli (Science Talents) - making experiments at the amusements
Thursday 11 July	Excursion to Louisiana and Kronborg, Midterm party at DTU (S-Huset)	Experimental examination. Tour around DTU (Technical University of Denmark) - Science show, history of technology, eco-car, Center for Electron Nanoscopy, radio dead room. Midterm Party at DTU (S-Huset) with live band ("Dødspop patruljen")
Friday 12 July	Excursion to Copenhagen City Hall, free time in Copenhagen	Excursion to Experimentarium, Copenhagen City Hall and Tivoli Friday Rock (artist: Marie Key and Fallulah)
Saturday 13 July	Moderation	Excursion to Roskilde Viking Museum, Roskilde Cathedral and Lejre Museum. Pizza in "Kings Garden".
Sunday 14 July	International Board Meeting, Official closing ceremony, Closing party at DTU (S-Huset)	Free time in Copenhagen and Canal tour. Official closing ceremony. Closing party at DTU (S-Huset)
Monday 15 July	Departure	Departure





Data sheet T

Data sheet: Table of physical parameters

Speed of light in vacuum	$c = 2.998 \times 10^{8}\ \mathrm{m\ s^{-1}}$
Planck's constant over 2π	$\hbar = 1.055 \times 10^{-34}\ \mathrm{J\ s}$
Gravitational constant	$G = 6.67 \times 10^{-11}\ \mathrm{m^3 kg^{-1} s^{-2}}$
Gravitational acceleration	$g = 9.82\ \mathrm{m\ s^{-2}}$
Elementary charge	$e = 1.602 \times 10^{-19}\ \mathrm{C}$
Electric permittivity of vacuum	$\varepsilon_0 = 8.854 \times 10^{-12}\ \mathrm{C^2\ J^{-1}\ m^{-1}}$
Electron mass	$m_e = 9.109 \times 10^{-31}\ \mathrm{kg}$
Avogadro constant	$N_\mathrm{A} = 6.022 \times 10^{23}\ \mathrm{mol^{-1}}$
Boltzmann constant	$k_\mathrm{B} = 1.381 \times 10^{-23}\ \mathrm{J\ K^{-1}}$
Stony meteorite, specific heat	$c_\mathrm{sm} = 1.2 \times 10^{3}\ \mathrm{J\ kg^{-1}K^{-1}}$
Stony meteorite, thermal conductivity	$k_\mathrm{sm} = 2.0\ \mathrm{W\ m^{-1}\ K^{-1}}$
Stony meteorite, density	$\rho_\mathrm{sm} = 3.3 \times 10^{3}\ \mathrm{kg\ m^{-3}}$
Stony meteorite, melting point	$T_\mathrm{sm} = 1.7 \times 10^{3}\ \mathrm{K}$
Stony meteorite, specific melting heat	$L_\mathrm{sm} = 2.6 \times 10^{5}\ \mathrm{J\ kg^{-1}}$
Silver, molar mass	$M_\mathrm{Ag} = 1.079 \times 10^{-1}\ \mathrm{kg\ mol^{-1}}$
Silver, density	$\rho_\mathrm{Ag} = 1.049 \times 10^{4}\ \mathrm{kg\ m^{-3}}$
Silver, specific heat capacity	$c_\mathrm{Ag} = 2.40 \times 10^{2}\ \mathrm{J\ kg^{-1}K^{-1}}$
Water, molar mass	$M_\mathrm{wa} = 1.801 \times 10^{-2}\ \mathrm{kg\ mol^{-1}}$
Water, density	$\rho_\mathrm{wa} = 0.998 \times 10^{3}\ \mathrm{kg\ m^{-3}}$
Water, specific heat capacity	$c_\mathrm{wa} = 4.181 \times 10^{3}\ \mathrm{J\ kg^{-1}K^{-1}}$
Water, heat of vaporization	$L_\mathrm{wa} = 2.260 \times 10^{6}\ \mathrm{J\ kg^{-1}}$
Water, boiling temperature	$T_{100} = 100\ ^\circ\mathrm{C} = 373.15\ \mathrm{K}$
Ice, density of glacier	$\rho_\mathrm{ice} = 0.917 \times 10^{3}\ \mathrm{kg\ m^{-3}}$
Steam, specific heat capacity	$c_\mathrm{st} = 2.080 \times 10^{3}\ \mathrm{J\ kg^{-1}\ K^{-1}}$
Earth, mass of the	$m_\mathrm{E} = 5.97 \times 10^{24}\ \mathrm{kg}$
Earth, radius of the	$R_\mathrm{E} = 6.38 \times 10^{6}\ \mathrm{m}$
Sun, mass of the	$m_\mathrm{S} = 1.99 \times 10^{30}\ \mathrm{kg}$
Sun, radius of the	$R_\mathrm{S} = 6.96 \times 10^{8}\ \mathrm{m}$
Average Sun-Earth distance	$a_\mathrm{E} = 1.50 \times 10^{11}\ \mathrm{m}$

Page 1 of 1

Theoretical problems

(see www.ipho2013.dk/ipho2013-problems.htm)

The Maribo Meteorite T1

Introduction

A meteoroid is a small particle (typically smaller than 1 m) from a comet or an asteroid. A meteoroid that impacts the ground is called a meteorite.

On the night of 17 January 2009 many people near the Baltic Sea saw the glowing trail or fireball of a meteoroid falling through the atmosphere of the Earth. In Sweden a surveillance camera recorded a video of the event, see Fig. 1.1(a). From these pictures and eyewitness accounts it was possible to narrow down the impact area, and six weeks later a meteorite with the mass 0.025 kg was found in the vicinity of the town Maribo in southern Denmark. Measurements on the meteorite, now named Maribo, and its orbit in the sky showed interesting results. Its speed when entering the atmosphere had been exceptionally high. Its age, 4.567×10^9 year, shows that it had been formed shortly after the birth of the solar system. The Maribo meteorite is possibly a part of Comet Encke.

The speed of Maribo

The fireball was moving in westerly direction, heading 285° relative to north, toward the location where the meteorite was subsequently found, as sketched in Fig. 1.1. The meteorite was found at a distance 195 km from the surveillance camera in the direction 230° relative to north.

1.1	Use this and the data in Fig. 1.1 to calculate the average speed of Maribo in the time interval between frames 155 and 161. The curvature of the Earth and the gravitational force on the meteoroid can both be neglected.	1.3

Through the atmosphere and melting?

The friction from the air on a meteoroid moving in the higher atmosphere depends in a complicated way on the shape and velocity of the meteoroid, and on the temperature and density of the atmosphere. As a reasonable approximation the friction force F in the upper atmosphere is given by the expression $F = k\rho_{atm}Av^2$, where k is a constant, ρ_{atm} the density of the atmosphere, A the projected cross-section area of the meteorite, and v its speed.

The following simplifying assumptions are made to analyze the meteoroid: The object entering the atmosphere was a sphere of mass $m_M = 30$ kg, radius $R_M = 0.13$ m, temperature $T_0 = 200$ K, and speed $v_M = 2.91 \times 10^4$ m/s. The density of the atmosphere is constant (its value 40 km above the surface of the Earth), $\rho_{atm} = 4.1 \times 10^{-3}$ kg/m^3, and the friction coefficient is $k = 0.60$.

1.2a	Estimate how long time after entering the atmosphere it takes the meteoroid to have its speed reduced by 10 % from v_M to $0.90\ v_M$. You can neglect the gravitational force on the meteoroid and assume, that it maintains its mass and shape.	0.7
1.2b	Calculate how many times larger the kinetic energy E_{kin} of the meteoroid entering the atmosphere is than the energy E_{melt} necessary for melting it completely (see data sheet).	0.3

The Maribo Meteorite T1

(a)

(b)

Frame	Time	Azimuth	Altitude
155	1.46 s	215°	19.2°
161	2.28 s	221°	14.7°
Landing at M		230°	0.0°

(c)

Figure 1.1 (a) Azimuth is the clockwise angular position from north in the horizontal plane, and altitude is the angular position above the horizon. A series of frames recorded by the surveillance camera in Sweden, showing the motion of Maribo as a fireball on its way down through the atmosphere. **(b)** The data from two frames indicating the time, the direction (azimuth) in degrees, as seen by the camera (C), and the height above the horizon (altitude) in degrees. **(c)** Sketch of the directions of the path (magenta arrow) of Maribo relative to north (N) and of the landing site (M) in Denmark as seen by the camera (C).

Heating of Maribo during its fall in the atmosphere

When the stony meteoroid Maribo entered the atmosphere at supersonic speed it appeared as a fire-ball because the surrounding air was glowing. Nevertheless, only the outermost layer of Maribo was heated. Assume that Maribo is a homogenous sphere with density ρ_{sm}, specific heat capacity c_{sm}, and thermal conductivity k_{sm} (for values see the data sheet). Furthermore, when entering the atmosphere, it had the temperature $T_0 = 200$ K. While falling through the atmosphere its surface temperature was constant $T_{\mathrm{s}} = 1000$ K due to the air friction, thus gradually heating up the interior.

The Maribo Meteorite T1

After falling a time t in the atmosphere, an outer shell of Maribo of thickness x will have been heated to a temperature significantly larger than T_0. This thickness can be estimated by dimensional analysis as the simple product of powers of the thermodynamic parameters: $x \approx t^{\alpha} \rho_{\mathrm{sm}}^{\beta} c_{\mathrm{sm}}^{\gamma} k_{\mathrm{sm}}^{\delta}$.

1.3a	Determine by dimensional (unit) analysis the value of the four powers α, β, γ, and δ.	0.6
1.3b	Calculate the thickness x after a fall time $t = 5$ s, and determine the ratio x/R_{M}.	0.4

The age of a meteorite

The chemical properties of radioactive elements may be different, so during the crystallization of the minerals in a given meteorite, some minerals will have a high content of a specific radioactive element and others a low content. This difference can be used to determine the age of a meteorite by radiometric dating of its radioactive minerals.

As a specific example, we study the isotope ^{87}Rb (element no. 37), which decays into the stable isotope ^{87}Sr (element no. 38) with a half-life of $T_{½} = 4.9 \times 10^{10}$ year, relative to the stable isotope ^{86}Sr. At the time of crystallization the ratio ^{87}Sr/^{86}Sr was identical for all minerals, while the ratio ^{87}Rb/^{86}Sr was different. As time passes on, the amount of ^{87}Rb decreases by decay, while consequently the amount of ^{87}Sr increases. As a result, the ratio ^{87}Sr/^{86}Sr will be different today. In Fig. 1.2(a), the points on the horizontal line refer to the ratio ^{87}Rb/^{86}Sr in different minerals at the time, when they are crystallized.

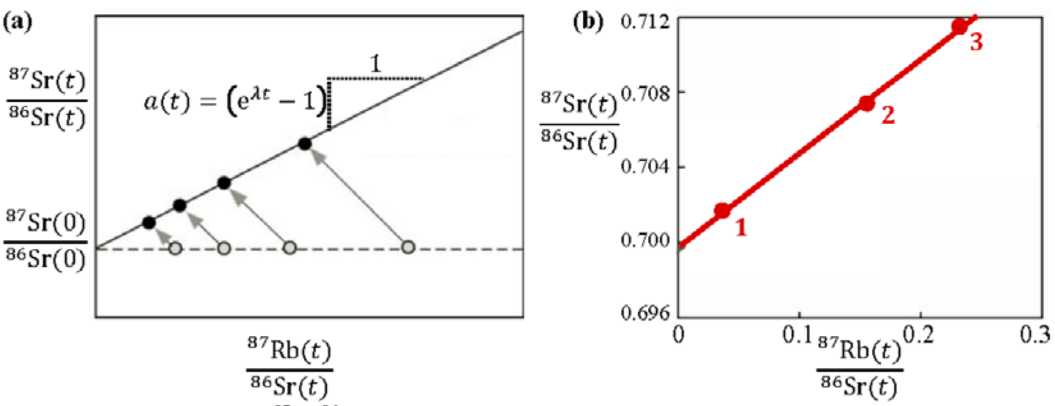

Figure 1.2 **(a)** The ratio ^{87}Sr/^{86}Sr in different minerals at the time $t = 0$ of crystallization (open circles) and at present time (filled circles). **(b)** The isochron-line for three different mineral samples taken from a meteorite at present time.

1.4a	Write down the decay scheme for the transformation of $^{87}_{37}$Rb to $^{87}_{38}$Sr.	0.3
1.4b	Show that the present-time ratio ^{87}Sr/^{86}Sr plotted versus the present-time ratio ^{87}Rb/^{86}Sr in different mineral samples from the same meteorite forms a straight line, the so-called isochron-line, with slope $a(t) = \left(e^{\lambda t} - 1\right)$. Here t is the time since the formation of the minerals, while λ is the decay constant inversely proportional to half-life $T_{½}$.	0.7
1.4c	Determine the age τ_{M} of the meteorite using the isochron-line of Fig. 1.2(b).	0.4

The Maribo Meteorite T1

Comet Encke, from which Maribo may originate

In its orbit around the Sun, the minimum and maximum distances between comet Encke and the Sun are $a_{\min} = 4.95 \times 10^{10}$ m and $a_{\max} = 6.16 \times 10^{11}$ m, respectively.

1.5	Calculate the orbital period t_{Encke} of comet Encke.	0.6

Consequences of an asteroid impact on Earth

65 million years ago Earth was hit by a huge asteroid with density $\rho_{\text{ast}} = 3.0 \times 10^3$ kg m^{-3}, radius $R_{\text{ast}} = 5.0$ km, and final speed of $v_{\text{ast}} = 2.5 \times 10^4$ m/s. This impact resulted in the extermination of most of the life on Earth and the formation of the enormous Chicxulub Crater. Assume that an identical asteroid would hit Earth today in a completely inelastic collision, and use the fact that the moment of inertia of Earth is 0.83 times that for a homogeneous sphere of the same mass and radius. The moment of inertia of a homogeneous sphere with mass M and radius R is $\frac{2}{5}MR^2$. Neglect any changes in the orbit of the Earth.

1.6a	Let the asteroid hit the North Pole. Find the maximum change in angular orientation of the axis of Earth after the impact.	0.7
1.6b	Let the asteroid hit the Equator in a radial impact. Find the change $\Delta\tau_{\text{vrt}}$ in the duration of one revolution of Earth after the impact.	0.7
1.6c	Let the asteroid hit the Equator in a tangential impact in the equatorial plane. Find the change $\Delta\tau_{\text{tan}}$ in the duration of one revolution of Earth after the impact.	0.7

Maximum impact speed

Consider a celestial body, gravitationally bound in the solar system, which impacts the surface of Earth with a speed v_{imp}. Initially the effect of the gravitational field of the Earth on the body can be neglected. Disregard the friction in the atmosphere, the effect of other celestial bodies, and the rotation of the Earth.

1.7	Calculate $v_{\text{imp}}^{\max}$, the largest possible value of v_{imp}.	1.6

Plasmonic Steam Generator T2

Introduction

In this problem we study an efficient process of steam production that has been demonstrated to work experimentally. An aqueous solution of spherical nanometer-sized silver spheres (nanoparticles) with only about 10^{13} particles per liter is illuminated by a focused light beam. A fraction of the light is absorbed by the nanoparticles, which are heated up and generate steam locally around them without heating up the entire water solution. The steam is released from the system in the form of escaping steam bubbles. Not all details of the process are well understood at present, but the core process is known to be absorption of light through the so-called collective electron oscillations of the metallic nanoparticles. The device is known as a plasmonic steam generator.

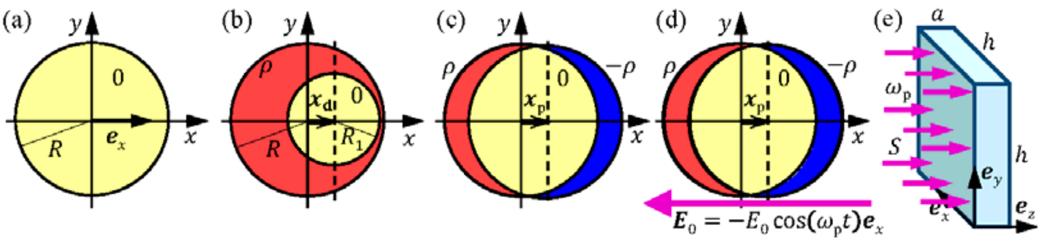

Figure 2.1 (a) A spherical charge-neutral nanoparticle of radius R placed at the center of the coordinate system. **(b)** A sphere with a positive homogeneous charge density ρ (red), and containing a smaller spherical charge-neutral region (0, yellow) of radius R_1, with its center displaced by $\boldsymbol{x}_\mathrm{d} = x_\mathrm{d}\, \boldsymbol{e}_x$. **(c)** The sphere with positive charge density ρ of the nanoparticle silver ions is fixed in the center of the coordinate system. The center of the spherical region with negative spherical charge density $-\rho$ (blue) of the electron cloud is displaced by $\boldsymbol{x}_\mathrm{p}$, where $x_\mathrm{p} \ll R$. **(d)** An external homogeneous electric field $\boldsymbol{E}_0 = -E_0 \boldsymbol{e}_x$. For time-dependent $\boldsymbol{E}_0$, the electron cloud moves with velocity $\boldsymbol{v} = \mathrm{d}\boldsymbol{x}_\mathrm{p}/\mathrm{d}t$. **(e)** The rectangular vessel $(h \times h \times a)$ containing the aqueous solution of nanoparticles illuminated by monochromatic light propagating along the z-axis with angular frequency ω_p and intensity S.

A single spherical silver nanoparticle

Throughout this problem we consider a spherical silver nanoparticle of radius $R = 10{,}0$ nm and with its center fixed at the origin of the coordinate system, see Fig. 2.1(a). All motions, forces and driving fields are parallel to the horizontal x-axis (with unit vector $\boldsymbol{e}_x$). The nanoparticle contains free (conduction) electrons moving within the whole nanoparticle volume without being bound to any silver atom. Each silver atom is a positive ion that has donated one such free electron.

2.1	Find the following quantities: The volume V and mass M of the nanoparticle, the number N and charge density ρ of silver ions in the particle, and for the free electrons their concentration n, their total charge Q, and their total mass m_0.	0.7

Plasmonic Steam Generator T2

The electric field in a charge-neutral region inside a charged sphere

For the rest of the problem assume that the relative dielectric permittivity of all materials is $\varepsilon = 1$. Inside a charged sphere of homogeneous charge density ρ and radius R is created a small spherical charge-neutral region of radius R_1 by adding the opposite charge density $-\rho$, with its center displaced by $\boldsymbol{x}_\mathrm{d} = x_\mathrm{d}\,\boldsymbol{e}_x$ from the center of the R-sphere, see Fig. 2.1(b).

2.2	Show that the electric field inside the charge-neutral region is homogenous of the form $\boldsymbol{E} = A\,(\rho/\varepsilon_0)\,\boldsymbol{x}_\mathrm{d}$, and determine the pre-factor A.	1.2

The restoring force on the displaced electron cloud

In the following, we study the collective motion of the free electrons, and therefore model them as a single negatively charged sphere of homogeneous charge density $-\rho$ with a center position $\boldsymbol{x}_\mathrm{p}$, which can move along the x-axis relative to the center of the positively charged sphere (silver ions) fixed at the origin of the coordinate system, see Fig. 2.1(c). Assume that an external force $\boldsymbol{F}_\mathrm{ext}$ displaces the electron cloud to a new equilibrium position $\boldsymbol{x}_\mathrm{p} = x_\mathrm{p}\,\boldsymbol{e}_x$ with $|x_\mathrm{p}| \ll R$. Except for tiny net charges at opposite ends of the nanoparticle, most of its interior remains charge-neutral.

2.3	Express in terms of $\boldsymbol{x}_\mathrm{p}$ and n the following two quantities: The restoring force $\boldsymbol{F}$ exerted on the electron cloud and the work W_el done on the electron cloud during displacement.	1.0

The spherical silver nanoparticle in an external constant electric field

A nanoparticle is placed in vacuum and influenced by an external force $\boldsymbol{F}_\mathrm{ext}$ due to an applied static homogeneous electric field $\boldsymbol{E}_0 = -E_0\boldsymbol{e}_x$, which displaces the electron cloud the small distance $|x_\mathrm{p}|$, where $|x_\mathrm{p}| \ll R$.

2.4	Find the displacement x_p of the electron cloud in terms of E_0 and n, and determine the amount $-\Delta Q$ of electron charge displaced through the yz-plane at the center of the nanoparticle in terms of n, R and $\mathrm{x_p}$.	0.6

The equivalent capacitance and inductance of the silver nanoparticle

For both a constant and a time-dependent field $\boldsymbol{E}_0$, the nanoparticle can be modeled as an equivalent electric circuit. The equivalent capacitance can be found by relating the work W_el, done on the separation of charges ΔQ, to the energy of a capacitor, carrying charge $\pm\Delta Q$. The charge separation will cause a certain equivalent voltage V_0 across the equivalent capacitor.

2.5a	Express the systems equivalent capacitance C in terms of ε_0 and R, and find its value.	0.7
2.5b	For this capacitance, determine in terms of E_0 and R the equivalent voltage V_0 that should be connected to the equivalent capacitor in order to accumulate the charge ΔQ.	0.4

Plasmonic Steam Generator T2

For a time-dependent field $\boldsymbol{E}_0$, the electron cloud moves with velocity $\boldsymbol{v} = v\,\boldsymbol{e}_x$, Fig. 2.1(d). It has the kinetic energy W_{kin} and forms an electric current I flowing through the fixed yz-plane. The kinetic energy of the electron cloud can be attributed to the energy of an equivalent inductor of inductance L carrying the current I.

2.6a	Express both W_{kin} and I in terms of the velocity v.	0.7
2.6b	Express the equivalent inductance L in terms of particle radius R, the electron charge e and mass m_e, the electron concentration n, and calculate its value.	0.5

The plasmon resonance of the silver nanoparticle

From the above analysis it follows that the motion, arising from displacing the electron cloud from its equilibrium position and then releasing it, can be modeled by an ideal LC-circuit oscillating at resonance. This dynamical mode of the electron cloud is known as the plasmon resonance, which oscillates at the so-called angular plasmon frequency ω_{p}.

2.7a	Find an expression for the angular plasmon frequency ω_{p} of the electron cloud in terms of the electron charge e and mass m_e, the electron density n, and the permittivity ε_0.	0.5
2.7b	Calculate ω_{p} in rad/s and the wavelength λ_{p} in nm of light in vacuum having angular frequency $\omega = \omega_{\mathrm{p}}$.	0.4

The silver nanoparticle illuminated with light at the plasmon frequency

In the rest of the problem, the nanoparticle is illuminated by monochromatic light at the angular plasmon frequency ω_{p} with the incident intensity $S = \frac{1}{2}c\varepsilon_0 E_0^2 = 1.00\ \mathrm{MW\ m^{-2}}$. As the wavelength is large, $\lambda_{\mathrm{p}} \gg R$, the nanoparticle can be considered as being placed in a homogeneous harmonically oscillating field $\boldsymbol{E}_0 = -E_0\cos(\omega_{\mathrm{p}}t)\,\boldsymbol{e}_x$. Driven by $\boldsymbol{E}_0$, the center $\boldsymbol{x}_{\mathrm{p}}(t)$ of the electron cloud oscillates at the same frequency with velocity $\boldsymbol{v} = \mathrm{d}\boldsymbol{x}_{\mathrm{p}}/\mathrm{d}t$ and constant amplitude x_0. This oscillating electron motion leads to absorption of light. The energy captured by the particle is either converted into Joule heating inside the particle or re-emitted by the particle as scattered light.

Joule heating is caused by random inelastic collisions, where any given free electron once in a while hits a silver ion and loses its total kinetic energy, which is converted into vibrations of the silver ions (heat). The average time between the collisions is $\tau \gg 1/\omega_{\mathrm{p}}$, where for silver nanoparticle we use $\tau = 5.24 \times 10^{-15}$ s.

2.8a	Find an expression for the time-averaged Joule heating power P_{heat} in the nanoparticle as well as the time-averaged current squared $\langle I^2 \rangle$, which includes explicitly the time-averaged velocity squared $\langle v^2 \rangle$ of the electron cloud.	1.0
2.8b	Find an expression for the equivalent ohmic resistance R_{heat} in an equivalent resistor-model of the nanoparticle having the Joule heating power P_{heat} due to the electron cloud current I. Calculate the numerical value of R_{heat}.	1.0

Plasmonic Steam Generator T2

The incident light beam loses some time-averaged power P_{scat} by scattering on the oscillating electron cloud (re-emission). P_{scat} depends on the scattering source amplitude x_0, charge Q, angular frequency ω_{p} and properties of the light (the speed of light c and permittivity ε_0 in vacuum). In terms of these four variables, P_{scat} is given by $P_{\text{scat}} = \frac{Q^2 x_0^2 {\omega_{\text{p}}}^4}{12\pi\varepsilon_0 c^3}$.

2.9	By use of P_{scat}, find an expression of the equivalent scattering resistance R_{scat} (in analogy with R_{heat}) in an equivalent resistor-model, and calculate its value.	1.0

The above equivalent circuit elements are combined into an *LCR* series circuit model of the silver nanoparticle, which is driven by a harmonically oscillating equivalent voltage $V = V_0 \cos(\omega_{\text{p}} t)$ determined by the electric field E_0 of the incident light.

2.10a	Derive expressions for the time-averaged power losses P_{heat} and P_{scat} involving the amplitude E_0 of the electric field in the incident light at the plasmon resonance $\omega = \omega_p$.	1.2
2.10b	Calculate the numerical value of E_0, P_{heat}, and P_{scat}.	0.3

Steam generation by light

An aqueous solution of silver nanoparticles is prepared with a concentration $n_{\text{np}} = 7.3 \times 10^{15}\ \text{m}^{-3}$. It is placed inside a rectangular transparent vessel of size $h \times h \times a = 10 \times 10 \times 1.0\ \text{cm}^3$ and illuminated by light at the plasmon frequency with the same intensity $S = 1.00\ \text{MW m}^{-2}$ at normal incidence as above, see Fig. 2.1(e). The temperature of the water is $T_{\text{wa}} = 20\ °\text{C}$ and we assume, in fair agreement with observations, that in steady state all Joule heating of the nanoparticle goes to the production of steam of temperature $T_{\text{st}} = 110\ °\text{C}$, without raising the temperature of the water.

The thermodynamic efficiency η of the plasmonic steam generator is defined by the power ratio $\eta = P_{\text{st}}/P_{\text{tot}}$, where P_{st} is the power going into the production of steam in the entire vessel, while P_{tot} is the total power of the incoming light that enters the vessel.

Most of the time any given nanoparticle is surrounded by steam instead of water, and it can thus be described as being in vacuum.

2.11a	Calculate the total mass per second μ_{st} of steam produced by the plasmonic steam generator during illumination by light at the plasmon frequency and intensity S.	0.6
2.11b	Calculate the numerical value of the thermodynamic efficiency η of the plasmonic steam generator.	0.2

The Greenlandic Ice Sheet T3

Introduction

This problem deals with the physics of the Greenlandic ice sheet, the second largest glacier in the world, Fig. 3.1(a). As an idealization, Greenland is modeled as a rectangular island of width $2L$ and length $5L$ with the ground at sea level and completely covered by incompressible ice (constant density ρ_{ice}), see Fig. 3.1(b). The height profile $H(x)$ of the ice sheet does not depend on the y-coordinate and it increases from zero at the coasts $x = \pm L$ to a maximum height H_{m} along the middle north-south axis (the y-axis), known as the ice divide, see Fig. 3.1(c).

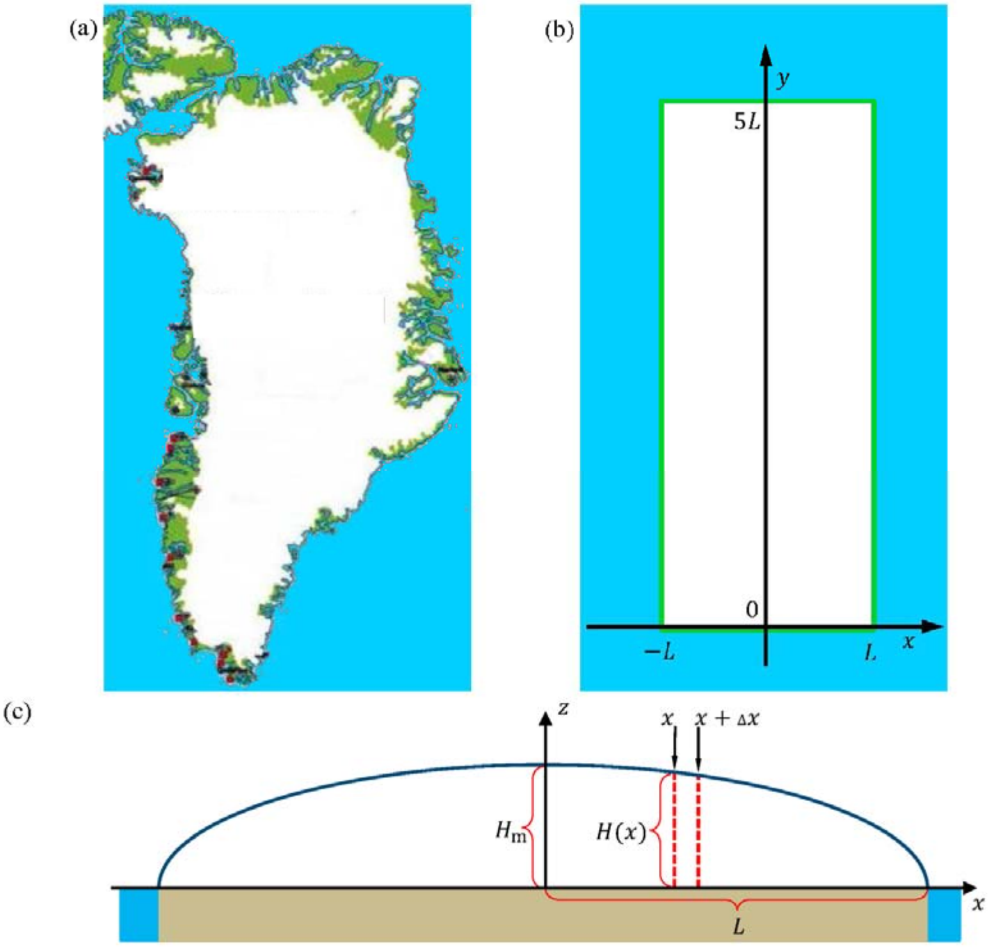

Figure 3.1 (a) A map of Greenland showing the extent of the ice sheet (white), the ice-free, coastal regions (green), and the surrounding ocean (blue). **(b)** The crude model of the Greenlandic ice sheet as covering a rectangular area in the xy-plane with side lengths $2L$ and $5L$. The ice divide, the line of maximum ice sheet height H_{m} runs along the y-axis. **(c)** A vertical cut (xz-plane) through the ice sheet showing the height profile $H(x)$ (blue line). $H(x)$ is independent of the y-coordinate for $0 < y < 5L$, while it drops abruptly to zero at $y = 0$ and $y = 5L$. The z-axis marks the position of the ice divide. For clarity, the vertical dimensions are expanded compared to the horizontal dimensions. The density ρ_{ice} of ice is constant.

The Greenlandic Ice Sheet T3

Two useful formulas

In this problem you can make use of the integral:

$$\int_0^1 \sqrt{1-x}\,\mathrm{d}x = \frac{2}{3}$$

and the approximation $(1+x)^a \approx 1 + ax$, valid for $|ax| \ll 1$.

The height profile of the ice sheet

On short time scales the glacier is an incompressible hydrostatic system with fixed height profile $H(x)$.

3.1	Write down an expression for the pressure $p(x,z)$ inside the ice sheet as a function of vertical height z above the ground and distance x from the ice divide. Neglect the atmospheric pressure.	0.3

Consider a given vertical slab of the ice sheet in equilibrium, covering a small horizontal base area $\Delta x \Delta y$ between x and $x + \Delta x$, see the red dashed lines in Fig. 3.1(c). The size of Δy does not matter. The net horizontal force component ΔF on the two vertical sides of the slab, arising from the difference in height on the center-side versus the coastal-side of the slab, is balanced by a friction force $\Delta F = S_\mathrm{b}\, \Delta x \Delta y$ from the ground on the base area $\Delta x \Delta y$, where $S_\mathrm{b} = 100$ kPa.

3.2a	For a given value of x, show that in the limit $\Delta x \to 0$, $S_\mathrm{b} = kH\, \mathrm{d}H/\mathrm{d}x$, and determine k	0.9
3.2b	Determine an expression for the height profile $H(x)$ in terms of ρ_ice, g, L, S_b and distance x from the divide. The result will show, that the maximum glacier height H_m scales with the half-width L as $H_\mathrm{m} \propto L^{1/2}$.	0.8
3.2c	Determine the exponent γ with which the total volume V_ice of the ice sheet scales with the area A of the rectangular island, $V_\mathrm{ice} \propto A^\gamma$.	0.5

A dynamical ice sheet

On longer time scale, the ice is a viscous incompressible fluid, which by gravity flows from the center part to the coast. In this model, the ice maintains its height profile $H(x)$ in a steady state, where accumulation of ice due to snow fall in the central region is balanced by melting at the coast. In addition to the ice sheet geometry of Fig. 3.1(b) and (c) make the following model assumptions:

1) Ice flows in the xz-plane away from the ice divide (the y-axis).
2) The accumulation rate c (m/year) in the central region is a constant.
3) Ice can only leave the glacier by melting near the coasts at $x = \pm L$.
4) The horizontal (x-)component $v_x(x) = \mathrm{d}x/\mathrm{d}t$ of the ice-flow velocity is independent of z.
5) The vertical (z-)component $v_z(z) = \mathrm{d}z/\mathrm{d}t$ of the ice-flow velocity is independent of x.

Consider only the central region $|x| \ll L$ close to the middle of the ice sheet, where height variations of the ice sheet are very small and can be neglected altogether, i.e. $H(x) \approx H_\mathrm{m}$.

3.3	Use mass conservation to find an expression for the horizontal ice-flow velocity $v_x(x)$ in terms of c, x, and H_m.	0.6

The Greenlandic Ice Sheet T3

From the assumption of incompressibility, i.e. the constant density ρ_{ice} of the ice, it follows that mass conservation implies the following restriction on the ice flow velocity components

$$\frac{dv_x}{dx} + \frac{dv_z}{dz} = 0.$$

3.4	Write down an expression for the z dependence of the vertical component $v_z(z)$ of the ice-flow velocity.	0.6

A small ice particle with the initial surface position (x_i, H_{m}) will, as time passes, flow as part of the ice sheet along a flow trajectory $z(x)$ in the vertical xz-plane.

3.5	Derive an expression for such a flow trajectory $z(x)$.	0.9

Age and climate indicators in the dynamical ice sheet

Based on the ice-flow velocity components $v_x(x)$ and $v_z(z)$, one can estimate the age $\tau(z)$ of the ice in a specific depth $H_{\text{m}} - z$ from the surface of the ice sheet.

3.6	Find an expression for the age $\tau(z)$ of the ice as a function of height z above ground, right at the ice divide $x = 0$.	1.0

An ice core drilled in the interior of the Greenland ice sheet will penetrate through layers of snow from the past, and the ice core can be analyzed to reveal past climate changes. One of the best indicators is the so-called $\delta^{18}\text{O}$, defined as

$$\delta^{18}\text{O} = \frac{R_{\text{ice}} - R_{\text{ref}}}{R_{\text{ref}}} \, 1000 \text{ ‰},$$

where $R = [^{18}\text{O}]/[^{16}\text{O}]$ denotes the relative abundance of the two stable isotopes ^{18}O and ^{16}O of oxygen. The reference R_{ref} is based on the isotopic composition of the oceans around Equator.

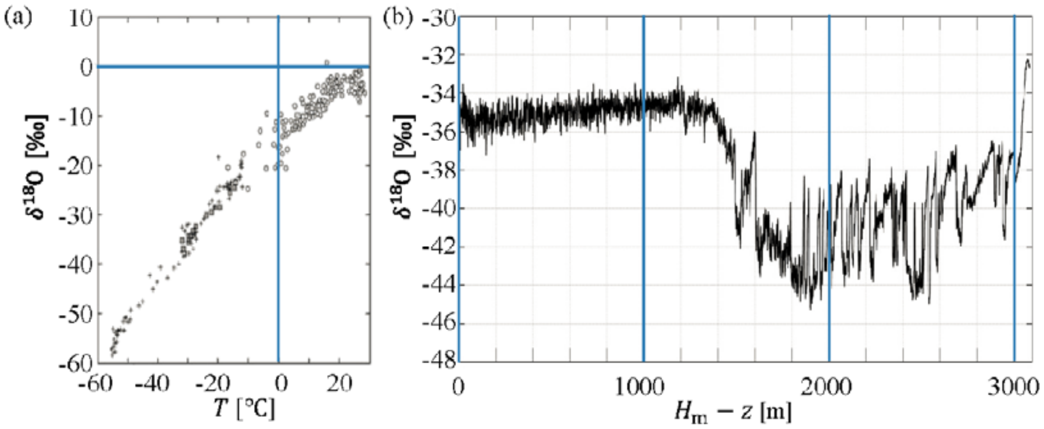

Figure 3.2 (a) Observed relationship between $\delta^{18}\text{O}$ in snow versus the mean annual surface temperature T. **(b)** Measurements of $\delta^{18}\text{O}$ versus depth $H_{\text{m}} - z$ from the surface, taken from an ice core drilled from surface to bedrock at a specific place along the Greenlandic ice divide where $H_{\text{m}} = 3060$ m.

The Greenlandic Ice Sheet T3

Observations from the Greenland ice sheet show that $\delta^{18}\mathrm{O}$ in the snow varies approximately linearly with temperature, Fig. 3.2(a). Assuming that this has always been the case, $\delta^{18}\mathrm{O}$ retrieved from an ice core at depth $H_\mathrm{m} - z$ leads to an estimate of the temperature T near Greenland at the age $\tau(z)$.

Measurements of $\delta^{18}\mathrm{O}$ in a 3060 m long Greenlandic ice core show an abrupt change in $\delta^{18}\mathrm{O}$ at a depth of 1492 m, Fig. 3.2(b), marking the end of the last ice age. The ice age began 120,000 years ago, corresponding to a depth of 3040 m, and the current interglacial age began 11,700 years ago, corresponding to a depth of 1492 m. Assume that these two periods can be described by two different accumulation rates, c_ia (ice age) and c_ig (interglacial age), respectively. You can assume H_m to be constant throughout these 120,000 years.

3.7a	Determine the accumulation rates c_ia and c_ig.	0.8
3.7b	Use the data in Fig. 3.2 to find the temperature change at the transition from the ice age to the interglacial age.	0.2

Sea level rise from melting of the Greenland ice sheet

A complete melting of the Greenlandic ice sheet will cause a sea level rise in the global ocean. As a crude estimate of this sea level rise, one may simply consider a uniform rise throughout a global ocean with constant area $A_\mathrm{O} = 3.61 \times 10^{14}\ \mathrm{m}^2$.

3.8	Calculate the average global sea level rise, which would result from a complete melting of the Greenlandic ice sheet, given its present area of $A_\mathrm{G} = 1.71 \times 10^{12}\mathrm{m}^2$ and $S_\mathrm{b} = 100\ \mathrm{kPa}$.	0.6

The massive Greenland ice sheet exerts a gravitational pull on the surrounding ocean. If the ice sheet melts, this local high tide is lost and the sea level will drop close to Greenland, an effect which partially counteracts the sea level rise calculated above.

To estimate the magnitude of this gravitational pull on the water, the Greenlandic ice sheet is now modeled as a point mass located at the ground level and having the total mass of the Greenlandic ice sheet. Copenhagen lies at a distance of 3500 km along the Earth surface from the center of the point mass. One may consider the Earth, without the point mass, to be spherically symmetric and having a global ocean spread out over the entire surface of the Earth of area $A_\mathrm{E} = 5.10 \times 10^{14}\mathrm{m}^2$. All effects of rotation of the Earth may be neglected.

3.9	Within this model, determine the difference $h_\mathrm{CPH} - h_\mathrm{OPP}$ between sea levels in Copenhagen (h_CPH) and diametrically opposite to Greenland (h_OPP).	1.8

The Maribo Meteorite T1

Solutions

1.1	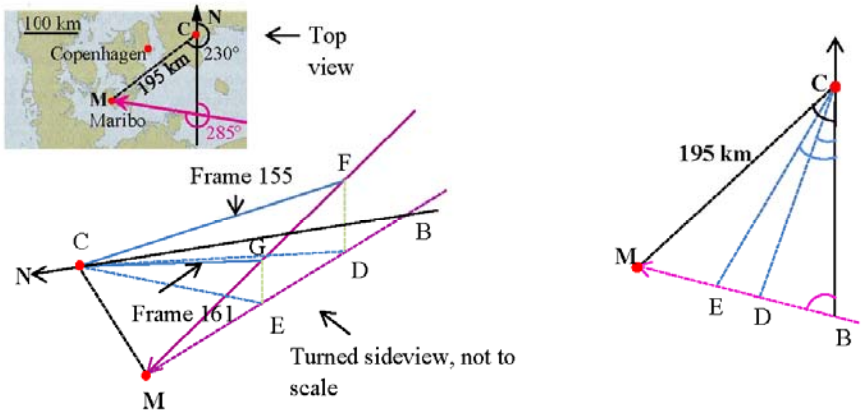 Top view: Triangle MBC: $\lvert CM\rvert = 195$ km, $\angle BCM = 230° - 180° = 50°$, and $\angle MBC = 75°$, so $\angle CMB = 180° - 75° - 50° = 55°$. Then $\lvert CB\rvert = \frac{\lvert CM\rvert \sin(\angle CMB)}{\sin(\angle MBC)} = 165.4$ km. Triangle DBC: $\lvert BC\rvert = 165.4$ km, $\angle BCD = 215° - 180° = 35°$,and $\angle DBC = 75°$, so $\angle CDB = 180° - 75° - 35° = 70°$. Then $\lvert CD\rvert = \frac{\lvert BC\rvert \sin(\angle DBC)}{\sin(\angle CDB)} = 170.0$ km. Triangle EBC: $\lvert BC\rvert = 165.4$ km, $\angle BCE = 221° - 180° = 41°$, and $\angle EBC = 75°$, so $\angle CEB = 180° - 75° - 41° = 64°$. Then $\lvert CE\rvert = \frac{\lvert BC\rvert \sin(\angle EBC)}{\sin(\angle CEB)} = 177.7$ km. Triangle EDC: $\angle DCE = 41° - 35° = 6°$. Horizontal distance traveled by Maribo: $\lvert DE\rvert = \frac{\lvert DC\rvert \sin(\angle DCE)}{\sin(\angle CED)} = 19.77$ km Side view: Triangle CDF: $\lvert DF\rvert = \lvert DC\rvert \tan(\angle FCD) = 59.20$ km Triangle CEG: $\lvert EG\rvert = \lvert CE\rvert \tan(\angle GCE) = 46.62$ km Thus vertical distance travelled by Maribo: $\lvert DF\rvert - \lvert EG\rvert = 12.57$ km. Total distance travelled by Maribo from frame 155 to 161: $\lvert FG\rvert = \sqrt{\lvert DE\rvert^2 + (\lvert DF\rvert - \lvert EG\rvert)^2} = 23.43$ km. The speed of Maribo is $v = \frac{23.43\text{ km}}{2.28\text{ s} - 1.46\text{ s}} = 28.6$ km/s	1.3

1.2a	Newton's second law: $m_M \frac{dv}{dt} = -k\rho_{atm}\pi R_M^2 v^2$ yields $\frac{1}{v^2}dv = -\frac{k\rho_{atm}\pi R_M^2}{m_M}dt$. By integration $t = \frac{m_M}{k\rho_{atm}\pi R_M^2}\left(\frac{1}{0.9} - 1\right)\frac{1}{v_M} = 0.88$ s. Alternative solution: The average force on the meteoroid when the speed decreases from v_M to $0.9\, v_M$ can be estimated to $F_{av} = -k\rho_{atm}\pi R_M^2\,(0.95\, v_M)^2$. Using that the acceleration is approximately constant, $a_{av} = -k\rho_{atm}\pi R_M^2\,(0.95\, v_M)^2/m_M$, results in $t = \frac{-0.1\, v_M}{a_{av}} = 0.87$ s.	0.7

The Maribo Meteorite T1

1.2b	$\frac{E_{\mathrm{kin}}}{E_{\mathrm{melt}}} = \frac{\frac{1}{2}v_{\mathrm{M}}^2}{c_{\mathrm{sm}}(T_{\mathrm{sm}}-T_0)+L_{\mathrm{sm}}} = \frac{4.2\times10^8}{2.1\times10^6} = 2.1\times10^2 \gg 1.$	0.3

1.3a	$[x] = [t]^{\alpha}[\rho_{\mathrm{sm}}]^{\beta}[c_{\mathrm{sm}}]^{\gamma}\,[k_{\mathrm{sm}}]^{\delta} = [\mathrm{s}]^{\alpha}[\mathrm{kg\ m^{-3}}]^{\beta}[\mathrm{m^2\ s^{-2}K^{-1}}]^{\gamma}\,[\mathrm{kg\ m\ s^{-3}K^{-1}}]^{\delta}$, so $[\mathrm{m}] = [\mathrm{kg}]^{\beta+\delta}[\mathrm{m}]^{-3\beta+2\gamma+\delta}[\mathrm{s}]^{\alpha-2\gamma-3\delta}[\mathrm{K}]^{-\gamma-\delta}$. Thus $\beta+\delta=0$, $-3\beta+2\gamma+\delta=1$, $\alpha-2\gamma-3\delta=0$, and $-\gamma-\delta=0$. From which $(\alpha,\beta,\gamma,\delta) = \left(+\frac{1}{2},-\frac{1}{2},-\frac{1}{2},+\frac{1}{2}\right)$ and $x(t)\approx\sqrt{\frac{k_{\mathrm{sm}}t}{\rho_{\mathrm{sm}}c_{\mathrm{sm}}}}$.	0.6
1.3b	$x(5\ \mathrm{s}) = 1.6\ \mathrm{mm}$ $\quad x/R_{\mathrm{M}} = 1.6\ \mathrm{mm}/130\ \mathrm{mm} = 0.012.$	0.4

1.4a	Rb-Sr decay scheme: ${}^{87}_{37}\mathrm{Rb} \to {}^{87}_{38}\mathrm{Sr} + {}^{\ 0}_{-1}\mathrm{e} + \bar{\nu}_{\mathrm{e}}$	0.3
1.4b	$N_{87\mathrm{Rb}}(t) = N_{87\mathrm{Rb}}(0)\mathrm{e}^{-\lambda t}$and Rb→Sr: $N_{87\mathrm{Sr}}(t) = N_{87\mathrm{Sr}}(0) + [N_{87\mathrm{Rb}}(0) - N_{87\mathrm{Rb}}(t)]$. Thus $N_{87\mathrm{Sr}}(t) = N_{87\mathrm{Sr}}(0) + (\mathrm{e}^{\lambda t}-1)N_{87\mathrm{Rb}}(t)$, and dividing by $N_{86\mathrm{Sr}}$ we obtain the equation of a straight line: $\frac{N_{87\mathrm{Sr}}(t)}{N_{86\mathrm{Sr}}} = \frac{N_{87\mathrm{Sr}}(0)}{N_{86\mathrm{Sr}}} + (\mathrm{e}^{\lambda t}-1)\frac{N_{87\mathrm{Rb}}(t)}{N_{86\mathrm{Sr}}}$.	0.7
1.4c	Slope: $\mathrm{e}^{\lambda t}-1 = a = \frac{0.712-0.700}{0.25} = 0.050$ and $T_{½} = \frac{\ln(2)}{\lambda} = 4.9\times10^{10}$ year. So $\tau_{\mathrm{M}} = \ln(1+a)\frac{1}{\lambda} = \frac{\ln(1+a)}{\ln(2)}T_{½} = 3.4\times10^9$ year .	0.4

1.5	Kepler's 3rd law on comet Encke and Earth, with the orbital semi-major axis of Encke given by $a = \frac{1}{2}(a_{\min}+a_{\max})$. Thus $t_{\mathrm{Encke}} = \left(\frac{a}{a_{\mathrm{E}}}\right)^{\frac{3}{2}} t_{\mathrm{E}} = 3.30\ \mathrm{year} = 1.04\times10^8\ \mathrm{s}$.	0.6

1.6a	For Earth around its rotation axis: Angular velocity $\omega_{\mathrm{E}} = \frac{2\pi}{24\,\mathrm{h}} = 7.27\times10^{-5}\ \mathrm{s^{-1}}$. Moment of inertia $I_{\mathrm{E}} = 0.83\frac{2}{5}m_{\mathrm{E}}R_{\mathrm{E}}^2 = 8.07\times10^{37}\ \mathrm{kg\ m^2}$. Angular momentum $L_{\mathrm{E}} = I_{\mathrm{E}}\omega_{\mathrm{E}} = 5.87\times10^{33}\ \mathrm{kg\ m^2s^{-1}}$. Asteroid: $m_{\mathrm{ast}} = \frac{4\pi}{3}R_{\mathrm{ast}}^3\rho_{\mathrm{ast}} = 1.57\times10^{15}$ kg and angular momentum $L_{\mathrm{ast}} = m_{\mathrm{ast}}v_{\mathrm{ast}}R_{\mathrm{E}} = 2.51\times10^{26}\ \mathrm{kg\ m^2s^{-1}}$. L_{ast} is perpendicular to L_{E}, so by conservation angular momentum: $\tan(\Delta\theta) = L_{\mathrm{ast}}/L_{\mathrm{E}} = 4.27\times10^{-8}$.The axis tilt $\Delta\theta = 4.27\times10^{-8}$ rad (so the North Pole moves $R_{\mathrm{E}}\,\Delta\theta = 0.27$ m).	0.7
1.6b	At vertical impact $\Delta L_{\mathrm{E}} = 0$ so $\Delta(I_{\mathrm{E}}\omega_{\mathrm{E}}) = 0$. Thus $\Delta\omega_{\mathrm{E}} = -\omega_{\mathrm{E}}(\Delta I_{\mathrm{E}})/I_{\mathrm{E}}$, and since $\Delta I_{\mathrm{E}}/I_{\mathrm{E}} = m_{\mathrm{ast}}R_{\mathrm{E}}^2/I_{\mathrm{E}} = 7.9\times10^{-10}$ we obtain $\Delta\omega_{\mathrm{E}} = -5.76\times10^{-14}\ \mathrm{s^{-1}}$. The change in rotation period is $\Delta T_{\mathrm{E}} = 2\pi\left(\frac{1}{\omega_{\mathrm{E}}+\Delta\omega_{\mathrm{E}}} - \frac{1}{\omega_{\mathrm{E}}}\right) \approx -2\pi\frac{\Delta\omega_{\mathrm{E}}}{\omega_{\mathrm{E}}^2} = 6.84\times10^{-5}$ s.	0.7
1.6c	At tangential impact L_{ast} is parallel to L_{E} so $L_{\mathrm{E}} + L_{\mathrm{ast}} = (I_{\mathrm{E}} + \Delta I_{\mathrm{E}})(\omega_{\mathrm{E}} + \Delta\omega_{\mathrm{E}})$ and thus $\Delta T_{\mathrm{E}} = 2\pi\left(\frac{1}{\omega_{\mathrm{E}}+\Delta\omega_{\mathrm{E}}} - \frac{1}{\omega_{\mathrm{E}}}\right) = 2\pi\left(\frac{I_{\mathrm{E}}+\Delta I_{\mathrm{E}}}{L_{\mathrm{E}}+L_{\mathrm{ast}}} - \frac{1}{\omega_{\mathrm{E}}}\right) = -3.62\times10^{-3}$ s.	0.7

The Maribo Meteorite T1

1.7	Maximum impact speed $v_{\text{imp}}^{\max}$ arises from three contributions: (I) The velocity v_{b} of the body at distance a_{E} (Earth orbit radius) from the Sun, $v_{\text{b}} = \sqrt{\frac{2Gm_S}{a_E}} = 42.1\ \text{km/s}$. (II) The orbital velocity of the Earth, $v_{\text{E}} = \frac{2\pi a_E}{1\ \text{year}} = 29.8\ \text{km/s}$. (III) Gravitational attraction from the Earth and kinetic energy seen from the Earth: $\frac{1}{2}(v_{\text{b}} + v_{\text{E}})^2 = -\frac{Gm_E}{R_E} + \frac{1}{2}\left(v_{\text{imp}}^{\max}\right)^2$. In conclusion: $v_{\text{imp}}^{\max} = \sqrt{(v_{\text{b}} + v_{\text{E}})^2 + \frac{2Gm_E}{R_E}} = 72.8\ \text{km/s}$.	1.6

	Total	**9.0**

Plasmonic Steam Generator T2

Solutions

A single spherical silver nanoparticle

2.1	Volume of the nanoparticle: $V = \frac{4}{3}\pi R^3 = 4.19 \times 10^{-24}\ \mathrm{m}^3$. Mass of the nanoparticle: $M = V\rho_{\mathrm{Ag}} = 4.39 \times 10^{-20}$ kg . Number of ions in the nanoparticle: $N = N_A \frac{M}{M_{\mathrm{Ag}}} = 2.45 \times 10^5$. Charge density $\rho = \frac{eN}{V} = 9.38 \times 10^9\ \mathrm{C\,m^{-3}}$, charge density $\rho = en$. Electrons' concentration $n = \frac{N}{V} = 5.85 \times 10^{28}\ \mathrm{m}^{-3}$. Total charge of free electrons $Q = eN = 3.93 \times 10^{-14}$ C. Total mass of free electrons $m_0 = m_e N = 2.23 \times 10^{-25}$ kg.	0.7

The electric field in a charge-neutral region inside a charged sphere

2.2	For a sphere with radius R and constant charge density ρ, for any point inside the sphere designated by radius-vector $\mathbf{r} = r\mathbf{e}_r$ $(r < R)$ Gauss's law yields directly $4\pi r^2 \varepsilon_0 \boldsymbol{E}_+ = \frac{4}{3}\pi r^3 \rho\, \boldsymbol{e}_r$, where $\boldsymbol{e}_r$ is the unit radial vector pointing away from the center of the sphere. Thus, $\boldsymbol{E}_+ = \frac{\rho}{3\varepsilon_0}\boldsymbol{r}$. Likewise, inside another sphere of radius R_1 and charge density $-\rho$ the field is $\boldsymbol{E}_- = \frac{-\rho}{3\varepsilon_0}\boldsymbol{r}'$, where $\boldsymbol{r}'$ is the radius-vector of the point in the coordinate system with the origin in the center of this sphere. Superposition of the two charge configurations gives the setup we want with $\boldsymbol{r}' = \boldsymbol{r} - \boldsymbol{x}_d$. So inside the charge-free region $\lvert \boldsymbol{r} - \boldsymbol{x}_{\mathrm{p}} \rvert < R_1$ the field is $\boldsymbol{E} = \boldsymbol{E}_+ + \boldsymbol{E}_- = \frac{\rho}{3\varepsilon_0}\mathbf{r} + \frac{-\rho}{3\varepsilon_0}(\boldsymbol{r} - \boldsymbol{x}_d)$ or $\boldsymbol{E} = \frac{\rho}{3\varepsilon_0}\boldsymbol{x}_d$ with pre-factor $A = \frac{1}{3}$	1.2

The restoring force on the displaced electron cloud

2.3	With $\boldsymbol{x}_{\mathrm{p}} = x_{\mathrm{p}}\,\boldsymbol{e}_x$ and $x_{\mathrm{p}} \ll R$ we have from above that approximately the field induced inside the particle is $\boldsymbol{E}_{\mathrm{ind}} = \frac{\rho}{3\varepsilon_0}\boldsymbol{x}_{\mathrm{p}}$. The number of electrons on the particle's border that produced $\boldsymbol{E}_{\mathrm{ind}}$ is negligibly smaller than the number of electrons inside the particle, so $\boldsymbol{F} \cong Q\boldsymbol{E}_{\mathrm{ind}} = (-eN)\frac{\rho}{3\varepsilon_0}\boldsymbol{x}_{\mathrm{p}} = -\frac{4\pi}{9\varepsilon_0}R^3 e^2 n^2\, x_p \boldsymbol{e}_x$ (note the antiparallel attractive force is proportional to the displacement that it is similar to Hooke's law). The work done on the electron cloud to shift it is $W_{\mathrm{el}} = -\int_0^{x_{\mathrm{p}}} F(x')\,\mathrm{d}x' = \frac{1}{2}\left(\frac{4\pi}{9\varepsilon_0}R^3 e^2 n^2\right) x_{\mathrm{p}}^2$	1.0

The spherical silver nanoparticle in an external constant electric field

2.4	Inside the metallic particle in the steady state the electric field must be equal to 0. The induced field (from 2.2 or 2.3) compensates the external field: $\boldsymbol{E}_0 + \boldsymbol{E}_{\mathrm{ind}} = 0$, so	0.6

Plasmonic Steam Generator T2

	$x_\mathrm{p} = \frac{3\varepsilon_0}{\rho} E_0 = \frac{3\varepsilon_0}{en} E_0$. Charge displaced through the yz-plane is the total charge of electrons in the cylinder of radius R and height x_p: $-\Delta Q = -\rho\, \pi R^2 x_\mathrm{p} = -\pi R^2\, ne\, x_\mathrm{p}$.	

The equivalent capacitance and inductance of the silver nanoparticle

2.5a	The electric energy W_el of a capacitor with capacitance C holding charges $\pm\Delta Q$ is $W_\mathrm{el} = \frac{\Delta Q^2}{2C}$. The energy of such capacitor is equal to the work (see 2.3) done to separate the charges (see 2.4), thus $C = \frac{\Delta Q^2}{2W_{el}} = \frac{9}{4}\varepsilon_0 \pi R = 6.26 \times 10^{-19}$ F.	0.7
2.5b	Equivalent scheme for a capacitor reads: $\Delta Q = CV_0$. Combining charge from (2.4) and capacitance from (2.5a) gives $V_0 = \frac{\Delta Q}{C} = \frac{4}{3} R\, E_0$.	0.4

2.6a	The kinetic energy of the electron cloud is defined as the kinetic energy of one electron multiplied by the number of electrons in the cloud $W_\mathrm{kin} = \frac{1}{2} m_e v^2 N = \frac{1}{2} m_e v^2 \left(\frac{4}{3}\pi R^3\, n\right)$. The current I is the charge of electrons in the cylinder of area πR^2 and height $v\Delta t$ divided by time Δt (or simply the time derivative of charge $-\Delta Q$), thus $I = -e\, nv\, \pi R^2$.	0.7
2.6b	The energy carried by current I in the equivalent circuit with inductance L is $W = \frac{1}{2} L\, I^2$ is, in fact, the kinetic energy of electrons W_kin. Taking the energy and current from (2.6a) gives $L = \frac{4\, m_e}{3\pi R n e^2} = 2.57 \times 10^{-14}$ H.	0.5

The plasmon resonance of the silver nanoparticle

2.7a	From the LC-circuit analogy we can directly derive $\omega_p = (LC)^{-1/2} = \sqrt{ne^2/3\varepsilon_0 m_e}$. Alternatively it is possible to use the harmonic law of motion in (2.3) and get the same result for the frequency.	0.5
2.7b	$\omega_\mathrm{p} = 7.88 \times 10^{15}$ rad/s, for light with angular frequency $\omega = \omega_\mathrm{p}$ the wavelength is $\lambda_\mathrm{p} = 2\pi c/\omega_\mathrm{p} = 239$ nm.	0.4

The silver nanoparticle illuminated with light at the plasmon frequency

2.8a	The velocity of an electron $v = \frac{dx}{dt} = -\omega x_0 \sin\omega t = v_0 \sin\omega t$. The time-averaged kinetic energy on the electron $\langle W_k\rangle = \langle\frac{m_e v^2}{2}\rangle = \frac{m_e}{2}\langle v^2\rangle$. During time τ each electron hits an ion one time. So the energy lost in the whole nanoparticle during time τ is $W_{heat} = N\,\langle\frac{m_e v^2}{2}\rangle = \frac{4}{3}\pi R^3 n\,\langle\frac{m_e v^2}{2}\rangle$. Time-averaged Joule heating power $P_\mathrm{heat} = \frac{1}{\tau} W_\mathrm{kin} = \frac{1}{2\tau} m_e \langle v^2\rangle \left(\frac{4}{3}\pi R^3\, n\right)$. The expression for current is taken from (2.6a), squared and averaged	1.0

Plasmonic Steam Generator T2

	$\langle I^2\rangle = (en\,\pi R^2)^2\,\langle v^2\rangle = \left(\frac{3Q}{4R}\right)^2\langle v^2\rangle$.	
2.8b	The average time between the collisions is $\tau \gg 1/\omega_p$, so each electron oscillates many times before it collides with an ion. The oscillating current $I = I_0 \sin\omega t = \pi R^2 nev_0 \sin\omega t$ produces the heat in the resistance R_{heat} equal to $P_{heat} = R_{heat}\langle I^2\rangle$, that together with results from (2.8a) leads to $R_{heat} = \frac{W_{kin}}{\tau\langle I^2\rangle} = \frac{2m_e}{3\pi ne^2 R\tau} = 2.46\ \Omega$.	1.0

2.9	For equivalent scattering resistance $R_{scat} = \frac{P_{scat}}{\langle I^2\rangle}$ and for harmonic oscillations we can average the velocity squared over one period of oscillations, so $\langle v^2\rangle = \frac{1}{2}\omega_p^2 x_0^2$. Together it yields $R_{scat} = \frac{Q^2 x_0^2\omega_p^4}{12\pi\varepsilon_0 c^3}\frac{16R^2}{9Q^2\langle v^2\rangle} = \frac{8\omega_0^2 R^2}{27\pi\varepsilon_0 c^3} = 2.45\ \Omega$.	1.0

2.10a	Ohm's law for a *LCR* serious circuit is $I_0 = \frac{V_0}{\sqrt{(R_{heat}+R_{scat})^2+\left(\omega L-\frac{1}{\omega C}\right)^2}}$. At the resonance frequency time-averaged voltage squared is $\langle V^2\rangle = Z_R^2\langle I^2\rangle = (R_{heat}+R_{scat})^2\langle I^2\rangle$. And from (2.5b) $\langle V^2\rangle = \frac{1}{2}V_0^2 = \frac{8}{9}R^2E_0^2$, so Ohm's law results in $\langle I^2\rangle = \frac{8R^2E_0^2}{9(R_{heat}+R_{scat})^2}$. The time-averaged power losses are $P_{heat} = R_{heat}\langle I^2\rangle = \frac{8R_{heat}R^2}{9(R_{heat}+R_{scat})^2}E_0^2$ and $P_{scat} = \frac{8R_{scat}R^2}{9(R_{heat}+R_{scat})^2}E_0^2 = \frac{R_{scat}}{R_{heat}}\langle P_{heat}\rangle$.	1.2
2.10b	Starting with the electric field amplitude $E_0 = \sqrt{2S/(\varepsilon_0 c)} = 27.4\ \mathrm{kV/m}$, we calculate $P_{heat} = 6.82\ \mathrm{nW}$ and $P_{scat} = 6.81\ \mathrm{nW}$.	0.3

Steam generation by light

2.11a	Total number of nanoparticles in the vessel: $N_{np} = h^2 a\, n_{np} = 7.3\times10^{11}$. Then the total time-averaged Joule heating power: $P_{st} = N_{np}P_{heat} = 4.98\ \mathrm{kW}$. This power goes into the steam generation: $P_{st} = \mu_{st}L_{tot}$, with $L_{tot} = c_{wa}(T_{100}-T_{wa}) + L_{wa} + c_{st}(T_{st}-T_{100}) = 2.62\times10^6\ \mathrm{J\,kg^{-1}}$. Thus the mass of steam produced in one second is: $\mu_{st} = \frac{P_{st}}{L_{tot}} = 1.90\times10^{-3}\ \mathrm{kg\,s^{-1}}$.	0.6
2.11b	The power of light incident on the vessel $P_{tot} = h^2 S = 0.01\mathrm{m}^2 \times 1\ \mathrm{MW\,m^{-2}} = 10.0\ \mathrm{kW}$, and the power directed for steam production by nanoparticles is given in 2.11a. Efficiency of the process is $\eta = \frac{P_{st}}{P_{tot}} = \frac{4.98\ \mathrm{kW}}{10.0\ \mathrm{kW}} = 0.498$.	0.2

	Total	**12.0**

The Greenlandic Ice Sheet T3

Solutions

3.1	The pressure is given by the hydrostatic pressure $p(x,z) = \rho_{\text{ice}} g(H(x) - z)$, which is zero at the surface.	0.3
3.2a	The outward force on a vertical slice at a distance x from the middle and of a given width Δy is obtained by integrating up the pressure times the area: $F(x) = \Delta y \int_0^{H(x)} \rho_{\text{ice}}\, g\, (H(x) - z)\, \mathrm{d}z \; = \frac{1}{2}\, \Delta y\, \rho_{\text{ice}}\, g\, H(x)^2$ which implies that $\Delta F = F(x) - F(x + \Delta x) = -\frac{\mathrm{d}F}{\mathrm{d}x}\Delta x = -\Delta y\, \rho_{\text{ice}}\, g\, H(x) \frac{\mathrm{d}H}{\mathrm{d}x}\Delta x$. This finally shows that $S_{\text{b}} = \frac{\Delta F}{\Delta x \Delta y} = -\, \rho_{\text{ice}}\, g\, H(x) \frac{\mathrm{d}H}{\mathrm{d}x}$ Notice the sign, which must be like this, since S_b was defined as positive and $H(x)$ is a decreasing function of x.	0.9
3.2b	To find the height profile, we solve the differential equation for $H(x)$: $-\frac{S_{\text{b}}}{\rho_{\text{ice}}\, g} = H(x) \frac{\mathrm{d}H}{\mathrm{d}x} = \frac{1}{2} \frac{\mathrm{d}}{\mathrm{d}x} H(x)^2$ with the boundary condition that $H(L) = 0$. This gives the solution: $H(x) = \sqrt{\frac{2 S_b L}{\rho_{\text{ice}}\, g}} \sqrt{1 - x/L}$ Which gives the maximum height $H_{\text{m}} = \sqrt{\frac{2 S_b L}{\rho_{\text{ice}}\, g}}$. Alternatively, dimensional analysis could be used in the following manner. First notice that $\mathcal{L} = [H_{\text{m}}] = [\rho_{\text{ice}}^{\alpha}\, g^{\beta} \tau_{\text{b}}^{\gamma} L^{\delta}]$. Using that $[\rho_{\rho_{\text{ice}}}] = \mathcal{M}\mathcal{L}^{-3}$, $[g] = \mathcal{L}\,\mathcal{T}^{-2}$, $[\tau_b] = \mathcal{M}\mathcal{L}^{-1}\mathcal{T}^{-2}$, demands that $\mathcal{L} = [H_{\text{m}}] = [\rho_i{}^{\alpha} g^{\beta} \tau_b{}^{\gamma} L^{\delta}] = \mathcal{M}^{\alpha+\gamma} \mathcal{L}^{-3\alpha+\beta-\gamma+\delta}\, \mathcal{T}^{-2\beta-2\gamma}$, which again implies $\alpha + \gamma = 0,\ -3\alpha + \beta - \gamma + \delta = 1,\ 2\beta + 2\gamma = 0$. These three equations are solved to give $\alpha = \beta = -\gamma = \delta - 1$, which shows that $H_{\text{m}} \propto \left(\frac{S_{\text{b}}}{\rho_{\rho_{\text{ice}}} g}\right)^{\gamma} L^{1-\gamma}$ Since we were informed that $H_{\text{m}} \propto \sqrt{L}$, it follows that $\gamma = 1/2$. With the boundary condition $H(L) = 0$, the solution then take the form $H(x) \propto \left(\frac{S_{\text{b}}}{\rho_{\text{ice}}\, g}\right)^{1/2} \sqrt{L - x}$ The proportionality constant of $\sqrt{2}$ cannot be determined in this approach.	0.8

The Greenlandic Ice Sheet T3

3.2c	For the rectangular Greenland model, the area is equal to $A = 10L^2$ and the volume is found by integrating up the height profile found in problem 3.2b: $V_{\mathrm{G,ice}} = (5L)2\int_0^L H(x)\,\mathrm{d}x = 10L\int_0^L \left(\frac{\tau_{\mathrm{b}} L}{\rho_{\mathrm{ice}} g}\right)^{1/2} \sqrt{1-x/L}\,\mathrm{d}x = 10H_{\mathrm{m}}L^2\int_0^1 \sqrt{1-\tilde{x}}\,\mathrm{d}\tilde{x}$ $= 10H_{\mathrm{m}}L^2\left[-\frac{2}{3}(1-\tilde{x})^{3/2}\right]_0^1 = \frac{20}{3}H_{\mathrm{m}}L^2 \propto L^{5/2}$, where the last line follows from the fact that $H_{\mathrm{m}} \propto \sqrt{L}$. Note that the integral need not be carried out to find the scaling with L. This implies that $V_{\mathrm{G,ice}} \propto {A_G}^{5/4}$ and the wanted exponent is $\gamma = 5/4$.	0.5
3.3	According to the assumption of constant accumulation c the total mass accumulation rate from an area of width Δy between the ice divide at $x = 0$ and some point at $x > 0$ must equal the total mass flux through the corresponding vertical cross section at x. That is: $\rho c x \Delta y = \rho \Delta y H_{\mathrm{m}} v_x(x)$, from which the velocity is isolated: $$v_x(x) = \frac{cx}{H_{\mathrm{m}}}$$	0.6
3.4	From the given relation of incompressibility it follows that $$\frac{\mathrm{d}v_z}{\mathrm{d}z} = -\frac{\mathrm{d}v_x}{\mathrm{d}x} = -\frac{c}{H_{\mathrm{m}}}$$ Solving this differential equation with the initial condition $v_z(0) = 0$, shows that: $$v_z(z) = -\frac{cz}{H_{\mathrm{m}}}$$	0.6
3.5	Solving the two differential equations $$\frac{\mathrm{d}z}{\mathrm{d}t} = -\frac{cz}{H_{\mathrm{m}}} \quad \text{and} \quad \frac{\mathrm{d}x}{\mathrm{d}t} = \frac{cx}{H_{\mathrm{m}}}$$ with the initial conditions that $z(0) = H_{\mathrm{m}}$, and $x(0) = x_i$ gives $$z(t) = H_{\mathrm{m}}\,\mathrm{e}^{-ct/H_{\mathrm{m}}} \quad \text{and} \quad x(t) = x_i\,\mathrm{e}^{ct/H_{\mathrm{m}}}$$ This shows that $z = H_{\mathrm{m}}\,x_i\,/x$, meaning that flow lines are hyperbolas in the xz-plane. Rather than solving the differential equations, one can also use them to show that $$\frac{\mathrm{d}}{\mathrm{d}t}(xz) = \frac{\mathrm{d}x}{\mathrm{d}t}z + x\frac{\mathrm{d}z}{\mathrm{d}t} = \frac{cx}{H_{\mathrm{m}}}z - x\frac{cz}{H_{\mathrm{m}}} = 0$$ which again implies that $xz = \mathrm{const}$. Fixing the constant by the initial conditions, again leads to the result that $z = H_{\mathrm{m}}x_i/x$.	0.9
3.6	At the ice divide, $x = 0$, the flow will be completely vertical, and the t-dependence of z found in 3.5 can be inverted to find $\tau(z)$. One finds that $\tau(z) = \frac{H_{\mathrm{m}}}{c}\ln\left(\frac{H_{\mathrm{m}}}{z}\right)$.	1.0

The Greenlandic Ice Sheet T3

3.7a	The present interglacial period extends to a depth of 1492 m, corresponding to 11,700 year. Using the formula for $\tau(z)$from problem 3.6, one finds the following accumulation rate for the interglacial: $$c_{\mathrm{ig}} = \frac{H_{\mathrm{m}}}{11{,}700 \text{ years}} \ln\left(\frac{H_{\mathrm{m}}}{H_{\mathrm{m}} - 1492\text{ m}}\right) = 0.1749 \text{ m/year}.$$ The beginning of the ice age 120,000 years ago is identified as the drop in $\delta^{18}\mathrm{O}$ in figure 3.2b at a depth of 3040 m. Using the vertical flow velocity found in problem 3.4, on has $\frac{\mathrm{d}z}{z} = -\frac{c}{H_{\mathrm{m}}}\mathrm{d}t$, which can be integrated down to a depth of 3040 m, using a stepwise constant accumulation rate: $$H_{\mathrm{m}} \ln\left(\frac{H_{\mathrm{m}}}{H_{\mathrm{m}} - 3040\text{ m}}\right) = -H_{\mathrm{m}} \int_{H_{\mathrm{m}}}^{H_{\mathrm{m}}-3040\text{ m}} \frac{1}{z}\mathrm{d}z$$ $$= \int_{11{,}700\text{ year}}^{120{,}000\text{ year}} c_{\mathrm{ia}}\,\mathrm{d}t + \int_{0}^{11{,}700\text{ year}} c_{\mathrm{ig}}\,\mathrm{d}t$$ $$= c_{\mathrm{ia}}(120{,}000\text{ year-}11{,}700\text{ year}) + c_{\mathrm{ig}}11{,}700\text{ year}$$ Isolating form this equation leads to $c_{\mathrm{ia}} = 0.1232$, i.e. far less precipitation than now.	0.8
3.7b	Reading off from figure 3.2b: $\delta^{18}\mathrm{O}$ changes from $-43{,}5$ ‰ to $-34{,}5$ ‰. Reading off from figure 3.2a, T then changes from -40 °C to -28 °C. This gives $\Delta T \approx 12$ °C.	0.2

3.8	From the area A_{G} one finds that $L = \sqrt{A_{\mathrm{G}}/10} = 4.14 \times 10^5$ m. Inserting numbers in the volume formula found in 3.2c, one finds that: $$V_{\mathrm{G,ice}} = \frac{20}{3} L^{5/2} \sqrt{\frac{2S_{\mathrm{b}}}{\rho_{\mathrm{ice}} g}} = 3.45 \times 10^{15}\text{ m}^3$$ This ice volume must be converted to liquid water volume, by equating the total masses, i.e. $V_{\mathrm{G,wa}} = V_{\mathrm{G,ice}} \frac{\rho_{\mathrm{ice}}}{\rho_{\mathrm{wa}}} = 3.17 \times 10^{15}\text{ m}^3$, which is finally converted to a sea level rise, as $h_{\mathrm{G,rise}} = \frac{V_{\mathrm{G,wa}}}{A_{\mathrm{o}}} = 8.79$ m.	0.6

The Greenlandic Ice Sheet T3

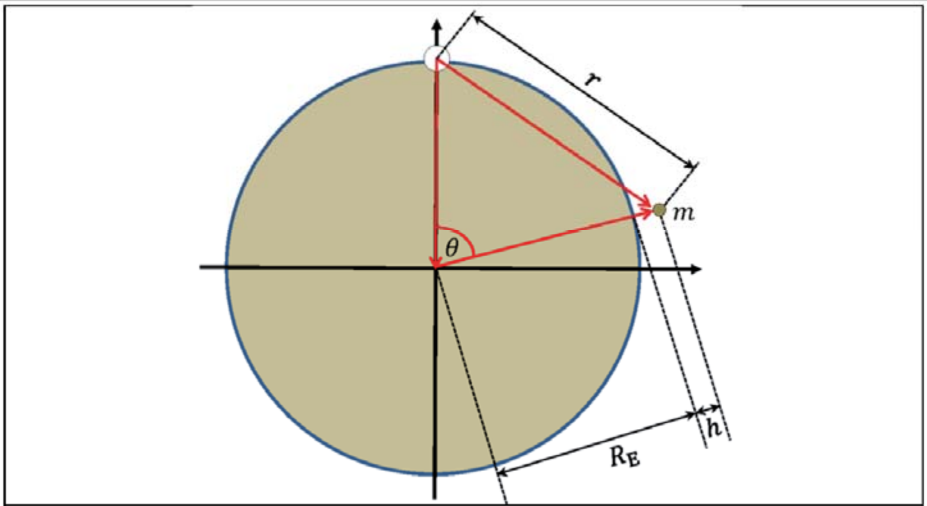

Figure 3.S1 Geometry of the ice ball (white circle) with a test mass m (small gray circle).

3.9	The total mass of the ice is $$M_{\text{ice}} = V_{\text{G,ice}}\,\rho_{\text{ice}} = 3.17\times10^{18}\text{ kg} = 5.31\times10^{-7}m_{\text{E}}$$ The total gravitational potential felt by a test mass m at a certain height h above the surface of the Earth, and at a polar angle θ (cf. figure 3.S1), with respect to a rotated polar axis going straight through the ice sphere is found by adding that from the Earth with that from the ice: $$U_{\text{tot}} = -\frac{Gm_{\text{E}}m}{R_{\text{E}}+h} - \frac{GM_{\text{ice}}m}{r} = -mgR_E\left(\frac{1}{1+h/R_E} + \frac{M_{ice}/m_E}{r/R_E}\right)$$ where $g = Gm_E/R_E^2$. Since $h/R_{\text{E}} \ll 1$ one may use the approximation given in the problem, $(1+x)^{-1} \approx 1-x,\ \|x\| \ll 1$, to approximate this by $$U_{\text{tot}} \approx -mgR_E\left(1 - \frac{h}{R_E} + \frac{M_{ice}/m_E}{r/R_E}\right).$$ Isolating h now shows that $h = h_0 + \frac{M_{ice}/m_E}{r/R_E}R_E$, where $h_0 = R_E + U_{\text{tot}}/(mg)$. Using again that $h/R_{\text{E}} \ll 1$, trigonometry shows that $r \approx 2R_{\text{E}}\|\sin(\theta/2)\|$, and one has: $$h(\theta) - h_0 \approx \frac{M_{\text{ice}}/m_{\text{E}}}{2\|\sin(\theta/2)\|}R_E \approx \frac{1.69\text{ m}}{\|\sin(\theta/2)\|}.$$ To find the magnitude of the effect in Copenhagen, the distance of 3500 km along the surface is used to find the angle $\theta_{\text{CPH}} = (3.5\times10^6\text{ m})/R_E \approx 0.549$, corresponding to $h_{\text{CPH}} - h_0 \approx 6.25$ m. Directly opposite to Greenland corresponds to $\theta = \pi$, which gives $h_{\text{OPP}} - h_0 \approx 1.69$ m. The difference is then $h_{\text{CPH}} - h_{\text{OPP}} \approx 4.56$ m, where h_0 has dropped out.	1.6

The Greenlandic Ice Sheet T3

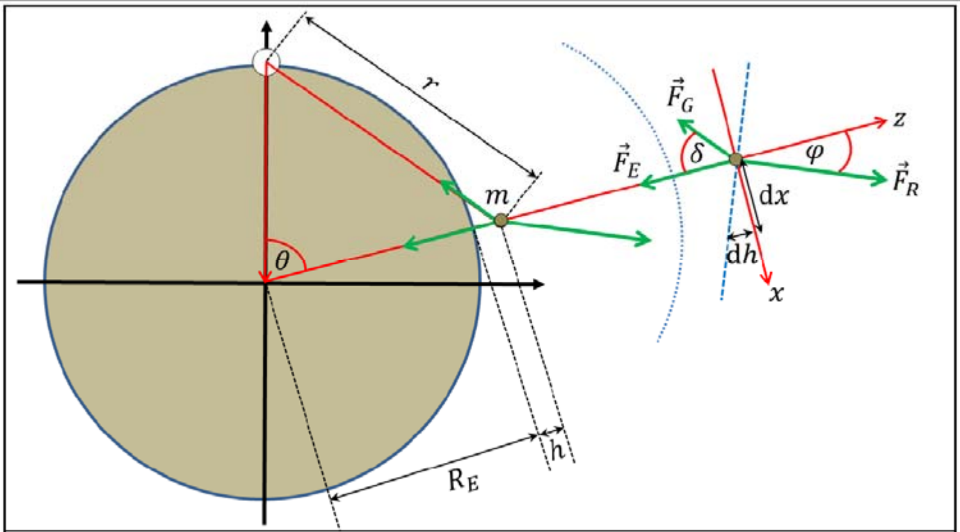

Figure 3.S2 Same figure as above, but with the relevant forces depicted and showed again outside figure for clarity. The blue dotted line indicates the Earth surface. The blue dashed line indicates the local sea level, growing towards Greenland and decreasing towards the south pole.

Approach with forces:

This problem can also be solved using forces. The basic equations for mechanical equilibrium of the test particle is then a simple matter of balancing the two gravitational forces, $\vec{F}_E$ and $\vec{F}_G$, with the reaction force from the Earth, $\vec{F}_R$. Given the angles indicated in Figure 3.S2, the force balance along locally vertical and horizontal directions, respectively, read

$$F_E + F_G\cos(\delta) = F_R\cos(\varphi)$$

and

$$F_G\sin(\delta) = F_R\sin(\varphi)$$

which can be divided to obtain (using that $\delta = \pi/2 - \theta/2$):

$$\begin{aligned}\tan(\varphi) &= \frac{F_G\sin(\delta)}{F_E + F_G\cos(\delta)}\\ &= \frac{F_G}{F_E}\cos(\theta/2)\frac{1}{1+(F_G/F_E)\sin(\theta/2)}\\ &\approx \frac{F_G}{F_E}\cos(\theta/2)\\ &= \frac{M_{ice}/m_E}{(r/R_E)^2}\cos(\theta/2)\\ &= \frac{M_{ice}/m_E}{4\sin^2(\theta/2)}\cos(\theta/2)\end{aligned}$$

where we have plugged in the gravitational forces and the relevant distances. We have also

The Greenlandic Ice Sheet T3

approximated the fraction, using that $M_{ice}/m_E = 5.31 \times 10^{-7} \ll 1$, which is only valid not too close to Greenland, i.e. for a certain size of θ. Since the local sea surface will be perpendicular to the reaction force, it is seen from figure 3.S2 that

$$\tan(\varphi) = \frac{dh}{dx} = \frac{dh}{d\theta}\frac{d\theta}{dx} = \frac{1}{R_E}\frac{dh}{d\theta}$$

whereby

$$\frac{dh}{d\theta} = R_E \frac{M_{ice}/m_E}{4\sin^2(\theta/2)}\cos(\theta/2)$$

The difference in sea levels in Copenhagen and opposite to Greenland can now be obtained by integrating this expression. That is

$$\begin{aligned} h_{\mathrm{CPH}} - h_{\mathrm{OPP}} &= R_E \frac{M_{ice}}{m_E}\int_{\pi}^{\theta_{CPH}} \frac{\cos(\theta/2)}{4\sin^2(\theta/2)}\, d\theta \\ &= R_E \frac{M_{ice}}{2\, m_E}\int_{1}^{\sin(\theta_{CPH}/2)} q^{-2}\, dq \\ &= R_E \frac{M_{ice}}{2\, m_E}\left(\frac{1}{\sin(\theta_{CPH}/2)} - 1\right) \end{aligned}$$

where we have made the substitution $q = \sin(\theta/2)$. Plugging in the numbers found above, we obtain again $h_{\mathrm{CPH}} - h_{\mathrm{OPP}} \approx 4.56$. Note that this solution strategy necessarily involves consideration of tangential force components alongside with the radial components.

	Total	**9.0**

The examinations, Tuesday 9 July (NBI) and Thursday 11 July (DTU)

(see more pictures at http://www.ipho2013.dk/ipho2013-photos.htm)





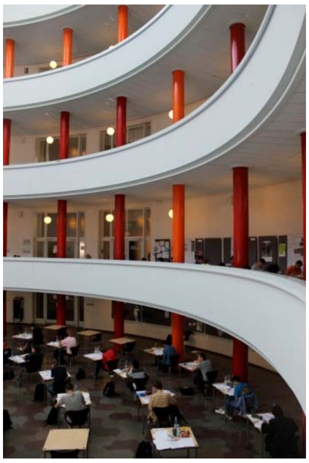










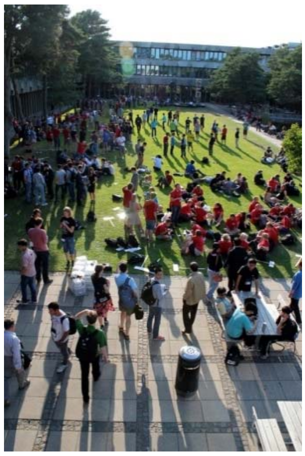

Experimental problems
(see www.ipho2013.dk/ipho2013-problems.htm)

Speed of light E1

Notice: All measurements and calculated values must be presented with SI units with an appropriate number of significant digits. Uncertainties required only when explicitly asked for.

1.0 Introduction

Experiments with a laser distance meter (LDM)

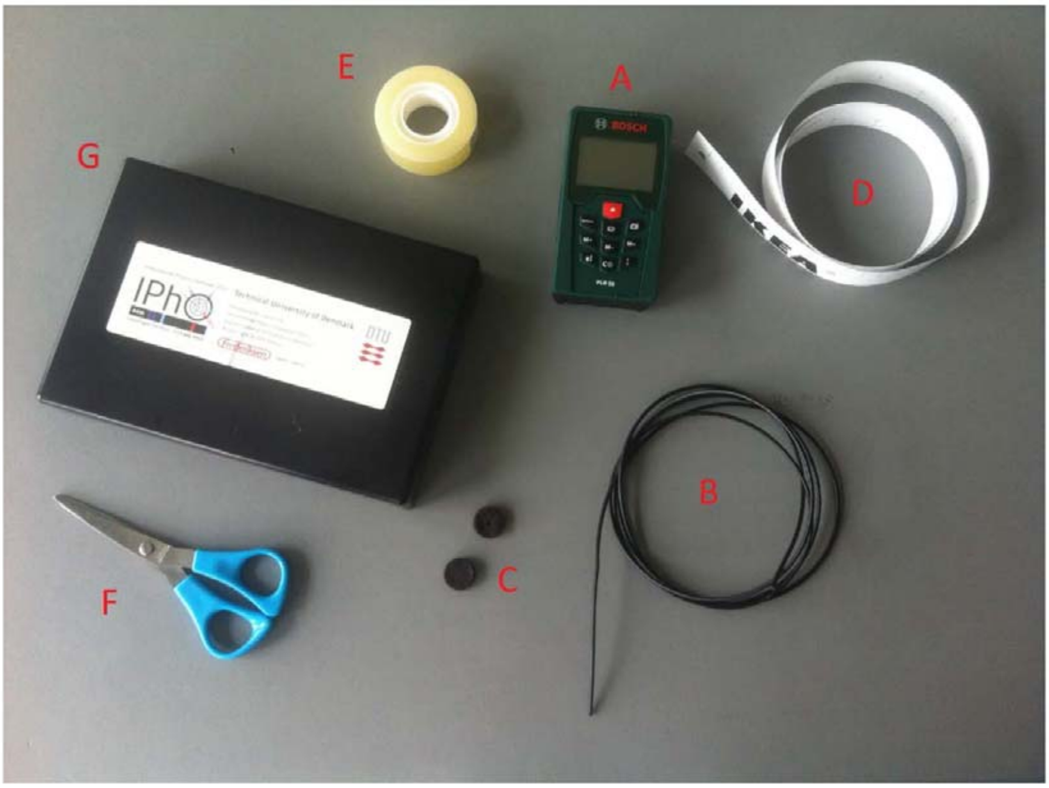

Figure 1.1 Equipment for the first experiments 1.1 and 1.2.

A: Laser distance meter

B: Fiber optic cable (approximately 1 m)

C: Self-adhesive black felt pads with hole

D: Tape measure

E: Tape

F: Scissors

G: Lid from the black box

A laser distance meter (LDM, see Fig. 1.2 and Fig. 1.3) consists of an emitter and a receiver. The emitter is a diode laser that emits a modulated laser beam, i.e. a laser beam for which the amplitude varies at a very high frequency. When the laser beam hits an object, light is reflected in all directions from the laser dot. Some of this light returns to the instrument's receiver which is situated

Speed of light E1

immediately next to the emitter. The instrument's telescope optics is focused on the laser dot and receives the light returned from the laser dot. The electronics of the instrument measures the time difference in the modulation of the received light signal relative to the emitted light signal. The delay t in the modulation is exactly the time it takes for the light to travel from emitter to receiver. The measured time is then converted to a value

$$y = \frac{1}{2}ct + k$$

This value y is shown in the instrument's display. Here, $c = 2.998 \cdot 10^8 \mathrm{ms}^{-1}$ is the speed of light. The constant k depends on the instrument setting; on the instrument you can switch between measuring the distance either from the rear end or from the front end of the instrument. When the laser distance meter is turned on, the default setting is to measure from the rear. **This setting shall be maintained during all measurements.**

Due to parallax, the LDM cannot measure any distance shorter than 5 cm. The maximum distance that can be measured is around 25 m. The shape of the instrument is such that the rear side is perpendicular to the laser beam as well as the front side. When the instrument is lying on the table the polarization is vertical (perpendicular to the display)

The diode laser is of class 2 with power < 1 mW and wavelength 635 nm. Manifacturer uncertainty for measurements is +/- 2 mm.

Warning: The instrument's diode laser can damage your eyes. Do not look into the laser beam and do not shine it into other people's eyes!

Settings for LDM

The above calculation of the distance y of course assumes that the light has been travelling at speed c. At the level of accuracy in this experiment, there is no need to distinguish between the speed of light in vacuum and in air, since the refractive index for dry, atmospheric air at normal pressure and temperature is $1.000\ 29 \approx 1.000$.

Speed of light E1

Figure 1.2 The unlabeled six buttons are irrelevant (they are used to calculate area and volume). The relevant buttons are:

A: On/off

B: Switch between measurement from the rear and the front of the instrument.

C: Indicator for measurement from the rear/front

D: Turn on laser/start measurement

E: Continuous measurement

F: Indicator for continuous measurement

Figure 1.3 The laser distance meter seen from the front end:

A: Receiver: Lens for the telescope focused on the laser dot

B: Emitter: Do not look into the laser beam!

1.1 Measurement with the laser distance meter

The instrument will perform a measurement when you press the button **D**, see Fig. 1.2.

1.1	Use the LDM to measure the distance H from the top of the table to the floor. Write down the uncertainty ΔH. Show with a sketch how you perform this measurement.	0.4

Speed of light E1

1.2 Experiment with the fiber optic cable

Figure 1.4 Diagram of a fiber optic cable.

You have been given a fiber optic cable of length approximately 1 m and diameter approximately 2 mm. The cable consists of two optical materials. The core (diameter approximately 1 mm) is made from a plastic with a high refractive index. The core is surrounded by a cladding made from a plastic with a slightly lower refractive index, and this is covered by a protective jacket of black plastic. Core and cladding serve as a wave guide for light shone into the cable, since the boundary between core and cladding will cause total reflection – and thereby prevent the light from leaving the core – as long as the angle of incidence is larger than the critical angle for total reflection. The light will therefore follow the core fiber, even if the cable bends, as long as it is not bent too much.

The LDM should now be set for continuous measurement (**E**, see Fig. 1.2), so that the display indication y updates approximately once per second. The LDM will automatically go into sleep mode after a few minutes. It can be reactivated by pushing the red start button.

Carefully and gently cover the lens of the receiver with one small, black felt pad (the other is a backup) with a hole of diameter 2 mm (see figure 1.3A). The adhesive side of the pad should be pressed softly against the lens. Insert a fiber optic cable of length x in the hole in the pad so that it touches the lens,

see Fig. 1.5.

Speed of light E1

Figure 1.5 (a) Felt pad and fiber optic cable. **(b)** Attaching the fiber optic cable.

The other end of the cable should be held against the emitter, so that it touches the glass in the middle of the laser beam. Now read off the y-value from the display. The supplied scissors should be used to cut the fiber optic cable into different lengths x.

Think <u>very</u> carefully before cutting the fiber optic cable, as you cannot get any more cable!!

Notice also that the LDM display might show a thermometer icon after a while in the continuous mode due to excessive heating of the electronics. If this happens, turn off the LDM for a while to cool off the instrument.

1.2a	Measure corresponding values of x and y. Set up a table with your measurements. Draw a graph showing y as a function of x.	1.8
1.2b	Use the graph to find the refractive index n_{co} for the material from which the core of the fiber optic cable is made. Calculate the speed of light v_{co} in the core of the fiber optic cable.	1.2

Speed of light E1

1.3 Laser distance meter at an angle from the vertical

In this part of the experiment you will need the equipment shown in Fig. 1.6.

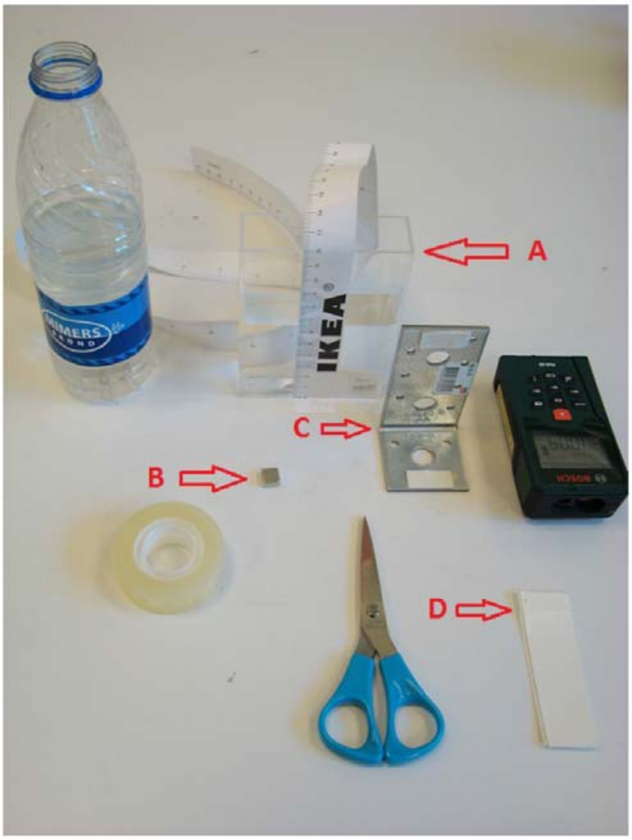

Figure 1.6 Equipment for experiment 1.3 shown in the figure:

A: Optical vessel with water and measuring tape

B: Magnet to secure the angle iron on top of the black box. (You find magnet placed on the angle iron).

C: Angle iron with self-adhesive foam pads

D: Self-adhesive foam pads

Remove the black felt pad from the lens. The LDM should now be placed in the following set-up: Place two self-adhesive foam pads on the angle iron, see A on Fig. 1.7.

Speed of light E1

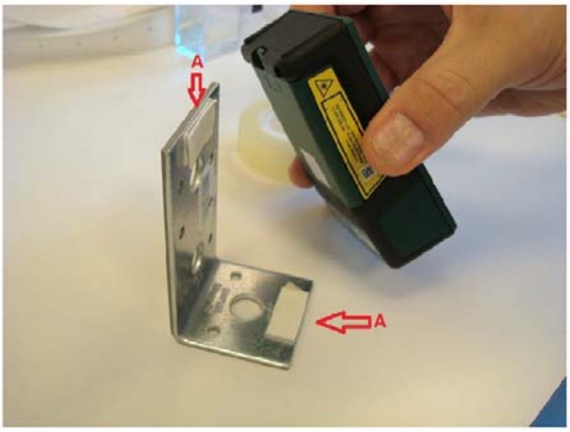

Figure 1.7 How to place the two self-adhesive foam pads on the angle iron.

The LDM should be carefully placed on the angle iron as shown in Fig. 1.8.

Figure 1.8 How to place the laser distance meter on the angle iron.

The angle iron with the LDM should be mounted on the black box as shown in Fig. 1.9. Secure the angle iron to the box with a magnet placed below inside the box. (The tiny magnet is found on the angle iron). It is important to mount the LDM exactly as in the photo, since the side of the box facing upwards slants by approximately 4 degrees. The laser beam should now be pointing unobstructedly downwards at an angle.

Speed of light E1

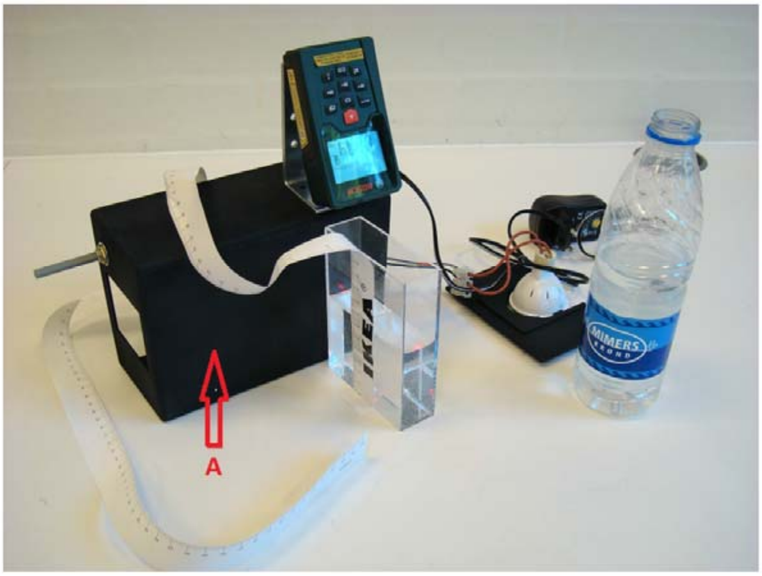

Figure 1.9 The experimental set-up. (The black box only serves as a support. The equipment behind the bottle is not used, though).

A: **Important: The bottom of the black box must face forward as shown. The side that faces upwards is slanting approximately 4 degrees with respect to the horizontal plane. Make sure that the angle θ_1 is the same all the time**

When the LDM is turned on and mounted as explained above, the laser beam will form an angle θ_1 with respect to the vertical direction. This angle, which must be the same throughout this experiment, must now be determined. The optical vessel is not needed here, so put it aside so far.

1.3a	Measure with the LDM the distance y_1 to the laser dot where the laser beam hits the table top. Then move the box with the LDM horizontally until the laser beam hits the floor. Measure the distance y_2 to the laser dot where the laser beam hits the floor. State the uncertainties.	0.2
1.3b	Calculate the angle θ_1 using only these measurements y_1, y_2 and H (from problem 1.1). Determine the uncertainty $\Delta\theta_1$.	0.4

Speed of light E1

1.4 Experiment with the optical vessel

Place the optical vessel so that the laser beam hits the bottom of the vessel approximately in the middle, see Fig. 1.10. Pour some water into the vessel. The depth of the water is x. Read off y on the display of the LDM.

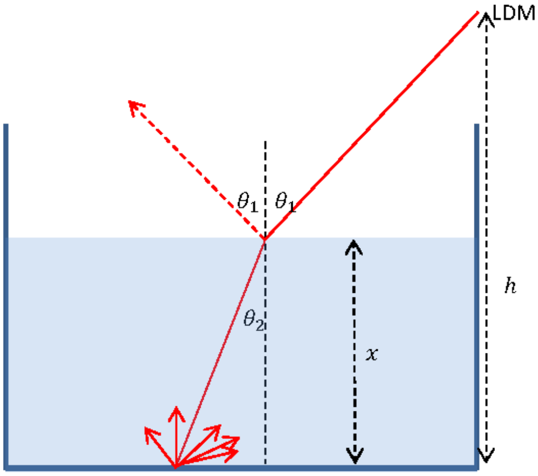

Figure 1.10 Diagram of laser beams in the optical vessel with water of depth x.

1.4a	Measure corresponding values of x and y. Set up a table with your measurements. Draw a graph of y as a function of x.	1.6
1.4b	Use equations to explain theoretically what the graph is expected to look like.	1.2
1.4c	Use the graph to determine the refractive index n_w for water.	1.2

Solar cells E2

2.0 Introduction

Equipment used for this experiment is displayed in Fig. 2.1.

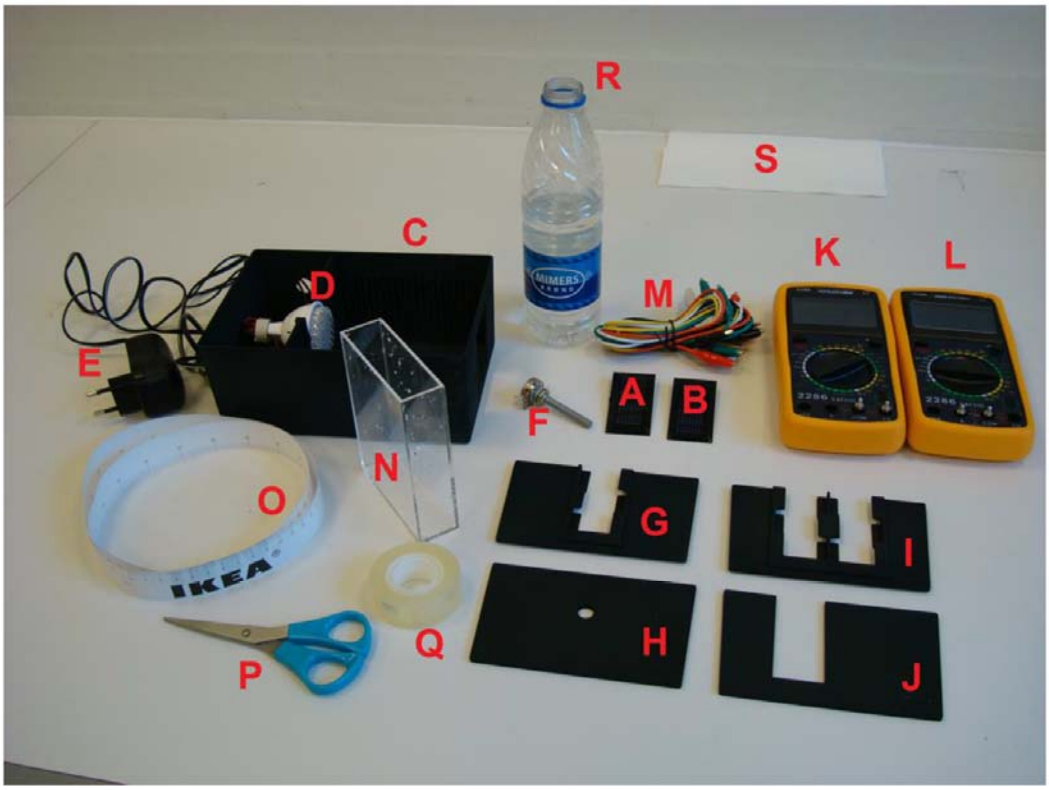

Figure 2.1 Equipment used for experiment E2.

List of equipment (see Fig. 2.1):

A: Solar cell

B: Solar cell

C: Box with slots for the mounting of light source, solar cells, etc.

D: LED-light source in holder

E: Power supply for light source D

F: Variable resistor

G: Holder for mounting single solar cell in the box C

H: Circular aperture for use in the box C

I: Holder for mounting two solar cells in the box C

Solar cells E2

J: Shielding plate for use in the box C
K: Digital multimeter
L: Digital multimeter
M: Wires with mini crocodile clips
N: Optical vessel (large cuvette)
O: Measuring tape
P: Scissors
Q: Tape
R: Water for filling the optical vessel N
S: Paper napkin for drying off excess water
T: Plastic cup for water from the optical vessel N (not shown in Fig. 2.1)
U: Plastic pipette (not shown in Fig. 2.1)
V: Lid for the box C (not shown in Fig. 2.1)

Data sheet: table of fundamental constants

Speed of light in vacuum	$c = 2.998 \times 10^{8}$ m s^{-1}
Elementary charge	$e = 1.602 \times 10^{-19}$ C
Boltzmann's constant	$k_B = 1.381 \times 10^{-23}$ J K^{-1}

A solar cell transforms part of the electromagnetic energy in the incident light to electric energy by separating charges inside the solar cell. In this way an electric current can be generated. Experiment E2 intents to examine solar cells with the use of the supplied equipment. This equipment consists of a box with holders for light source and solar cells along with various plates and a lid. The variable resistor should be mounted in the box, see Fig. 2.2. One of the three terminals on the resistor has been removed, since only the two remaining terminals are to be used. Also supplied are wires with mini crocodile clips and two solar cells (labeled with a serial number and the letter A or B) with terminals on the back. The two solar cells are similar but can be slightly different. The two multimeters have been equipped with terminals for designated use as ammeter and voltmeter, respectively, see Fig. 2.3. Finally, the experiment will make use of an optical vessel together with some drinking water from the bottle.

Solar cells E2

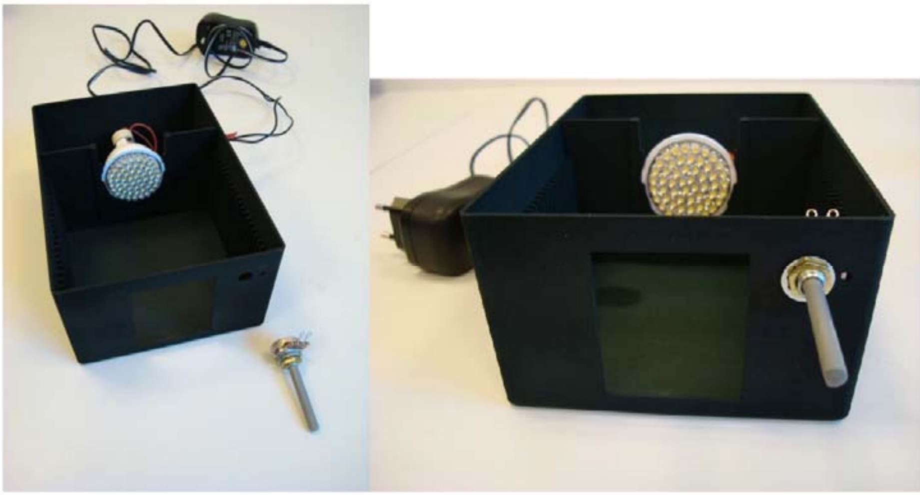

Figure 2.2 (a) Box with light source and resistor for mounting. **(b)** The resistor mounted in the box. Notice that the small pin on the resistor fits in the hole to the right of the shaft.

Figure 2.3 Multimeters equipped with terminals for use as ammeter **(left)** and voltmeter **(right)**, respectively. The instrument is turned on by pressing "POWER" in the top left corner. The instrument turns off automatically after a certain idle time. It can measure direct current and voltage (=) as well as alternating current and voltage (~). The internal resistance in the voltmeter is 10 MΩ regardless of the measuring range. The potential difference over the ammeter is 200 mV at full reading, regardless of the measuring range. In case of overflow the display will show "1", and you need to select a higher measuring range. The "HOLD" button (top right corner) should not be pushed, except if you want to freeze a measurement.

Solar cells E2

WARNING: ***Do not use the multimeter as an ohmmeter on the solar cells since the measuring current can damage them. When changing the measuring range on the multimeters, please turn the dial with caution. It can be unstable and may break. Check whether there is a number under the decimal point when measuring – if the dial is not fully in place, the multimeter will not measure, even if there are digits in the display.***

Notice: Do not change the voltage on the power supply. It must be 12 V throughout the experiment. (The power supply for the light source should be connected to the outlet (230 V ~) at your table.)

Notice: Uncertainty considerations are only expected when explicitly mentioned.

Notice: All measured and calculated values must be given in SI units.

Notice: For all measurements of currents and voltages in this experiment, the LED-light source is supposed to be on.

Solar cells E2

2.1 The dependence of the solar cell current on the distance to the light source

For this question you will measure the current, I, generated by the solar cell when in a circuit with the ammeter, and determine how it depends on the distance, r, to the light source. The light is produced *inside* the individual light diodes and r is therefore to be measured as shown in Fig. 2.4.

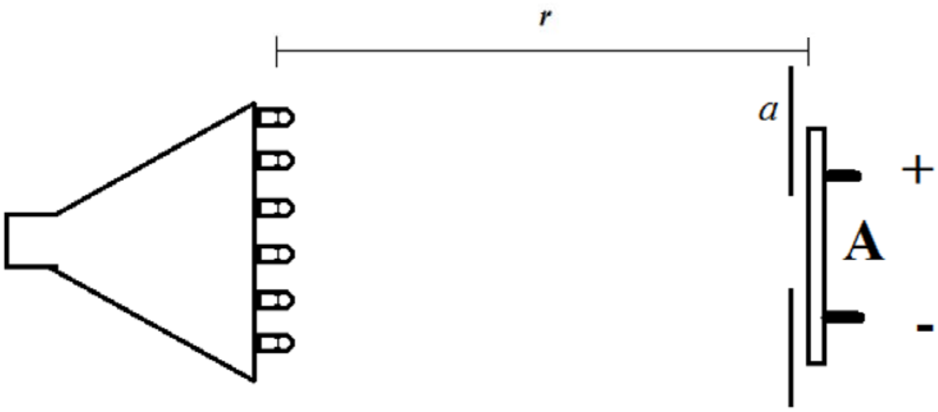

Figure 2.4 Top view of setup for question 2.1. Note the aperture a immediately in front of the solar cell A. The distance is measured from inside the light diode to the surface of the solar cell.

Do not change the measuring range on the ammeter in this experiment: the internal resistance of the ammeter depends on the measuring range and affects the current that can be drawn from the solar cell. State the serial numbers of the light source and of solar cell A on your answer sheet. Mount the light source in the U-shaped holder (the light source has a tight fit in the holder, so be patient when mounting it. Mount solar cell A in the single holder and place it together with the circular aperture immediately in front of the solar cell. The current I as a function of the distance r to the light source can, when r is not too small, be approximated by

$$I(r) = \frac{I_a}{1 + \frac{r^2}{a^2}}$$

where I_a and a are constants.

2.1a	Measure I as a function of r, and set up a table of your measurements.	1.0
2.1b	Determine the values of I_a and a by the use of a suitable graphical method.	1.0

Solar cells E2

2.2 Characteristic of the solar cell

Remove the circular aperture. Mount the variable resistor in the box as shown on Fig. 2.2. Place the light source in slot number 0, furthest away from the resistor. Mount solar cell A in the single holder *without the circular aperture* in slot number 10. Build a circuit as shown in Fig. 2.5, so that you can measure the characteristic of the solar cell, i.e. the terminal voltage U of the solar cell as a function of the current I in the circuit consisting of solar cell, resistor and ammeter.

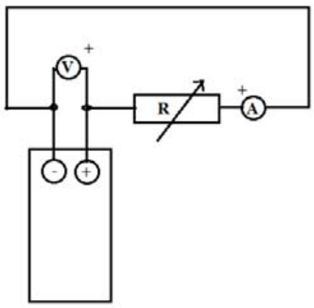

Figure 2.5 Electrical diagram for measuring the characteristic in question 2.2.

2.2a	Make a table of corresponding measurements of U and I.	0.6
2.2b	Graph voltage as function of current	0.8

2.3 Theoretical characteristic for the solar cell

For the solar cells in this experiment, the current as function of the voltage is given by the equation

$$I = I_{\text{max}} - I_0 \left(\exp\left(\frac{eU}{\eta k_B T} \right) - 1 \right)$$

where the parameters I_{max}, I_0 and η are constant at a given illumination. We take the temperature to be $T = 300$ K. The fundamental constants e and k_B are the elementary charge and Boltzmann's constant, respectively.

2.3a	Use the graph from question 2.2b to determine I_{max} .	0.4

The parameter η can be assumed to lie in the interval from 1 to 4. For some values of the potential difference U, the formula can be approximated by

$$I \approx I_{\text{max}} - I_0 \exp\left(\frac{eU}{\eta k_B T} \right)$$

2.3b	Estimate the range of values of U for which the mentioned approximation is good. Determine graphically the values of I_0 and η for your solar cell.	1.2

Solar cells E2

2.4 Maximum power for a solar cell

2.4a	The maximum power that the solar cell can deliver to the external circuit is denoted P_{max}. Determine P_{max} for your solar cell through a few, suitable measurements. (You may use some of your previous measurements from question 2.2).	0.5
2.4b	Estimate the optimal load resistance R_{opt}, i.e. the total external resistance when the solar cell delivers its maximum power to R_{opt}. State your result with uncertainty and illustrate your method with suitable calculations.	0.5

2.5 Comparing the solar cells

Mount both solar cells (A and B) in the double holder in slot number 15, see Fig. 2.6.

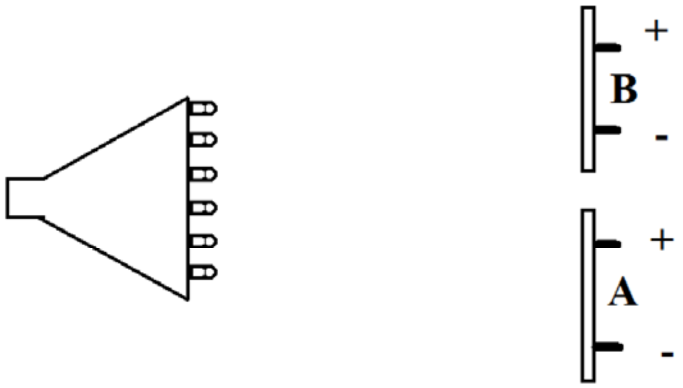

Figure 2.6 Top view of light source and solar cells in question 2.5.

2.5a	Measure, for the given illumination: - The maximum potential difference U_A that can be measured over solar cell A. - The maximum current I_A that can be measured through solar cell A. Do the same for solar cell B.	0.5
2.5b	Draw electrical diagrams for your circuits showing the wiring of the solar cells and the meters.	0.3

Solar cells E2

2.6 Couplings of the solar cells

The two solar cells can be connected in series in two different ways as shown in Fig. 2.7. There are also two different ways to connect them in parallel (not shown in the figure).

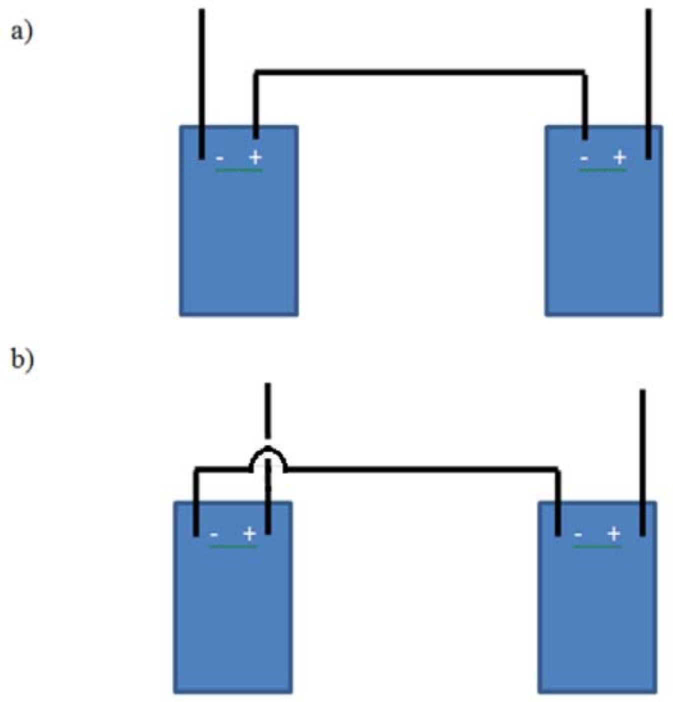

Figure 2.7 Two ways to connect the solar cells in series for question 2.6. The two ways to connect them in parallel are not shown.

2.6	Determine which of the four arrangements of the two solar cells yields the highest possible power in the external circuit when one of the solar cells is shielded with the shielding plate (J in Fig. 2.1). Hint: You can estimate the maximum power quite well by calculating it from the maximum voltage and maximum current measured from each configuration. Draw the corresponding electrical diagram.	1.0

2.7 The effect of the optical vessel (large cuvette) on the solar cell current

Mount the light source in the box and place solar cell A in the single holder with the circular aperture immediately in front, so that there is approximately 50 mm between the solar cell and the light source. Place the empty optical vessel immediately in front of the circular aperture as shown in Fig. 2.8.

Solar cells E2

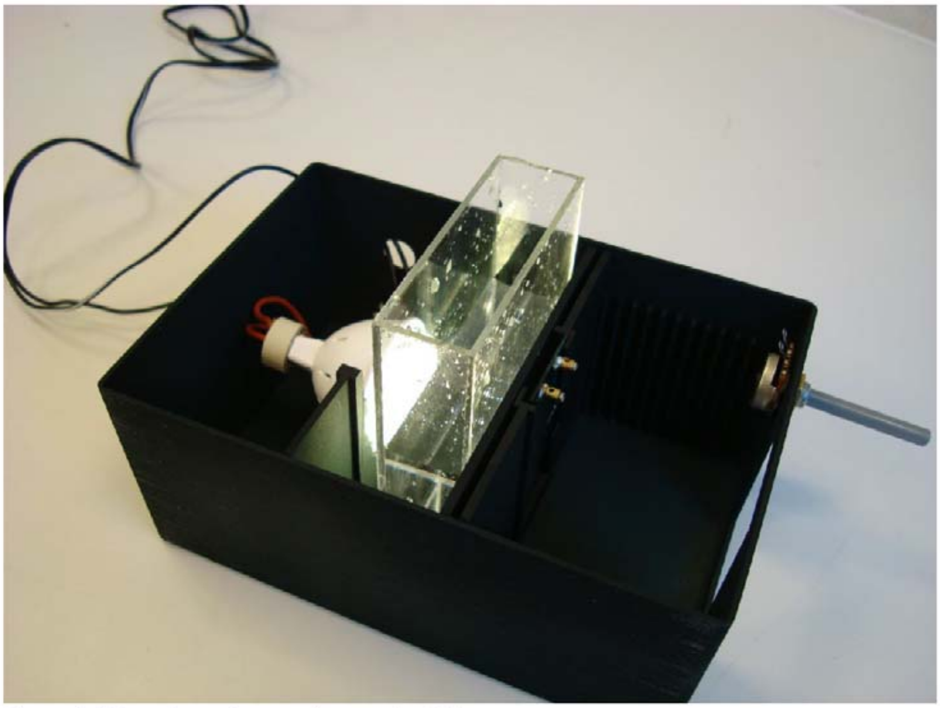

Figure 2.8 Experimental set-up for question 2.7.

2.7a	Measure the current I, now as a function of the height, h, of water in the vessel, see Fig. 2.8. Make a table of the measurements and draw a graph.	1.0
2.7b	Explain with only sketches and symbols why the graph looks the way it does.	1.0

Mount the light source in the box and place solar cell A in the single holder so that the distance between the solar cell and the light source is maximal. Place the circular aperture immediately in front of the solar cell.

2.7c	For this set-up do the following: - Measure the distance r_1 between the light source and the solar cell and the current I_1. - Place the empty vessel immediately in front of the circular aperture and measure the current I_2. - Fill up the vessel with water, almost to the top, and measure the current I_3.	0.6
2.7d	Use your measurements from 2.7c to find a value for the refractive index n_w for water. Illustrate your method with suitable sketches and equations. You may include additional measurements.	1.6

Experimental solutions
(see www.ipho2013.dk/ipho2013-solutions.htm)

Speed of light (solution) E1

In this document decimal comma is used instead of decimal point in graphs and tables

1.1	Use the LDM to measure the distance H from the top of the table to the floor. Write down the uncertainty ΔH. Show with a sketch how you perform this measurement.	0.4

$H = 907$ mm ± 2 mm. See the sketch in the figure corresponding to 1.3b. It must appear how the height is measured with the LDM in the rear mode.

1.2a	Measure corresponding values of x and y. Set up a table with your measurements. Draw a graph showing y as a function of x.	1.8

Here, a 2 m cable is used, but 1 m is sufficient. There should be about 8 lengths evenly distributed in the interval from 0 m to 1 m.

x	y
m	m
0,103	0,177
0,176	0,232
0,348	0,396
0,546	0,517
0,617	0,570
0,839	0,748
1,025	0,885
1,107	0,950
1,750	1,459
2,000	1,642

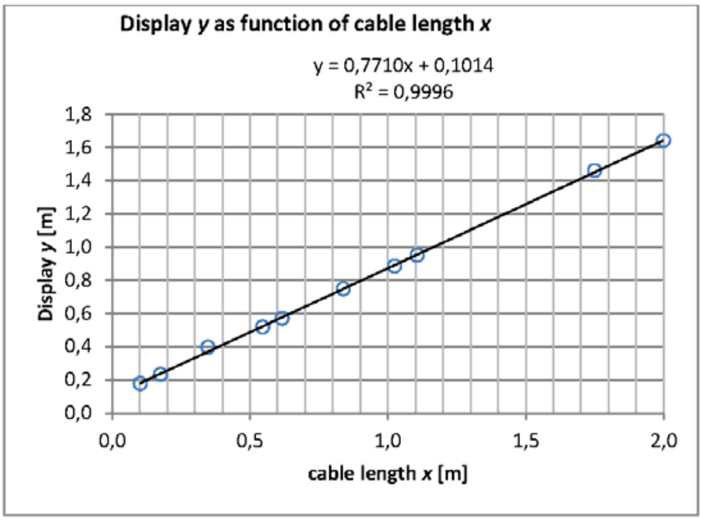

Speed of light (solution) E1

1.2b	Use the graph to find the refractive index n_{co} for the material from which the core of the fiber optic cable is made. Calculate the speed of light v_{co} in the core of the fiber optic cable.	1.2

The refractive index is twice the gradient of the linear graph, $n_{co} = 2 \cdot 0.7710 \approx 1.54$.

The reason for that is that the travel time for a light pulse

$$t = \frac{x}{v_{co}} = \frac{x n_{co}}{c}$$

The display will therefore show $y = \frac{1}{2}ct + k \Leftrightarrow y = \frac{1}{2}n_{co}x + k$.

The speed of light in the core of the cable is $v_{co} = \frac{c}{n_{co}} = \frac{2{,}998 \cdot 10^8 \frac{\text{m}}{\text{s}}}{2 \cdot 0.7710} \approx 1.95 \cdot 10^8 \, \frac{\text{m}}{\text{s}}$

1.3a	Measure with the LDM the distance y_1 to the laser dot where the laser beam hits the table top. Then move the box with the LDM horizontally until the laser beam hits the floor. Measure the distance y_2 to the laser dot where the laser beam hits the floor. State the uncertainties.	0.2

$y_1 = 312 \text{ mm} \pm 2 \text{ mm}$, $y_2 = 1273 \text{ mm} \pm 2 \text{ mm}$

1.3b	Calculate the angle θ_1 using only these measurements y_1, y_2 and H (from problem 1.1). Determine the uncertainty $\Delta\theta_1$.	0.4

$$\theta_1 = \cos^{-1}\left(\frac{H}{y_2 - y_1}\right) = \cos^{-1}\left(\frac{907 \text{ mm}}{961 \text{ mm}}\right) = 19.30^\circ$$

(see the figure)

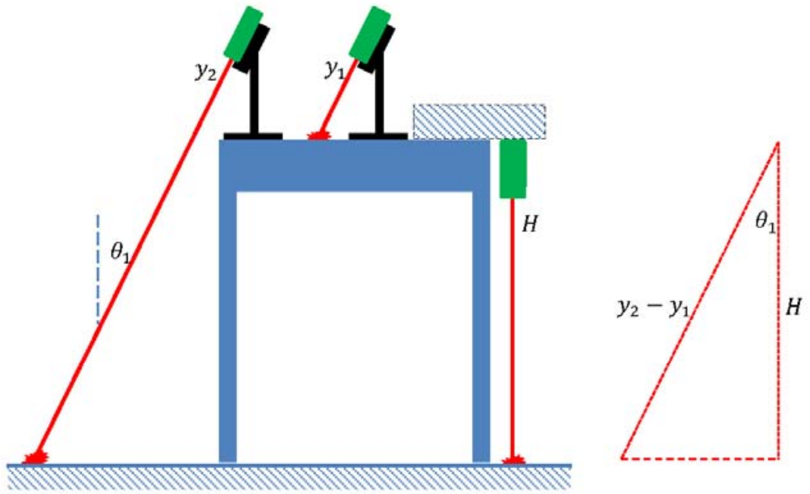

Speed of light (solution) E1

Measuring the horizontal part of some triangle is very inaccurate because of the size of the laser dot. No marks will be awarded for that. Using $\delta = 2$ mm as the uncertainty of y_1, y_2 and H, the uncertainty of θ_1 can be calculated as follows:

$$\Delta \cos\theta_1 = \Delta\left(\frac{H}{y_2 - y_1}\right)$$

Using simple derivatives yields

$$\tan\theta_1 \cdot \Delta\theta_1 = \frac{\delta}{H} + \frac{2\delta}{y_2 - y_1}$$

$$\Delta\theta_1 = \frac{\left(\frac{\delta}{H} + \frac{2\delta}{y_2 - y_1}\right)}{\tan\theta_1} \cdot \frac{180°}{\pi} = \frac{\left(\frac{2}{907} + \frac{4}{961}\right)}{\tan 19{,}30°} \cdot \frac{180°}{\pi} \approx 1°$$

Otherwise, using min/max method

$$\Delta\theta_1 = \theta_{1\max} - \theta_1 = \cos^{-1}\left(\frac{H_{\min}}{y_{2\max} - y_{1\min}}\right) = \cos^{-1}\left(\frac{905 \text{ mm}}{965 \text{ mm}}\right) - \cos^{-1}\left(\frac{907 \text{ mm}}{961 \text{ mm}}\right) = 1.0°$$

Alternatively, calculate $\Delta\theta_1$ using $\Delta(y_2 - y_1) = \sqrt{(\Delta y_1)^2 + (\Delta y_2)^2} = \sqrt{2}\delta$ and then

$$\tan\theta_1 \cdot \Delta\theta_1 = \sqrt{\left(\frac{\delta}{H}\right)^2 + \frac{2\delta^2}{(y_2 - y_1)^2}}$$

Also, accept $\delta = 1$ mm and $\Delta\theta_1 = 0.5°$.

1.4a	Measure corresponding values of x and y. Set up a table with your measurements. Draw a graph of y as a function of x.	1.6

x [mm]	y [mm]
4	450
17	454
27	457
32	459
39	461
51	466
58	467
66	471
76	473
82	476
90	478
96	480

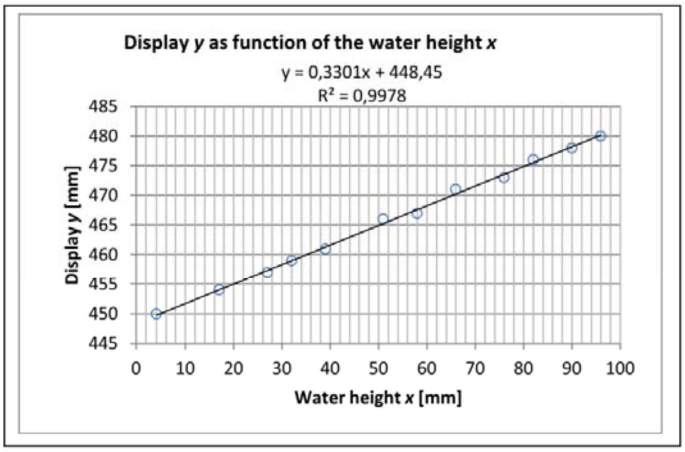

Speed of light (solution) E1

1.4b	Use equations to explain theoretically what the graph is expected to look like.	1.2

The time it takes the light to reach the water surface is

$$t_1 = \frac{(h-x)/\cos\theta_1}{c}$$

From the water surface to the bottom the light uses the time

$$t_2 = \frac{x/\cos\theta_2}{v}$$

Total travel time forth and back

$$t = 2t_1 + 2t_2 = 2\frac{(h-x)/\cos\theta_1}{c} + 2\frac{x/\cos\theta_2}{v} = 2\frac{h-x}{c\cos\theta_1} + 2\frac{nx}{c\cos\theta_2}$$

Hence, the display will show (we simply write $n = n_w$)

$$y = ½ct + k = \left(\frac{n}{\cos\theta_2} - \frac{1}{\cos\theta_1}\right)x + \frac{h}{\cos\theta_1} + k$$

which is a linear function of x. Then, using a trigonometric identity and Snell's law,

$$\cos\theta_2 = \sqrt{1-\sin^2\theta_2} = \sqrt{1-\frac{\sin^2\theta_1}{n^2}}.$$

From this the gradient α is found to be

$$\alpha = \frac{n}{\sqrt{1-\frac{\sin^2\theta_1}{n^2}}} - \frac{1}{\cos\theta_1} = \frac{n^2}{\sqrt{n^2-\sin^2\theta_1}} - \frac{1}{\cos\theta_1}$$

1.4c	Use the graph to determine the refractive index n_w for water.	1.2

Knowing the gradient α from the graph, the index of refraction n is found by solving this equation. Introducing a practical parameter,

$$p = \alpha + \frac{1}{\cos\theta_1}$$

the above equation becomes

$$p = \frac{n_w^2}{\sqrt{n_w^2 - \sin^2\theta_1}} \Leftrightarrow n_w^4 - p^2 n_w^2 + p^2\sin^2\theta_1 = 0$$

with the solution

$$n_w = \sqrt{\frac{p^2 \pm \sqrt{p^4 - 4p^2\sin^2\theta_1}}{2}} = \frac{\sqrt{2}}{2}p\sqrt{1 \pm \sqrt{1-\left(\frac{2\sin\theta_1}{p}\right)^2}}$$

From the graph is found $\alpha = 0.3301$, which leads to $p = 1.388356$ and hence

$$n_w = 1.34676 \approx 1.347.$$

All solutions with $n_w < 1$ are omitted.

Speed of light (solution) E1

Another and more elegant way of finding n_w is to use Snell's law in the equation

$$\alpha = \frac{n_w}{\cos\theta_2} - \frac{1}{\cos\theta_1} = \frac{\sin\theta_1}{\sin\theta_2\cos\theta_2} - \frac{1}{\cos\theta_1} = \frac{2\sin\theta_1}{\sin 2\theta_2} - \frac{1}{\cos\theta_1}$$

This yields

$$\sin 2\theta_2 = \frac{2\sin\theta_1}{\alpha + \frac{1}{\cos\theta_1}}$$

From here θ_2 can be calculated leading to $n_w = \frac{\sin\theta_1}{\sin\theta_2}$. This method also only uses the graph and the angle θ_1, and measurement of θ_2 is not involved).

The table value for pure water at normal conditions is $n_w = 1.331$ at the wavelength $\lambda = 635$ nm.

The following approximations can be used: For small angles

$$n_w \approx \frac{\sqrt{2}}{2} p \sqrt{1 + 1 - \frac{1}{2}\left(\frac{2\sin\theta_1}{p}\right)^2} \approx p\sqrt{1 - \left(\frac{\sin\theta_1}{p}\right)^2} \approx p\left(1 - \frac{1}{2}\left(\frac{\sin\theta_1}{p}\right)^2\right)$$

For very small angles, we get

$$n_w \approx p \approx \alpha + 1$$

It is much simpler, but not recommendable, to do the experiment with very small $\theta_1 \approx 0$.
Reflections in the water surface will ruin the signal from the bottom.

Solar cells (solution) E2

2.1 The dependence of the solar cell current on the distance to the light source

$$I(r) = \frac{I_a}{1 + \frac{r^2}{a^2}}$$

2.1a	Measure I as a function of r, and set up a table of your measurements.	1.0
2.1b	Determine the values of I_a and a by the use of a suitable graphical method.	1.0

slot #	r	I	$1/I$	r^2
	mm	mA	1/mA	mm^2
3	9.0	5.440	0.184	81
4	14.5	5.290	0.189	210
5	20.0	5.010	0.200	400
6	25.5	4.540	0.220	650
7	31.0	3.840	0.260	961
8	36.5	3.230	0.310	1332
9	42.0	2.730	0.366	1764
10	47.5	2.305	0.434	2256
11	53.0	1.985	0.504	2809
12	58.5	1.730	0.578	3422
13	64.0	1.485	0.673	4096
14	69.5	1.305	0.766	4830
15	75.0	1.140	0.877	5625
16	80.5	1.045	0.957	6480
17	86.0	0.930	1.075	7396
18	91.5	0.840	1.190	8372
19	97.0	0.755	1.325	9409
20	102.5	0.690	1.449	10506

$$I\left(1 + \frac{r^2}{a^2}\right) = I_a$$

$$r^2 = I_a a^2 \cdot \frac{1}{I} - a^2$$

$$a^2 = 1200\ \text{mm}^2 \pm 100\ \text{mm}^2,$$

$$a = 35\ \text{mm} \pm \pm 2\ \text{mm}$$

$$I_a a^2 = \frac{10870-0}{1.50-0.15} \cdot \frac{\text{mm}^2}{\text{mA}^{-1}} = 8051.85 \ldots \text{mm}^2\text{mA}$$

$$I_a = \frac{8051.85 \frac{\text{mm}^2}{\text{mA}^{-1}}}{1200\ \text{mm}^2} = 6.7\ \text{mA} \pm 0.5\ \text{mA}$$

$$(I_a a^2)_{\min} = \frac{10700-0}{1.50-0.14} \cdot \frac{\text{mm}^2}{\text{mA}^{-1}} = 7867.6 \ldots \text{mm}^2\text{mA}$$

$$\rightarrow I_{a,\max} = \frac{(I_a a^2)_{\min}}{a^2{}_{\min}} = \frac{7867.6\ \text{mm}^2\text{mA}}{1100\ \text{mm}^2} = 7.2\ \text{mA}$$

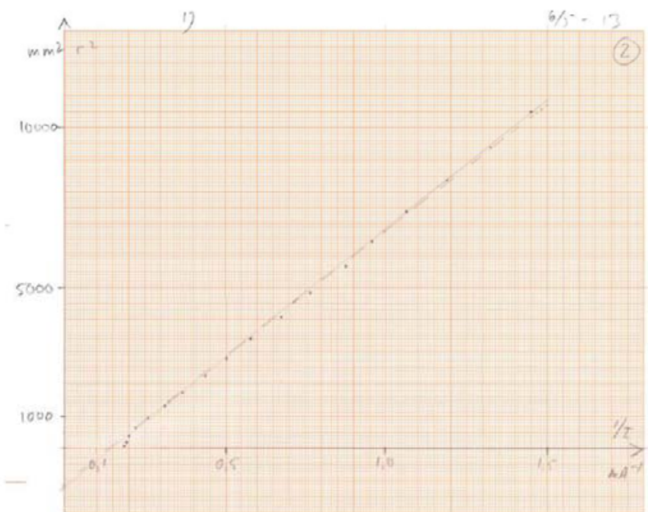

Page 1 of 12

Solar cells (solution) E2

2.2 Characteristic of the solar cell

2.2a	Make a table of corresponding measurements of U and I.	0.6
2.2b	Graph voltage as a function of current	0.8

I	U
mA	V
0.496	0.532
1.451	0.531
5.05	0.526
8.88	0.52
14.05	0.509
31.1	0.395
25.3	0.471
21.6	0.488
30.6	0.41
31.9	0.364
32.6	0.299
32.6	0.313
33.1	0.239
33.4	0.085
33.3	0.138
33.4	0.096
33.4	0.058
33.5	0.046
33.5	0.045
1.05	0.529
27.8	0.454
15.9	0.503
22.3	0.483
26.8	0.458
29.2	0.435

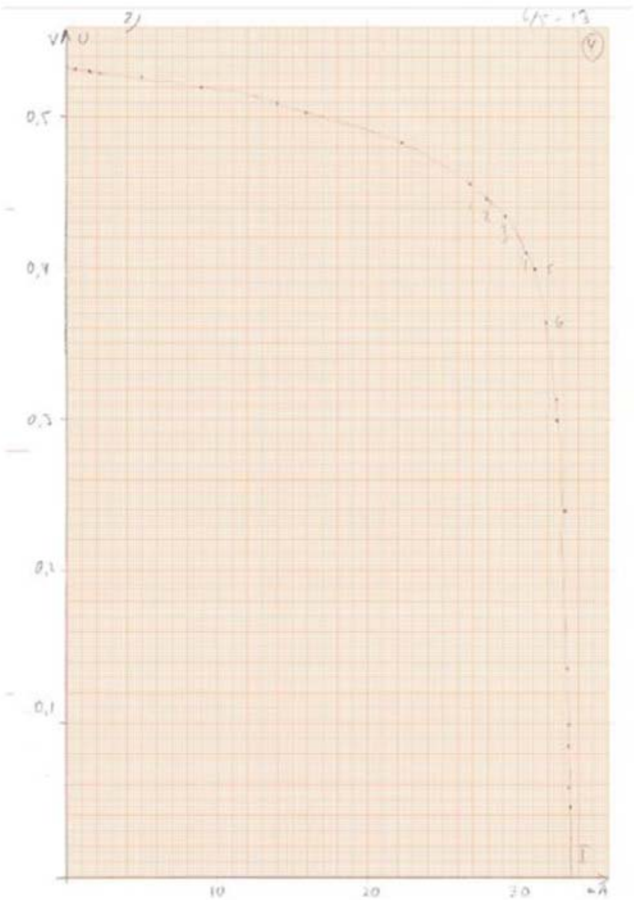

Solar cells (solution) E2

2.3 Theoretical characteristic for the solar cell

2.3a	Use the graph from question 2.2b to determine $I_{\max}$.	0.4
2.3b	Estimate the range of values of U for which the mentioned approximation is good. Determine graphically the values of I_0 and η for your solar cell.	1.2

$I = I_{\max}$ for $U = 0 \rightarrow I_{\max} = 33.5$ mA

$\eta k_B T < 4 \cdot 1.381 \cdot 10^{-23}\text{J/K} \cdot 300\text{ K} = 0.103\text{ eV}$

$$I = I_{\max} - I_0\left(\exp\left(\frac{eU}{\eta k_B T}\right) - 1\right) \approx I_{\max} - I_0 \exp\left(\frac{eU}{\eta k_B T}\right)$$

for $U > 0.4\,V$ where $\exp\left(\frac{eU}{\eta k_B T}\right) > \exp(4) \gg 1$

$$\ln\left(\frac{I_{\max} - I}{\text{mA}}\right) = \frac{e}{\eta k_B T}U + \ln\left(\frac{I_0}{\text{mA}}\right) \qquad \frac{e}{\eta k_B T} = \frac{4.03 - (-7.7)}{0.56\text{ V}} = 20.95\text{ V}^{-1}$$

$$I_0 = e^{-7.7}\text{mA} = 0.45\ \mu A \qquad \rightarrow \boldsymbol{\eta} = \frac{e/(k_B T)}{20.95\text{ V}^{-1}} = 1.85$$

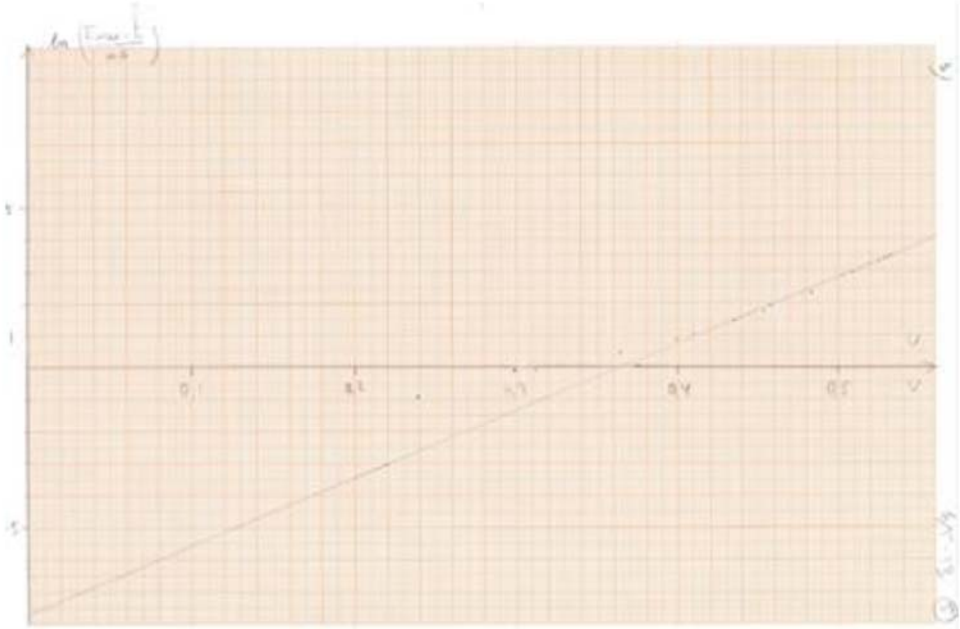

Solar cells (solution) E2

2.4 Maximum power for a solar cell

2.4a	The maximum power that the solar cell can deliver to the external circuit is denoted P_{max}. Determine P_{max} for your solar cell through a few, suitable measurements. (You may use some of your previous measurements from question 2.2)	0.5
2.4b	Estimate the optimal load resistance R_{opt}, i.e. the total external resistance when the solar cell delivers its maximum power to R_{opt}. State your result with uncertainty and illustrate your method with suitable calculations.	0.5

I	U	P	
mA	V	mW	
26.8	0.458	12.2744	1
27.8	0.454	12.6212	2
29.2	0.435	12.7020	3
30.6	0.410	12.5460	4
31.1	0.395	12.2845	5

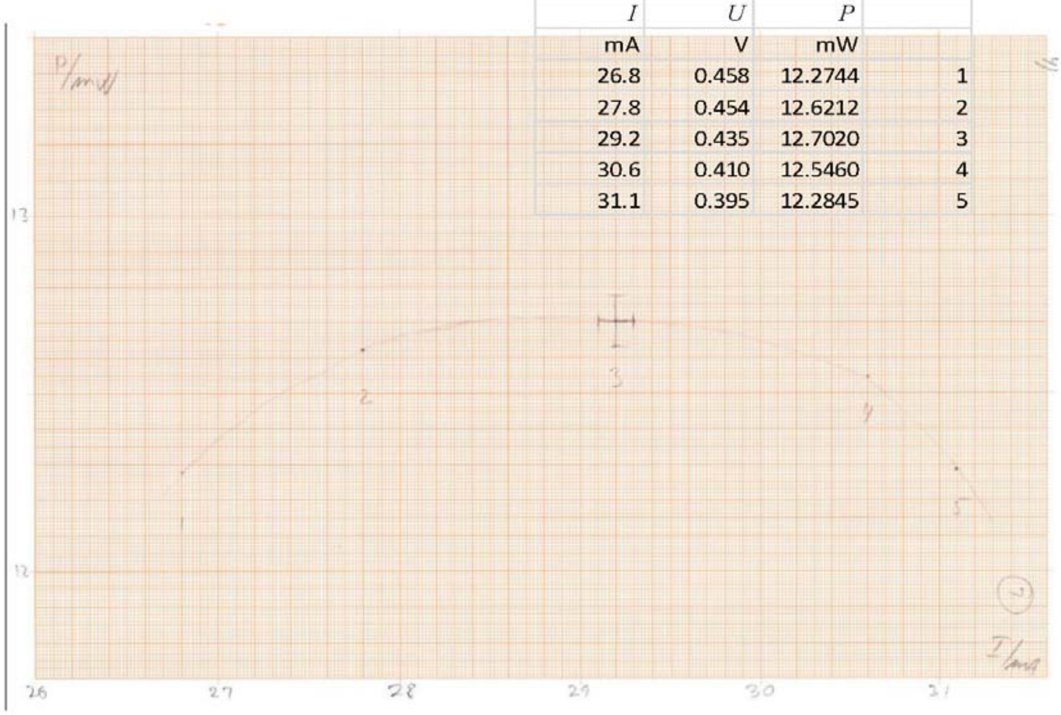

$P_{max} = (12.7 \pm 0.1)\text{mW at } I = (28.8 \pm 0.2)\text{mA}$

$$R_{opt} = \frac{P_{max}}{I_{opt}^2} = \frac{12.71\text{mW}}{(28.8\text{mA})^2} = (15.3 \pm 0.3)\Omega$$

Solar cells (solution) E2

2.5 Comparing the solar cells

2.5a	Measure, for the given illumination: - The maximum potential difference U_A that can be measured over solar cell A. - The maximum current I_A that can be measured through solar cell A. Do the same for solar cell B.	0.5
2.5b	Draw electrical diagrams for your circuits showing the wiring of the solar cells and the meters.	0.3

2.5a. U_A=0.512 V I_A=16.465 mA U_B=0.480 V I_B = 16.325 mA

2.5b.

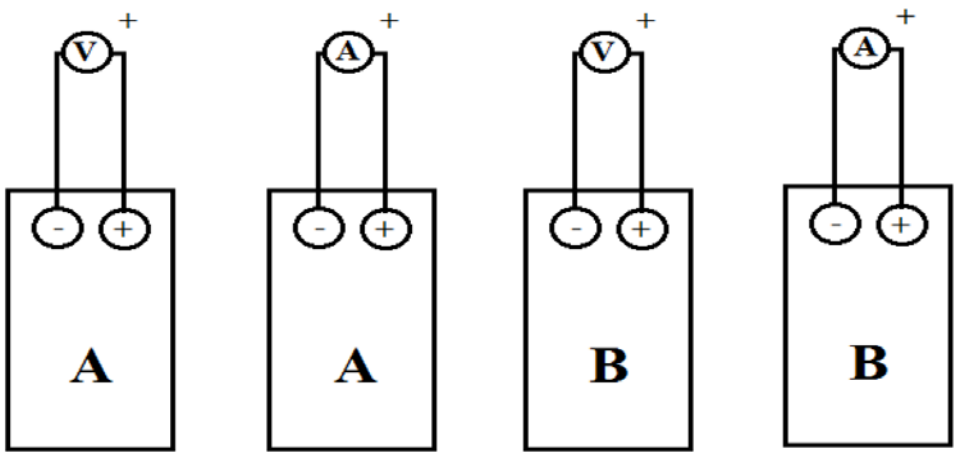

Solar cells (solution) E2

2.6 Couplings of the solar cells

2.6	Determine which of the four arrangements of the two solar cells yields the highest possible power in the external circuit when one of the solar cells is shielded with the shielding plate (J in Fig. 2.1). Draw the corresponding electrical diagram.	1.0

Two approaches:

Approach 1: use a constant setting of the variable resistor to simulate a constant external load.

Approach 2: use the hint given in the question and measure values of maximal U and maximal I independently (no variable resistor involved).

In the following only measurements for approach 1 are presented.

a.

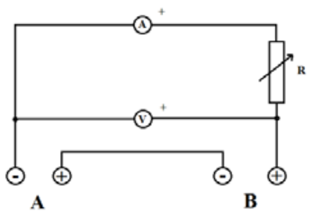

Unshielded (adjusting R for reasonable P)

13.10 mA; 0.794 V; 10.4 mW

A shielded: 0.37 mA; 0.022 V

B shielded: 0.83 mA; 0.049 V

b.

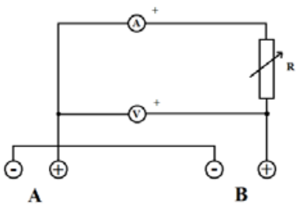

R like in a.

A shielded: 1.47 mA; 0.088 V

B shielded: -2.82 mA; -0.170 V

c.

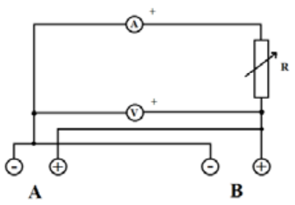

R like in a.

A shielded: 6.89 mA; 0.415 V

B shielded: 6.905 mA; 0.4165 V

Solar cells (solution) E2

d.

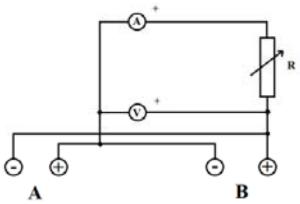

R like in a.

A shielded: 7.14 mA; 0.436 V

B shielded: -7.76 mA; -0.474 V

Conclusion: Best power: Set-up d with B shielded. (Solar cell A slightly better than B).

(2.7 on next page)

Solar cells (solution) E2

2.7 The effect of the optical vessel (large cuvette) on the solar cell current

2.7a	Measure the current I, now as a function of the height, h, of water in the vessel, see Fig. 2.8. Make a table of the measurements and draw a graph.	1.0
2.7b	Explain with only sketches and symbols why the graph looks the way it does.	1.0
2.7c	For this set-up do the following: - Measure the distance r_1 between the light source and the solar cell, and the current I_1. - Place the empty vessel immediately in front of the circular aperture and measure the current I_2. - Fill up the vessel with water, almost to the top, and measure the current I_3.	0.6
2.7d	Use your measurements from 2.7c to find a value for the refractive index n_w for water. Illustrate your method with suitable sketches and equations. You may include additional measurements.	1.6

2.7a

h mm	I mA
2	2.54
22	2.55
28	2.56
34	2.57
38	2.42
42	2.21
45	2.13
46	2.08
48	2.15
49	2.54
50	2.97
52	3.36
53	3.61
57	3.96
59	3.99
63	3.89
67	3.6
69	3.49
72	3.47

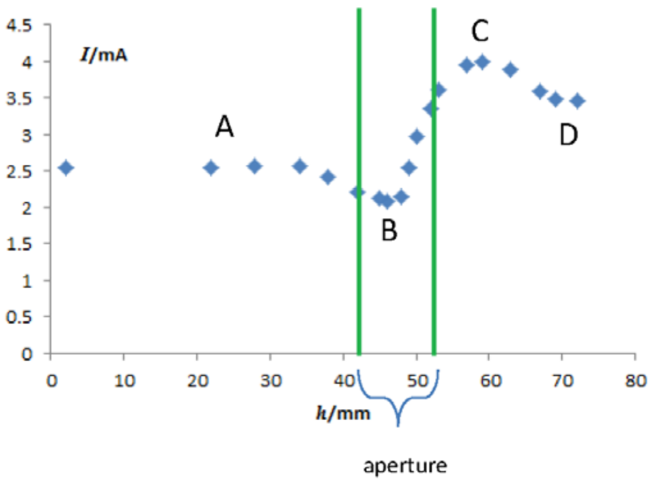

Solar cells (solution) E2

2.7b ***Exemple*** drawings for position A, B, C and D on previous graph:

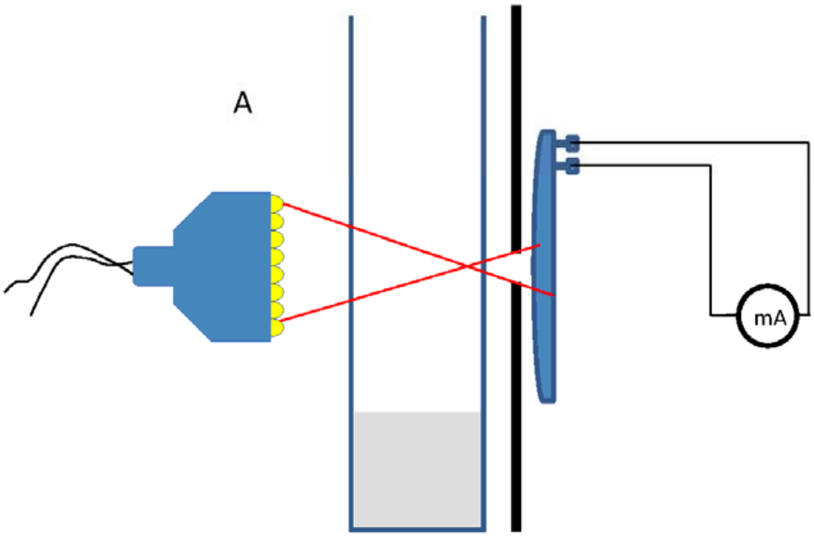

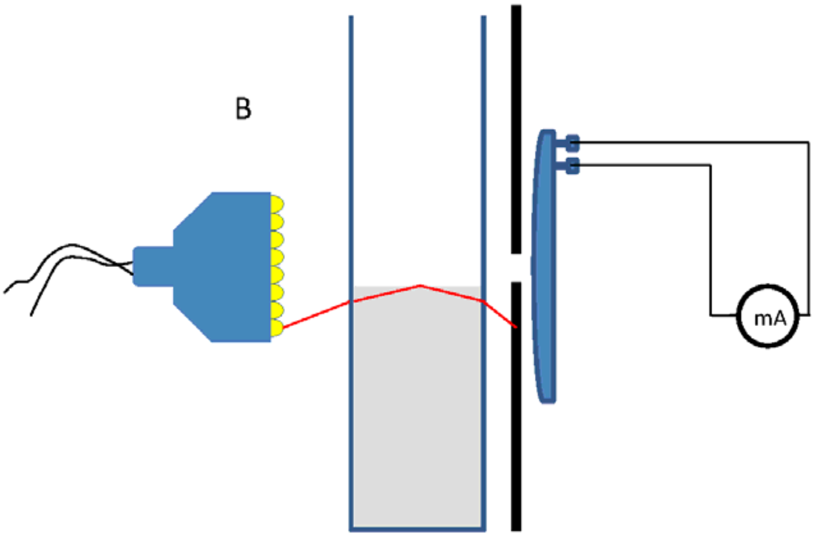

Solar cells (solution) E2

C

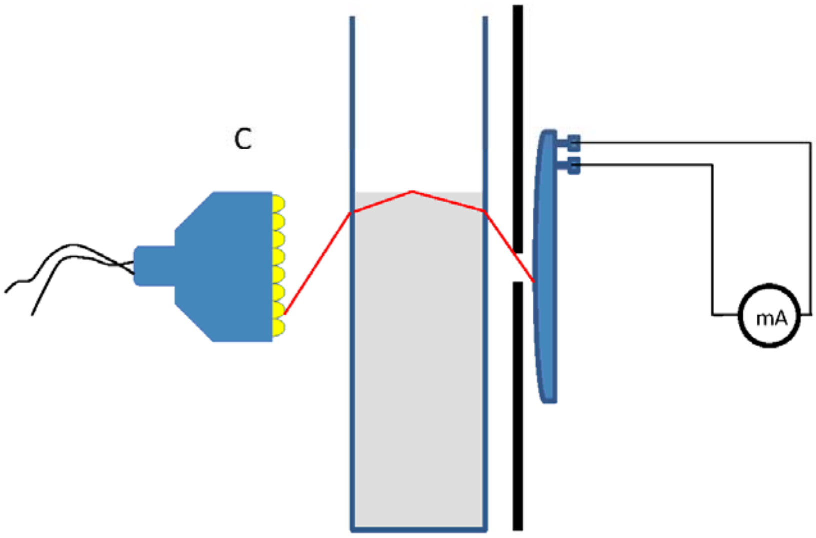

D

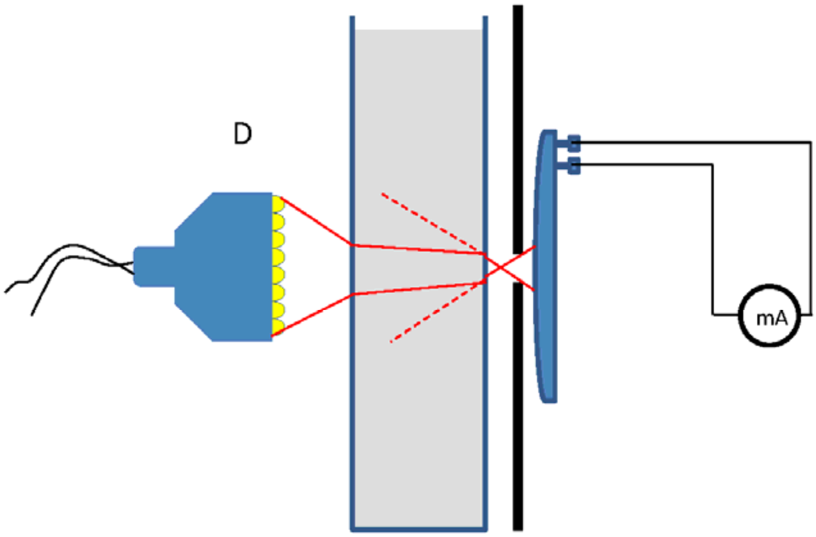

Solar cells (solution) E2

2.7c NOTE: The exemplar measurements are from a different lamp than in 2.1. For a solution to 2.7d using the distance graph it is necessary to refer to the graph below.
$r_1 = 103.5$ mm; $I_1 = 0.81$ mA; $I_2 = 0.705$ mA; $I_3 = 0.85$ mA

$$\frac{1}{I_3} \cdot \frac{I_2}{I_1} = 1.024 \text{ mA}^{-1} \sim r_c^2 = 8800 \text{ mm}^2 \sim r_c = 93.8 \text{ mm}$$

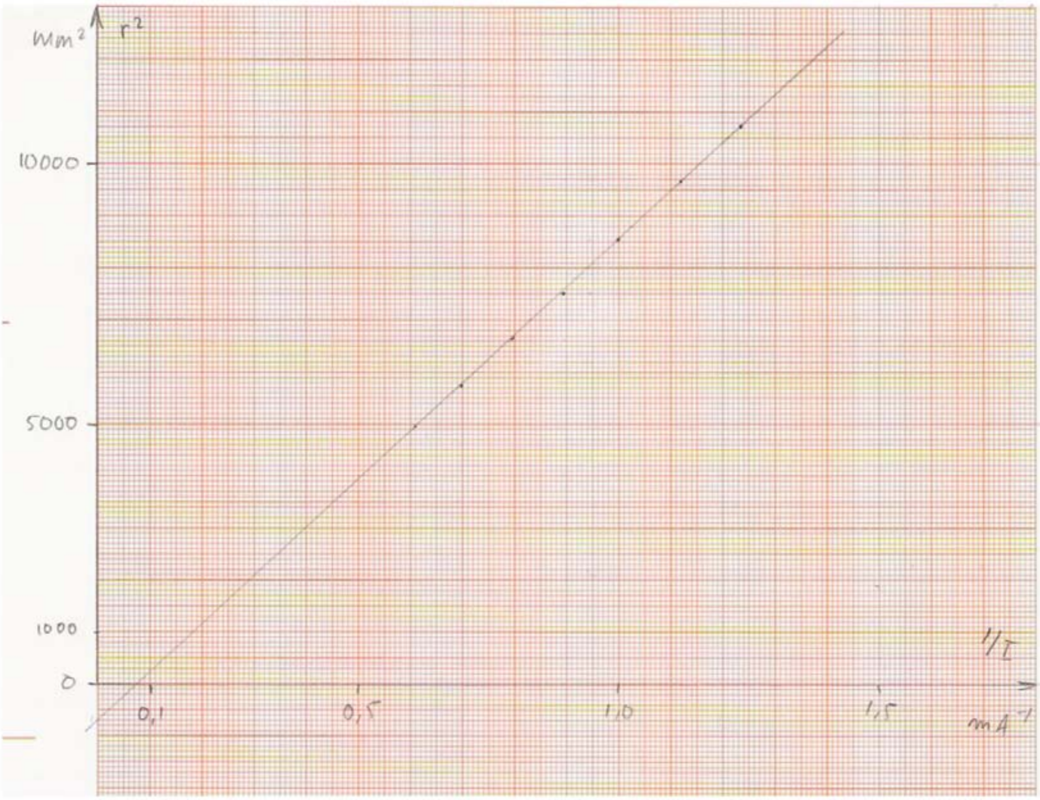

Solar cells (solution) E2

2.7d

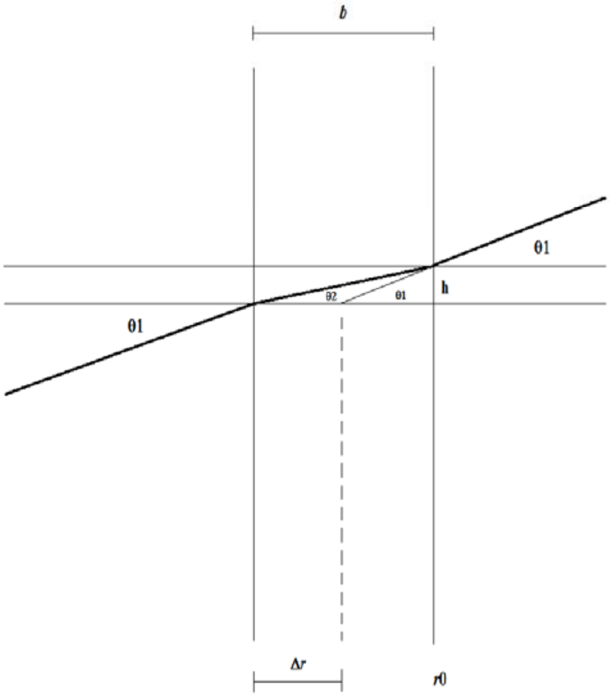

$$h = (b - \Delta r)\tan\theta_1 = b\tan\theta_2 \Rightarrow \frac{b}{b-\Delta r} = \frac{\tan\theta_1}{\tan\theta_2} \approx \frac{\sin\theta_1}{\sin\theta_2} = n \text{, da } \theta_2 < \theta_1 << 1.$$

$$n_W \approx \frac{b}{b - \Delta r} = \frac{b}{b - (r_1 - r_c)} = \frac{26.0\text{ mm}}{26.0\text{ mm} - (103.5 - 93.8)\text{mm}} = 1.6$$

NOTE: Better results may be obtained. The uncertainty is rather large in this method because of the subtraction of two large numbers for Δr

A different method is to determine the shift by actually moving the set-up and perhaps making an interpolation in directly measured data.

Minutes of the Meetings of the International Board during the 44th International Physics Olympiad in Copenhagen, Denmark 7 – 15 July 2013

(see IPhO syllabus, statutes etc. at http://ipho.phy.ntnu.edu.tw)

1. A total number of 374 contestants from the following 82 countries were present at the 44th International Physics Olympiad (IPhO): Armenia, Australia, Austria, Azerbaijan, Bangladesh, Belarus, Belgium, Bolivia, Bosnia & Herzegovina, Brazil, Bulgaria, Canada, China, Colombia, Croatia, Cuba, Cyprus, Czech Republic, Denmark, Ecuador, El Salvador, Estonia, Finland, France, Georgia, Germany, Greece, Hong Kong, Hungary, Iceland, India, Indonesia, Iran, Ireland, Israel, Italy, Japan, Kazakhstan, Kuwait, Kyrgyzstan, Latvia, Liechtenstein, Lithuania, Macau, Macedonia, Malaysia, Mexico, Moldova, Mongolia, Montenegro, Netherlands, Nigeria, Norway, Pakistan, Peru*, Poland, Portugal, Puerto Rico, Republic of Korea, Romania, Russia, Saudi Arabia, Serbia, Singapore, Slovakia, Slovenia, South Africa, Spain, Sri Lanka, Suriname, Sweden, Switzerland, Syria, Taiwan, Tajikistan, Thailand, Turkey, Turkmenistan, Ukraine, United Kingdom, USA, Vietnam.

* participated by leaders, but no student.

2. Results of marking papers by the organizers were presented.
The best score (47.0 points) was achieved by Mr. Attila Szabó from Hungary (the overall winner of the 44th IPhO). The following minimal points for awarding the medals and the honorable mention were established according to the Statutes:

Gold Medal	38.6 points
Silver Medal	29.5 points
Bronze Medal	21.5 points
Honorable Mention	16.7 points

According to the above minima, 41 Gold Medals, 64 Silver Medals, 101 Bronze Medals, and 64 Honorable Mentions were awarded. The grade lists of the awardees were distributed to all the delegation leaders in print.

3. In addition to the regular prizes, the following special prizes were awarded:

The Overall Winner:	Mr. Attila Szabó, Hungary
The Best in Theory:	Mr. Attila Szabó, Hungary
The Best in Experiment	Mr. Calvin Lin Huang, USA

Special Prizes of European Physical Society
- Ms. Katerina Marinova Naydenova, Bulgaria
- Mr. Attila Szabó, Hungary

Special Prizes of Association of Asia Pacific Physical Societies
- Ms. Tran Thi Thu Huong, Vietnam
- Mr. Zhang Chengkai, People`s Republic of China

4. The following three leaders were designated by the International Board (IB) to serve as consultants to the local academic committee for grading the examination papers: Prof. Jaan Kalda (Estonia), Prof. Askar Davletov (Kazakhstan), and Prof. Matthew Verdon (Australia).

5. The President of IPhOs, Prof. Hans Jordens, proposed to invite Kazakhstan to host the IPhO in 2014 to replace the originally arranged hosting country, Slovenia, who had withdrawn from organizing the IPhO2014 for economic reasons. The proposal was unanimously accepted by the International Board. The President expressed his gratitude to Kazakhstan Government for her kind and timely support to keep the continuity of conducting IPhO.

6. The representative of the Indian delegation, Prof. Vijay Singh, reconfirmed the hosting of IPhO 2015 in India and gave a short presentation about the ongoing preparation for the event.

7. The President of IPhOs announced the formal establishment of a legal body of fund-raising bank account, "*The Foundation of International Physics Olympiad*", which was affiliated to IPhO. He nominated, for the time being, Prof. Yohanes Surya from Indonesia as the treasurer. During the IB meeting in the next IPhO 2014, the IB will take a vote on the rules for the election of the treasurer. The elections for the treasurer will be held during the IPhO 2015. The President had used part of the donated fund of the Foundation to support Cuba team to participate in this Olympiad by offering two roundtrip air flight tickets to Copenhagen.

8. The International Board discussed a proposal on amending the Article #5 of the IPhO Statutes about using pocket calculator in the contest. The proposal was drafted by the calculator-committee composed of Dr. Matthew Verdon (Australia), Dr. Eli Raz (Israel), and Dr. Martin Swift (Iceland), who were designated by the IPhO Secretariat. This proposal was overwhelmingly carried by 114 votes to 12. The total number of IB members present at the meeting was 138. The concerned part of the Article #5 of the IPhO Statutes has been amended as the following:

"*Contestants may bring into the examination drawing instruments and approved calculators. No other aids may be brought into the examination*."

Additionally, the Regulations to the Article #5 of the IPhO Statutes have been amended by adding the following new sentences:

"*A calculator shall be an approved calculator if it is not a graphical calculator, its display has no more than three lines, and if its user memory is completely cleared immediately prior to each examination. The host country may provide calculators to students which are approved calculators. If the country chooses to do this then the team leaders of the countries attending IPhO must be advised of the exact model at least two months in advance of the competition. Students who bring their own approved calculators shall be permitted to use them*."

9. The International Board discussed a proposal submitted by Prof. Jaan Kalda (the principal organizer of IPhO 2012 in Estonia), regarding the amendment of the Regulations to the Article #4 of IPhO Statutes, concerning the voluntary fee. After the earlier discussions in the Advisory Committee, there were two different versions of the amendment on the issue of voluntary fee as the following, along with the concerned current regulation of the IPhO Statutes:

Current Regulation: "*The host country may ask the delegations for a voluntary contribution to the obligatory costs*."

Version 1: "*The host country may ask the delegations for a voluntary contribution to the obligatory costs, Those delegations which have not made the requestedcontribution are not eligible to send observers and visitors.*"

Version 2: "*The host country may ask the delegations for a contribution to the obligatory costs. Delegations with economic difficulties may ask waving this fee by sending a motivated appeal to the Secretariat of the IPhO.*"

The version 2 was carried by 98 votes to 33; while the version 1 was rejected with 63 votes in favour and 65 votes against.

10. For revising the current Syllabus of IPhO, the President invited the following six leaders to form a "*Syllabus Committee*": Dr. Lasse Franti (Finland), Dr. Helmuth Mayr (Austria), Dr. Stefan Petersen (Germany), Dr. Matthew Vernon (Australia), Dr. Andrzej Kotlicki (Canada), and Dr. Jaan Kalda (Estonia).

11. The Secretary of IPhOs, Prof. Ming-Juey Lin, on behalf of the IPhO Secretariat, reported the process and result of the election of IPhO Presidency. Since there was only one candidate, Prof. Hans Jordens, for the election of the new IPhO President, according to the IPhO Statutes, the Secretary officially announced that Prof. Hans Jordens was accepted as the new President of IPhOs for the next five-year term from 2013 to 2018.

12. The current Secretary of IPhOs will have his term expired in 2014. According to the IPhO Statutes, the election of the new Secretary of the term 2014-2019 will be held in next IPhO in Kazakhstan.

13. On behalf of all the participants, the President of IPhOs expressed his gratitude to Prof. Niels Hartling (Head of the Organizing Committee), Prof. Henrik Bruus (Head of the Academic Committee), Dr. Christian Thune Jacobsen, Prof. Jens Paaske. Dr. Jens Ulrik Lefmann, Dr. Michael Clasen Jacobsen and all other members involved in organizing the IPhO 2012 for excellent preparation and conduction of the 44th International Physics Olympiad. Deep thanks were also conveyed to the Danish Ministry of Children and Education, Technical University of Denmark, Niels Bohr Institute, University of Copenhagen, and all the sponsors, graders, guides and other people who contributed to the success of the Olympiad.

14. The Kazakhstan delegates disseminated printed materials about the 45th IPhO in 2014 to all the delegations and described present state of the preparatory works to ensure smooth organization of the next Olympiad.

15. At the Closing Ceremony of the Olympiad, on behalf of the organizers of the next International Physics Olympiad, Dr. Yernur Rysmagambetov announced that the 45th International Physics Olympiad would be held in Astana, Kazakhstan from July 13 to 21, 2014 and cordially invited all the participating countries to attend the competition.

....	....	………………...
Prof. Hans Jordens President of IPhOs	Prof. Ming-Juey Lin Secretary of IPhOs	Prof. Niels Hartling Head of the Organizing Committee of the IPhO 2013

Copenhagen, Denmark, 14 July 2013

The daily IPhO newsletter "Hafnium"

(www.ipho2013.dk/ipho2013-newsletter.htm)

Chief editor: Turi K. Schäffer **Photographer: Miriam Ortwed**

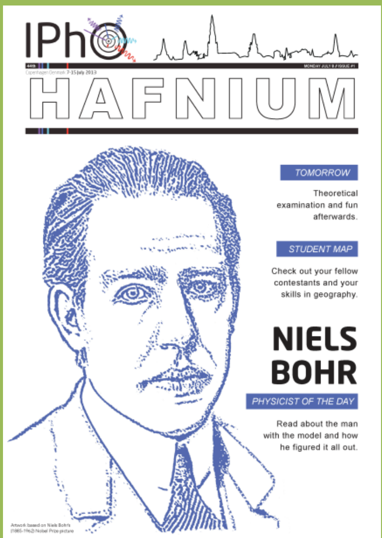

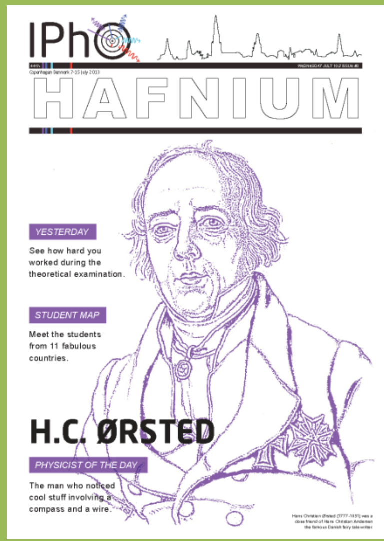

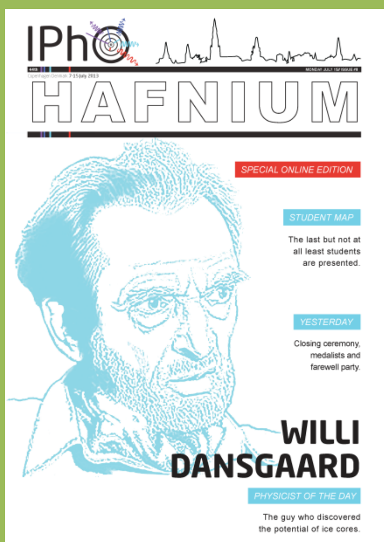

IPhO 44th Copenhagen Denmark 7-15 July 2013

World Capital of Physics, Copenhagen 2013

In 2012, Estonia launched a new tradition of nominating the hosting city of IPhO as The World Capital of Physics. Tartu became the World Capital of Physics of 2012. In Tartu, Denmark got the baton, i.e. the so-called Chronicle Book, from Estonia.

During IPhO-2013 Denmark followed up the new tradition: On Friday 12 July, the president of the municipal council of Copenhagen, Jesper Christensen, welcomed all students, leaders, observers, guides and visitors to Copenhagen City Hall and announced Copenhagen as the World Capital of Physics 2013. Afterwards, he handed over the Chronicle Book to Mrs. Sholpan Kirabayveva, Head of the Committee organizing the IPhO-2014 in Astana, Kazakhstan, the next World Capital of Physics of 2014.

After the ceremony, everybody got the famous Copenhagen City Hall Pancakes.




Results, some statistics
(http://www.ipho2013.dk/ipho2013-results.htm)

Number of participating

Countries:	82
Students:	374 (18 women = 4.8%)
Leaders:	156
Observers:	73
Visitors:	20

Number of medals

Gold:	41 (11.0%)	G	= 11.0% [minimum 8%, thus 3.0% more G]
Silver:	64 (17.1%)	G+S	= 28.1% [minimum 25%, thus 0.1% more S]
Bronze:	101 (27.0%)	G+S+B	= 55.1% [minimum 50%, thus 2.0% more B]
Hon.Men.:	64 (17.1%)	G+S+B+HM	= 72.2% [minimum 67%, thus 0.1% more HM]
Others:	104 (27.8%)		

Point limits for medals (max score 50)

Gold	awarded for 38.6 points or more
Silver	awarded for 29.5 points or more
Bronze	awarded for 21.5 points or more
Hon.Men.	awarded for 16.7 points or more

Best individual scores

Best overall score	47.0 (max 50.0) Hungary
Best theory score	29.5 (max 30.0) Hungary
Best experiment score	18.4 (max 20.0) USA

IPhO 2013 cumulated scores given
by markers and leaders, as well as the final result after moderation

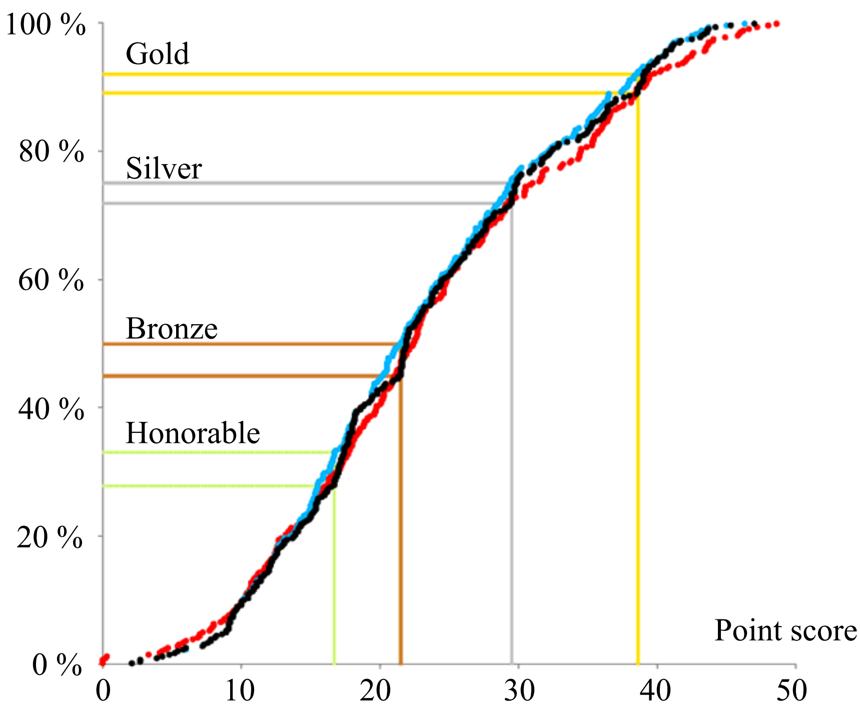

Results - gold medalists (www.ipho2013.dk/ipho2013-results-gold.htm)

Country	Name
Hungary	Szabó Attila
China	Zhang Chengkai
China	Zhang Zhengxing
Singapore	Sean Seet Xiang En
United States	Kevin Zhou
Taiwan	Wen-Yu Chang
Russian Federation	Daniil Kalinov
United States	Calvin Lin Huang
China	Yu Yue
Vietnam	Bui Quang Tu
Singapore	Daniel Mark Keat Kay
Poland	Jakub Supeł
Singapore	Lim Jeck
Iran	Amir Zare
Lithuania	Daumantas Kavolis
Thailand	Bhurint Siripanthong
Singapore	Tan Wei Liang Byorn
Bulgaria	Katerina Marinova Naydenova
Republic of Korea	Changhyon Lee
Republic of Korea	Jaewon Kim
Vietnam	Ngo Phi Long
Thailand	Peerasak Sae-Ung
China	Wang Sizhen
United States	Jeffrey Yan
Thailand	Kittipatr Poopong
Republic of Korea	Donghoi Kim
China	Jiang Jiaqi
Taiwan	Yu-Kai Lo
Republic of Korea	Jaeha Lee
Russian Federation	Ivan Maslov
Iran	Mohamadreza Lotfinamin
Republic of Korea	Sangsu Jeong
Iran	Koosha Rezaiezadeh
Hungary	Kovács Áron Dániel
Romania	Dan-Cristian Andronic
India	Prafulla Susil Dhariwal
Taiwan	Zong-You Luo
Israel	Dan Karliner
Russian Federation	Maksim Velikanov
Romania	Cristian-Alexandru Frunza
Russian Federation	Ilya Fradkin

Results - silver medalists (www.ipho2013.dk/ipho2013-results-silver.htm)

Singapore	Ashwin Venkidachalam
Hungary	Juhász Péter
Romania	Tudor Ciobanu
India	Shouvanik Chakrabarti
India	Abhijit Lavania
India	Yash Gupta
India	Abhishek Anand
Romania	Sebastian Florin Dumitru
Israel	Ofer Moshe Kopelevitch
Bulgaria	Yordan Stefanov Yordanov
France	Jean Douçot
Estonia	Andres Põldaru
Hong Kong	Man Siu Hang
United States	Samuel Zbarsky
Japan	Yuichi Enoki
Japan	Tasuku Omori
Iran	Nader Mostaan
Russian Federation	Mikhail Kurenkov
Taiwan	Ching-Chung Hsueh
Thailand	Sorawich Wathanapenpaiboon
Hong Kong	Shing Ming Tony
Hong Kong	Tam Pok Man
Vietnam	My Duy Hoang Long
Austria	Oliver Edtmair
France	Sébastien Chevaleyre
Estonia	Kristo Ment
United States	Jeffrey Cai
France	Matthieu De Rochemonteix
Belarus	Aliaksandr Hancharuk
Australia	Dmitry Brizhinev
Poland	Adam Krasuski
Belarus	Ivan Mitskovets
Estonia	Kaur Aare Saar
Republic of Moldova	Cristian Zanoci
France	Anatole Gosset
Israel	Guy Segall
Turkey	Atinc Cagan Sengul
Kazakhstan	Mussa Rajamov
Kazakhstan	Aidar Zhetessov
Germany	Sascha Lill
Serbia	Milan Krstajić
Kazakhstan	Amir Bralin
Macao	Chon Man Sou
Poland	Jakub Mrożek
United Kingdom	Matei Filip Mandache
France	Cédric Viry

Czech Republic	Lubomír Grund
Hungary	Jenei Márk
Brazil	Fabio Kenji Arai
Ukraine	Volodymyr Biloshytskyi
Canada	Henry Wu
United Kingdom	Yuting Li
Turkey	Fatih Serdar Saglam
United Kingdom	Daniel Yeelun Hu
Kazakhstan	Nurislam Tursynbek
Turkmenistan	Nazar Ilamanov
Republic of Moldova	Nicoleta Colibaba
Germany	Lucas Rettenmeier
Taiwan	Chuan-I Yen
Romania	Denis Turcu
Belarus	Maksim Litskevich
Israel	Gil Ad Kishony
Thailand	Kann Ruaytae
Germany	Lars Dehlwes

Results - bronze medalists (www.ipho2013.dk/ipho2013-results-bronze.htm)

Japan	Hidenobu Ema
Indonesia	I Made Gita Narendra Kumara
Bulgaria	Kaloyan Georgiev Metodiev
Japan	Kenji Ueda
Serbia	Ivan Tanasijević
Serbia	Uroš Ristivojević
Serbia	Luka Bojović
Australia	Liam Hayes
Japan	Hiromitsu Sawaoka
Germany	Michael Sonner
Lithuania	Gintautas Kamuntavičius
Montenegro	Petar Tadic
Belarus	Aliaksei Duduk
Slovakia	Patrik Turzák
Germany	David Schmidt
Bosnia and Herzegovina	Nudžeim Selimović
Estonia	Kristjan Kongas
Kazakhstan	Dinmukhammed Nurbek
Croatia	Antonio Bjelčić
Indonesia	Paulus Anthony Halim
Hong Kong	Wong Yiu Man
United Kingdom	Elango Madhivanan
Lithuania	Vilda Kornelija Markevičiūtė
Hong Kong	Lum Kai Chun
Italy	Federico Belliardo

Canada	Bailey Gu
Ukraine	Oleksii Lubynets
Ukraine	Igor Sholom
Indonesia	Mikael Harseno Subianto
Turkmenistan	Dovran Amanov
Turkey	Ekin Akyurek
Ukraine	Artem Oliinyk
Czech Republic	Miroslav Hanzelka
Latvia	Māris Seržāns
United Kingdom	George Thomas Fortune
Israel	Jacoby Shoham Joshoa
Iran	Amirparsa Zivari
Indonesia	Joshua Christian Nathanael
Liechtenstein	Lukas Lang
Vietnam	Le Duy Anh
Republic of Moldova	Ilie Popanu
Brazil	Fernando Frota Junior
Netherlands	Arthur Christianen
Hungary	Papp Roland
Slovakia	Tomáš Gonda
Austria	Christian Schuster
Belarus	Akvukh Jeims Aye
Netherlands	Tim Baanen
Macao	Chon Lok Lei
Slovenia	Žiga Krajnik
Armenia	Gevorg Martirosyan
Greece	Stavros Efthymiou
Malaysia	Yeoh Chin Vern
Poland	Kacper Oreszczuk
Italy	Leonardo Fiore
Bulgaria	Kaloyan Ognyanov Darmonev
Czech Republic	Jiří Guth
Turkey	Huseyin Anil Gunduz
Ukraine	Taras Antoshchuk
Syria	Osama Yaghi
Denmark	Frederik Ravn Klausen
Netherlands	Freddie Hendriks
Slovakia	Ján Ondráš
Latvia	Sergejs Blakunovs
Mongolia	Duinkharjav Budmonde
Croatia	Samuel Bosch
Armenia	Arsen Vasilyan
Italy	Michele Fava
Canada	Hao Zhe Sheng
Switzerland	Alain Rossier
Australia	Jack Spilecki
Finland	Tomi Mäkinen
Vietnam	Tran Thi Thu Huong

Mexico	Jose Alberto De La Paz Espinosa
Slovakia	Jakub Kvorka
Italy	Roberto Albesiano
Australia	Simon Swan
Armenia	Vardges Mambreyan
Australia	Eric Huang
Sri Lanka	Herath M. Kosala Sananthana Herath
Lithuania	Vilius Čepaitis
Turkey	Bilal Cark
Estonia	Joonas Kalda
Mexico	Eduardo Israel Acosta Reynoso
Bulgaria	Ivan Krasimirov Poryazov
Georgia	Sandru Maludze
Brazil	Guilherme Renato Martins Unzer
Armenia	Aleksandr Petrosyan
Slovenia	Michel Adamič
Brazil	Jose Luciano De Morais Neto
Belgium	Nick Van Den Broeck
Saudi Arabia	Mohammad Alhejji
Portugal	Tomás M.D.O. De Albuquerque Reis
Italy	Luigi Pagano
Serbia	Ilija Burić
Saudi Arabia	Ali Alhulaymi
Cyprus	Andreas Stavrou
Brazil	Matheus Carius Castro
Switzerland	William Borgeaud
Belgium	Gaëtan Cassiers
Macao	Ka Kit Kong

Results – honorable mentions (www.ipho2013.dk/ipho2013-results-honorable.htm)

Mexico	Jorge Torres Ramos
Georgia	Giorgi Tskhadadze
Latvia	Rūdolfs Treilis
Nepal	Pradeep Niroula
Austria	Florian Kanitschar
Tajikistan	Adhamzhon Shukurov
Republic of Moldova	Dinu Purice
Lithuania	Justinas Rumbutis
Mexico	Siddhartha Emmanuel Morales Guzman
Netherlands	Jozef Barnabas Houben
Canada	Shun Da Suo
Georgia	Sergi Chalauri
Denmark	Markus Emil Jacobsen
Saudi Arabia	Ibrahim Alnami
Turkmenistan	Omargeldi Atanov
Switzerland	Sven Pfeiffer
Mexico	Leonel Medina Varela
Sweden	Emil Ejbyfeldt

Croatia	Matej Vilić
Slovenia	Bine Brank
Kyrgyzstan	Salizhan Kylychbekov
Netherlands	Matthijs Niels Albert Vernooij
Mongolia	Zorigoo Garid
Macao	Chi Chong Lam
Nigeria	Ayomide Andrae Bamidele
Turkmenistan	Dovrangeldi Jumageldiyev
Poland	Kamil Kaczmarek
Colombia	Daniel Eduardo Fajardo Fajardo
Bosnia and Herzegovina	Slavko Ivanović
Denmark	Michael Blom Hermansen
Syria	Ghadeer Shaaban
Mongolia	Bat-Erdene Bat-Amgalan
Spain	Marc Santigosa I Pinilla
Switzerland	Rafael Winkler
Finland	Timo Takala
Finland	Einari Junter
Nepal	Niranjan Bhujel
Sweden	Andréas Sundström
Sweden	Henrik Gingsjö
Spain	Raul Gonzalez Molina
Spain	Francisco Javier Gonzalez Rodriguez
Latvia	Luka Ivanovskis
Armenia	Razmik Hovhannisyan
Macao	Pui Un Tang
Finland	Heikki Oskari Timonen
Finland	Joonas Latukka
Iceland	Pétur Rafn Bryde
Czech Republic	Jakub Rösler
El Salvador	Alejandra María Fuentes Núñez
Belgium	Engelen Wouter
Austria	Florian Riedl
Spain	Pablo Gomez Perez
Iceland	Snorri Tómasson
Canada	Jiaxi (Jannis) Mei
Georgia	Mikkeil Gobejishvili
Puerto Rico	Logan Brendan Abel
Austria	Moritz Theissing
Switzerland	Quentin Wenger
Bosnia and Herzegovina	Suad Krilašević
Colombia	Jorge Alberto Garcia Perez
Bosnia and Herzegovina	Enes Kriještorac
Bangladesh	Kinjol Barua
Malaysia	Poh Wai Chang
Saudi Arabia	Abdulmohsen Alowayed

Special prizes

Special prizes from
The International Phyiscs Olympiad
presented by Prof. Jens Paaske, Niels Bohr Inst.

- Best experimental result:
  Calvin Lin Huang, USA

- Best theoretical result:
  Szabó Attila, Hungary

- Best overall result:
  Szabó Attila, Hungary

Special prizes from The Association of the Asian Pacific Physical Societies
presented by IPhO secretary Ming-Juey Lin

- Best performing female Asian participant:
  Tran Thi Thu Huong, Vietnam

- Best performing male Asian participant:
  Zhang Chengkai, China

Special prizes from
The European Physical Society
presented by IPhO President Hans Jordens

- Best performing female European participant:
  Katerina M. Naydenova, Bulgaria

- Best performing male European participant:
  Szabó Attila, Hungary

The closing ceremony of the 44th International Physics Olympiad
DTU, Sunday 14 July 2013 (see the video at www.ipho2013.dk)

1. Opening at 16:00 by the New Bigband led by Andreas Vetö and
show hosts Flemming Enevold and Sofie Lassen-Kahlke

2. Speech. Bertel Haarder, MP and vice-chairman of the Danish Parliament

3. Show. Royal Danish Ballet: Josephine Berggren and Charles Andersen



4. Speech. President of IPhO, Dr. Hans Jordens

5. Awarding of Honorable Mention by Prof. Henrik Bruus



6. Awarding of Bronze Medals by President of IPhO 2013 Niels Hartling

7. Show. Andrea Pellegrini performs two songs by Carl Nielsen


8. Awarding of Silver Medals by Dean of Undergraduate Studies and Student Affairs at
Technical University of Denmark, Dr. Martin Etchells Vigild

9. Show. Andrea Pellegrini and Flemming Enevold perform a song by H.C. Andersen



10. Awarding of Gold Medals by President of IPhO, Dr. Hans Jordens
11. Awarding of Special Prizes by Prof. Jens Paaske, Prof. Ming-Juey Lin, Secretary of IPhO, and Dr. Hans Jordens, President of IPhO.


12. Closing of IPhO 2013. Scientific Coordinator of IPhO 2013, Professor Henrik Bruus and presentation of the IPhO banner by the Danish IPhO Team

13. Presentation of IPhO 2014.
Head of the IPhO 2014 Committee, Mrs. Sholpan Kirabayveva
Member of the IPhO 2014 Academic Committee, Mr. Pavel Levchenko
Member of the IPhO 2014 Academic Committee, Mr. Yernur Rysmagambetov


14. Closing show. Safri Duo